# Wheat- associated bacterial and fungal communities during the interaction of *Fusarium graminearum* and *Trichoderma gamsii* T6085

**and**

# Infection of a CRISPR/Cas9 derived green-fluorescent protein labeled *Leptosphaeria maculans* strain on *Brassica napus*

**By**

**Dhathuge Waththe Gedara Arshani Srimali Alukumbura**

**A Thesis submitted to the Faculty of Graduate Studies of**
**The University of Manitoba**
**in partial fulfilment of the requirements of the degree**

**MASTER OF SCIENCE**

**Department of Plant Science**
**University of Manitoba**
**Winnipeg**

**Copyright © 2022 by D. W. G. Arshani Srimali Alukumbura**

## ACKNOWLEDGMENTS

I would like to thank my supervisor Dr. Dilantha Fernando and my co-supervisor, Dr. Matthew Bakker, for having me as a graduate student. I am really grateful for your support and guidance throughout these two years. The encouragements and feedback you provided were really valuable for me to do my best and improve my research, writing, and presentation skills. I learned a lot from you both. Thank you very much for that. Thank you to my committee members, Dr. Ana Badea, Dr. Maria Antonia Heriquez and Dr. Teresa De Kievit. Thank you for all the guidance, feedback and encouragement you gave me during these two years. I am really grateful for that.

Thank you, Paula Parks, for all the help you gave me during the lab and greenhouse work and for always making us smile. I really appreciate your work in Dr Fernado's lab. Thank you, for everything.

Thank you to entire lab members from Dr. Fernando's lab and Dr. Bakker's lab for all the support you gave me. Thank you, Zhongwei Zou, Fei Lu and Shuanglong Huang, for your guidance during my research work. I am really grateful for all the guidance you provided on this project. Thank you, Liang Zhao, for reviewing my thesis. Thank you, Shaima Eissa, for doing DNA extractions. Also, I would like to thank Dr. Matthew McDougall and Wesley Johnson from the chemistry department for all the help you provided during Illumina sequencing.

Thank you to my fellow graduate students Sachithrani Kannangara, Anuradha Jayathissa and Janice Fajardo, for all the help you gave me during these two years and for all the fun we had together. It would be so hard if you guys weren't there. I really appreciate all your support.

Finally, I am thankful for my parents Palitha & Champika Alukumbura, my sister Sachini Alukumbura and my husband Mayantha Kurera for your love and care. Without your support, it would be a tough two years. Thanks a lot for that.

## DEDICATION

To my beloved family

## TABLE OF CONTENTS

ACKNOWLEDGMENTS ..... ii
DEDICATION ..... iii
LIST OF TABLES ..... vii
LIST OF FIGURES ..... viii
ABSTRACT ..... xii
1.0 GENERAL INTRODUCTION ..... 1
2.0 LITERATURE REVIEW ..... 3
2.1 Plant diseases caused by fungal pathogens ..... 3
2.2 Wheat - *Fusarium* interactions and FHB management ..... 3
2.2.1 Wheat ..... 3
2.2.2 The Fusarium head blight disease in wheat ..... 4
2.2.3 Plant microbiome interactions ..... 7
2.2.4 Biological control for plant disease management ..... 8
2.2.4.1 Genus *Trichoderma* ..... 10
2.2.4.1.1 *Trichoderma gamsii* as a potential biocontrol agent ..... 12
2.2.5 Impact of biocontrol agent on pathogens ..... 13
2.2.6 Impact of biocontrol agents on the broader microbial community ..... 14
2.3 Canola – *Leptosphaeria* interaction ..... 15
2.3.1 Canola ..... 16
2.3.2 Blackleg disease in canola ..... 18
2.3.3 *Leptosphaeria* spp. ..... 19
2.3.4 Blackleg resistance in *Brassica napus* ..... 21
2.3.4.1 Gene for gene interaction between host and the pathogen ..... 22
2.3.5 Fungal transformation ..... 23
2.3.5.1 *Agrobacterium tumefaciens*-mediated transformation ..... 24
2.3.6 CRISPR for gene editing ..... 26
2.3.7 Fluorescent proteins ..... 28
2.3.7.1 Green fluorescent protein as a marker ..... 29
2.4. Research questions ..... 30
3.0 CHAPTER 1 ..... 31
Wheat-associated bacterial and fungal communities during the interaction of *Fusarium graminearum* and *Trichoderma gamsii* T6085 ..... 31
3.1 ABSTRACT ..... 32
3.2 INTRODUCTION ..... 33
3.3 MATERIALS AND METHODS ..... 36

3.3.1 The field experimental setup ..... 36
3.3.2 Quantitative PCR ..... 37
3.3.3 Amplicon sequencing ..... 38
3.3.4 Data analysis ..... 39
3.4 RESULTS ..... 40
3.4.1 The variation in *T. gamsii* T6085 abundance in different wheat tissues ..... 40
3.4.2 The variation in *F. graminearum* abundance due to *T. gamsii* T6085 treatment ..... 41
3.4.3 Variations in *F. graminearum* abundance in different wheat tissues over time ..... 43
3.4.4 Relative abundances of different bacteria and fungi associated with different tissues. 44
3.4.5 Variations in the microbial community due to treatment and over time ..... 46
3.4.6 Variation in microbial diversity ..... 48
3.5 DISCUSSION ..... 54
4.0 CHAPTER 2 ..... 59
Infection of a CRISPR/Cas9 derived green-fluorescent protein labeled *Leptosphaeria maculans* strain on *Brassica napus* ..... 59
4.1 ABSTRACT ..... 60
4.2 INTRODUCTION ..... 61
4.3 MATERIALS AND METHODS ..... 64
4.3.1 Fungal material and inoculum preparation ..... 64
4.3.2 Fungal DNA extraction ..... 64
4.3.3 Characterization of the avirulence gene profile ..... 64
4.3.3.1 Genotypic identification ..... 65
4.3.3.2 Phenotypic identification ..... 66
4.3.4 The examination of the pathogenicity of mJN3 and JN3 isolates ..... 66
4.3.5 Development of a transgenic fungus ..... 67
4.3.5.1 The pRM-eGFP vector ..... 67
4.3.5.2 Plasmid DNA extraction and the transformation of *A. tumefaciens* cells by electroporation ..... 68
4.3.5.3 Antibiotic sensitivity test of the JN3 and mJN3 isolates ..... 69
4.3.5.4 *Agrobacterium tumefaciens*-mediated transformation of *L. maculans* isolates ..... 69
4.3.5.5 Fluorescence microscopic confirmation of GFP expressing fungi ..... 70
4.3.6.6 PCR amplification of *egfp* gene in transformed fungal isolates ..... 70
4.3.5.7 Mitotic stability test for the fungal transformants ..... 70
4.3.5.8 The disease forming ability of GFP transformants ..... 70
4.3.5.9 Fluorescent microscopic observation of the spores and hyphae of the selected mJN3gfp and JN3gfp isolates ..... 71
4.3.5.10 Fluorescent microscopic observation of the selected mJN3gfp and JN3gfp isolates in live plant tissues ..... 71
4.4 RESULTS ..... 72
4.4.1 The avirulence gene profile of the mJN3 and the JN3 isolates ..... 72
4.4.2 Pathogenicity of mJN3 and JN3 isolates ..... 72
4.4.3 Transformation of *A. tumefaciens* cells by electroporation ..... 73

4.4.4 Antibiotic sensitivity testing of the mJN3 and JN3 isolates ..... 74
4.4.5 *A. tumefaciens*-mediated transformation ..... 75
4.4.6 Confirmation of the presence of the *egfp* gene within the transformants by PCR ..... 76
4.4.7 The mitotic stability test ..... 76
4.4.8 The disease forming ability of GFP transformants ..... 76
4.4.9 Fluorescent microscopic observation of the selected mJN3gfp and JN3gfp isolates ..... 78
4.4.10 The growth of mJN3gfp in *B. napus* cotyledons comparative to the JN3gfp ..... 80
4.5 DISCUSSION ..... 82
5.0 GENERAL DISCUSSION AND CONCLUSIONS ..... 85
6.0 REFERENCES ..... 89
7.0 APPENDICES ..... 115
7.1 List of abbreviations ..... 115

## LIST OF TABLES

**Table 3.1.** Number of wheat tissue samples collected at different time points for the microbiome analysis..... 36

**Table 3.2.** The PCR programs for each PCR reaction performed during amplicon generation, addition of indices, and for qPCR..... 37

**Table 3.3**. Differentially abundant bacterial and fungal taxa compared to Treatment 1 (control treatment) in crop residue, wheat spikes, and kernel samples..... 47

**Table 4.1**. The nucleotide sequences of each primer pair used to amplify the avirulence genes in L. maculans isolates..... 65

**Table 4.2.** The resistance genes present in each differential line of *B. napus* plants are used for phenotypic characterization of *L. maculans* avirulence genes..... 66

**Table 4.3.** The deduced phenotypes of different *Brassica* varieties in response to the infection of mJN3 and JN3 isolates..... 72

**Table 4.4.** The disease scores and the inferred phenotypes in Westar after inoculating with different *L. maculans* strains..... 77

## LIST OF FIGURES

**Figure 2.1.** The life cycle of *F. graminearum*. *F. graminearum* overwinters within crop residue and mainly infects wheat plants during anthesis. *F. graminearum*'s sexual (ascospores) spores are released from perithecia, and the asexual (macroconidia) spores are released from sporodochia. The ascospores and macroconidia infect wheat plant from flowering stage to hard dough stage of wheat kernels contaminating them with mycotoxins. ..... 6

**Figure 2.2.** The genetic relationship among six natural *Brassica* spp. A, B and C represent three major genomes shared by each other. These three major genomes are present within diploid (AA, BB and CC) and allotetraploid (AABB, BBCC and AACC) *Brassica* species. ..... 17

**Figure 2.3**. The blackleg disease incidence over 22 years from 1998 to 2020 in western Canadian canola fields. Manitoba shows the highest blackleg incidences, and in Manitoba, more than 15% of canola plants infected with the blackleg disease in 2020 (The Canola Council of Canada, 2021). ..... 19

**Figure 2.4**. Life cycle of the blackleg pathogen. The *L. maculans* overwinters within crop residue and infects canola plants during spring, forming leaf lesions and stem cankers. Stem cankers are detrimental to canola plants. ..... 21

**Figure 2.5**. A summary of *A. tumefaciens* mediated transformation of fungi. 1: Acetosyringone in the culture media triggers the expression of virulence genes. 2: The virulence genes expressed, and virulence proteins cut the T-DNA region. 3: The virulence proteins transfer the T-DNA region through the type IV secretion system. At this point, the virulence proteins are bound to the T- DNA region. The T-DNA with virulence proteins enter the host nucleus with the help of nuclear localization signals. 4: The T-DNA integrates into the host genome. ..... 25

**Figure 3.1.** Variation in *T. gamsii* abundance in A: crop residue; B: wheat spikes; C: wheat kernels across different treatments. $T_{cr}0$, $T_{cr}1$ and $T_{cr}2$ indicate the different time points at which the crop residue samples were collected, while $T_{sp}0$, $T_{sp}1$, $T_{sp}2$ and $T_{sp}3$ indicate the various time points at which the wheat spikes samples were collected. The x-axis labels Trt1 (Control), Trt2 (*T. gamsii* T6085 applied on spikes at anthesis), Trt3 (*T. gamsii* T6085 applied in soil on crop residue), and Trt4 (*T. gamsii* T6085 applied both in soil on crop residue and on spikes at anthesis) indicates the four different treatments we used in the experiment. The box plots show the 1$^{st}$ quartile, median 3$^{rd}$ quartile, and data set outliers. The changes in *T. gamsii* abundance across different treatments was not significant in crop residue, wheat spikes and wheat kernels (ANOVA with Tukey HSD, $p>0.05$). ..... 40

**Figure 3.2.** The impact of *T. gamsii* T6085 application on *F. graminearum* abundance. A: *F. graminearum* abundance in crop residue; B: *F. graminearum* abundance in wheat spikes; C: *F. graminearum* abundance in wheat kernels. $T_{cr}0$, $T_{cr}1$ and $T_{cr}2$ indicate the different time points at which the crop residue samples were collected, while $T_{sp}0$, $T_{sp}1$, $T_{sp}2$ and $T_{sp}3$ indicate the various time points at which the wheat spikes samples were collected. The x-axis labels Trt1 (Control), Trt2 (*T. gamsii* T6085 applied on spikes at anthesis), Trt3 (*T. gamsii* T6085 applied in soil on crop residue), and Trt4 (*T. gamsii* T6085 applied both in soil on crop residue and on spikes at anthesis)

indicates the four different treatments we used in the experiment. The box plots show the 1st quartile, median 3rd quartile, and data set outliers. The changes in *F. graminearum* abundance due to *T. gamsii* T6085 treatment was not significant in crop residue, wheat spikes and wheat kernels (ANOVA with Tukey HSD, $p>0.05$). ..... 42

**Figure 3.3.** Variation of *F. graminearum* abundance over time in A: crop residue ($nT_{cr}0=14$, $nT_{cr}1=15$, $nT_{cr}2=20$) and B: wheat spikes ($nT_{sp}0=17$, $nT_{sp}1=16$, $nT_{sp}2=20$, $nT_{sp}3=20$) tissues. $T_{cr}0$, $T_{cr}1$ and $T_{cr}2$ indicate the different time points at which the crop residue samples were collected, while $T_{sp}0$, $T_{sp}1$, $T_{sp}2$ and $T_{sp}3$ indicate the different time points at which the wheat spikes samples were collected. Different colors of the legends represent different treatments including Trt1 (Control), Trt2 (*T. gamsii* T6085 applied on spikes at anthesis), Trt3 (*T. gamsii* T6085 applied onto crop residue at the soil surface) and Trt4 (*T. gamsii* T6085 applied onto both crop residue at the soil surface and onto spikes at anthesis). The box plot shows the 1st quartile, median and the 3rd quartile of the data set. Different letters indicate statistically significant difference ($p<0.05$). The *F. graminearum* abundance was significantly higher at the $T_{cr}0$ time point in the residue (Tukey HSD, $p<0.05$), and it decreased over time. The *F. graminearum* abundance is lower during $T_{sp}0$ to $T_{sp}2$ time points in wheat spikes and it reaches a significantly higher abundance at $T_{sp}3$ time point (ANOVA with Tukey HSD, $p<0.05$). ..... 43

**Figure 3.4**. The relative abundances of different bacteria and fungi present in different samples. A: bacteria in residue B: bacteria in spikes C: bacteria in kernels D: fungi in residue E: fungi in spikes F: fungi in kernels. The legends show the ten most abundant bacterial and fungal genera in each tissue, and different colors represent different genera. ..... 45

**Figure 3.5**. The variation in the microbial communities associated with crop residue, wheat spikes and kernels due to the application of *T. gamsii* T6085 were minimal. The plots are principal coordinates ordinations derived from pairwise community dissimilarity values (Bray-Curtis index). A: crop residue-associated bacteria; B: wheat spikes-associated bacteria; C: wheat kernels-associated bacteria; D: crop residue-associated fungi; E: wheat spikes-associated fungi; F: wheat kernels-associated fungi. The red colour indicates the *T. gamsii* T6085 treated samples while the blue colour indicates the untreated samples. The ellipses represent 95% confidence level. ..... 46

**Figure 3.6**. There was progressive change in bacterial and fungal communities over time. The variations were more prominent in crop residue-associated microbial communities, compared to wheat spikes-associated microbial communities. The plots are principal coordinates ordinations derived from pairwise community dissimilarity values (Bray-Curtis index). A: crop residue-associated bacteria; B: crop residue-associated fungi; C: wheat spikes-associated bacteria; D: wheat spikes-associated fungi. $T_{cr}0$, $T_{cr}1$ and $T_{cr}2$ indicate the different time points at which the crop residue samples were collected, while $T_{sp}0$, $T_{sp}1$, $T_{sp}2$ and $T_{sp}3$ indicate the various time points at which the wheat spikes samples were collected. ..... 48

**Figure 3.7**. OTU richness in different tissues, among treatments and over time. A: bacteria in residue; B: bacteria in wheat spikes; C: bacteria in wheat kernels; D: fungi in crop residue; E: fungi in wheat spikes; F: fungi in wheat kernels. $T_{cr}0$, $T_{cr}1$ and $T_{cr}2$ indicate the different time points at which the crop residue samples were collected, while $T_{sp}0$, $T_{sp}1$, $T_{sp}2$ and $T_{sp}3$ indicate the various time points at which the wheat spikes samples were collected. The Trt1 (Control), Trt2 (*T. gamsii* T6085 applied on spikes at anthesis), Trt3 (*T. gamsii* T6085 applied in soil on crop residue) and

Trt4 (*T. gamsii* T6085 applied both in soil on crop residue and on spikes at anthesis) indicates the four different treatments we used in the experiment. The box plots demonstrate the 1st quartile, median, 3rd quartile and the outliers of the data set. Different letters indicate statistically significant difference ($p<0.05$). The OTU richness values were not significantly different among different treatments in crop residue, wheat spikes and wheat kernels. However, there were significant changes in species richness between different time points in some tissues (ANOVA with Tukey HSD, $p<0.05$). ..... 50

**Figure 3.8**. Shannon diversity index for microbial communities associated with different tissues, among treatments and over time. A: bacteria in residue; B: bacteria in wheat spikes; C: bacteria in kernels; D: fungi in residue; E: fungi in wheat spikes; F: fungi in kernels. $T_{cr}0$, $T_{cr}1$ and $T_{cr}2$ indicate the different time points at which the crop residue samples were collected, while $T_{sp}0$, $T_{sp}1$, $T_{sp}2$ and $T_{sp}3$ indicate the various time points at which the wheat spikes samples collected. The Trt1 (Control), Trt2 (*T. gamsii* T6085 applied on spikes at anthesis), Trt3 (*T. gamsii* T6085 applied in soil on crop residue) and Trt4 (*T. gamsii* T6085 applied both in soil on crop residue and on spikes at anthesis) indicates the four different treatments we used in the experiment. The box plots demonstrate the 1st quartile, median, 3rd quartile and the outliers of the data set. Different letters indicate statistically significant difference ($p<0.05$). The Shannon index values did not change due to the treatments but did change over time (ANOVA with Tukey HSD, $p<0.05$). ... 52

**Figure 4.1**. The pRM-eGFP vector (8414 bp) contains the egfp gene that encodes for enhanced GFP and the ble gene, which confers the resistance to phleomycin. The constitutive expression of the egfp gene is regulated by the *PgpdA* promoter. The ble gene is under the control of the *PtrpC* promoter and the *TtrpC* terminator. The vector backbone consists of the Kanamycin resistance gene (*KanR*). The LB and RB indicate the left border and the right border of the T-DNA region, respectively. ..... 68

**Figure 4.2.** The growing Agrobacterium tumefaciens cells in LB media after transferring the pRM-eGFP vector into the bacterial cells by electroporation. The bacterial colonies appeared within 3 days of incubation at 30 ℃ in the dark. ..... 74

**Figure 4.3**. The growing mJN3 (first row) and JN3 (second row) isolates at 4 different concentrations of phleomycin A and E: 0 µg/mL, B and F: 25 µg/mL, C and G: 50 µg/mL and D and H: 100 µg/mL in V8 media. The cultures were incubated at room temperature for 10 days under fluorescent light. The mJN3 showed a minimal growth at 25 µg/ml, and its development was completely inhibited at 50 µg/ml and 100 µg/ml concentrations. All tested concentrations of phleomycin inhibited the growth of JN3 for 10 days. ..... 75

**Figure 4.4**. The gel image demonstrates the PCR amplified product of the egfp gene from the extracted DNA of transformed *L. maculans* isolates. A: mJN3gfp isolates; B: JN3gfp isolates. PC: positive control: NC: Negative control. The bands that are similar to the positive control were within the range of 600bp-700bp. A 100-1500 bp ladder was used for reference..... 76

**Figure 4.5**. Fluorescent microscopic images of mycelia of different GFP expressing *L. maculans* transformants after inoculating into cotyledons of Westar under the EVOS M5000 microscope using the 1.25× objective. The images were taken after 11 dpi. A: JN3gfp1; B: JN3gfp2; C: JN3gfp3; D: JN3gfp4; E: JN3gfp5; F: mJN3gfp1; G: mJN3gfp2; H: mJN3gfp3; I: mJN3gfp4; J:

mJN3gfp5; K: mJN3gfp6; L: mJN3gfp7; M: mJN3gfp8; N: mJN3gfp9; O: mJN3gfp10; P: Negative control. The scale bar represents 2 050µm. ..... 78

**Figure 4.6**. The mycelia and the pycnidiospores transformed *L. maculans* isolates with egfp gene. A: mJN3gfp2 and B: JN3gfp2. The slides were prepared using the slide culture technique. The images were taken after 10 days of incubation of the slide cultures at room temperature under the fluorescent light. The images were taken under the EVOS M5000 microscope using the 40× objective. The images in the left side were taken using the GFP channel and the right side were taken using the TRANS channel. The scale bar represents 2 050µm. ..... 79

**Figure 4.7**. The mycelial growth of the transformed *L. maculans* isolates with egfp gene. A: mJN3gfp2 after 11 dpi; B: JN3gfp2 after 11 dpi; C: mJN3gfp2 after 14 dpi; D: JN3gfp2 after 14 dpi; E: mJN3gfp2 after 17 dpi; F: JN3gfp2 after 17 dpi. The images were taken under the Zeiss Axio Imager Z1 Microscope using the 5× objective. The scale bar represents 200µm. ..... 80

**Figure 4.8**. The mycelial growth of transformed *L. maculans* isolates; mJN3gfp2 and LmGFP isolates in *B. napus* cotyledons after 11 and 14 dpi. A and B: mJN3gfp2 after 11 dpi; C and D: mJN3gfp2 after 14 dpi; E and F: LmGFP after 11 dpi; G and H: LmGFP after 14 dpi. The images were taken using two microscopes: the EVOS M5000 microscope using the 1.25× objective [A, C, E and G (scale bar represent 2 050µm)] and the Zeiss Axio Imager Z1 Microscope using the 5× objective [B, D, F and H (scale bar represent 200µm)]. ..... 81

## ABSTRACT

Alukumbura, Arshani. M.Sc., The University of Manitoba, December, 2021. Wheat-associated bacterial and fungal communities during the interaction of *Fusarium graminearum* and *Trichoderma gamsii* T6085 and infection of a CRISPR/Cas9 derived green-fluorescent protein labeled *Leptosphaeria maculans* strain on *Brassica napus*. Major professors: Dr. Dilantha Fernando and Dr. Matthew Bakker.

The microbial diseases in agriculturally important crops have become a critical problem in countries all around the world. The plant diseases caused by various pathogens are unique and require different management strategies to prevent spreading. The Fusarium head blight (FHB) disease in wheat and the blackleg disease in canola are two major diseases that have been reported all around the world. While the primary causative agents of FHB are *Fusarium graminearum* and *Fusarium culmorum,* the primary causative agent of the blackleg disease is the *Leptosphaeria maculans*. All these pathogens are Ascomycetes and feed on decaying plant material. They can survive throughout the winter within dead plant material and initiate infections during spring and summer. The first objective of the current work was to analyze the microbiome associated with wheat plants and to evaluate the effectiveness of the biocontrol method for FHB management in wheat. This work examined the impact of inoculation with *Trichoderma gamsii* strain T6085 as a biocontrol agent on the natural bacterial and fungal community associated with wheat plants. The effect of *T. gamsii* T6085 on the microbial communities in wheat tissues was minimal. However, the current *T. gamsii* T6085 application method needs to be improved to have a good inhibition in the growth of *F. graminearum.* The second objective of this work was to understand the behaviour of a mutant *L. maculans* isolate generated through the CRISPR/Cas9 gene engineering technique. The mutant and its wild-type progenitor were tagged with the *egfp* gene, which expressed the green fluorescent reporter protein. The transformation of *L. maculans* with the *egfp* gene led to a decrease in their pathogenicity. According to the results, the mutant *L. maculans* isolate can colonize the plant tissues, but the plant defence responses inhibit its growth through a hypersensitive reaction.

# 1.0 GENERAL INTRODUCTION

The microorganisms and plants have been co-evolved during their evolution, changing genetic traits of each other enforced by natural selection. The interaction between the plants and their surrounding microbiota has contributed a lot to the earth's diversity. However, the beginning of the agriculturally based societies has made a massive impact on the natural interaction between the plants and the harmful microbes. The agricultural environments are less diverse and simple eco-systems which have created a favorable environment for the pathogens to adapt rapidly (Occhipinti, 2013). Therefore, the plant diseases caused by pathogenic microbes in domesticated crops have been a critical issue since the beginning of agricultural societies (McDonald and McDermott, 1993).

The diseases caused by plant pathogens have led to significant yield losses in various crops worldwide, creating a massive impact on the agricultural and food industries. Nevertheless, the global food demand is increasing rapidly. It is predicted that the global population will reach 9 billion by 2050. Therefore, the global food supply needs to be increased by 50% to supply a sufficient amount of food to feed the whole population (Jaggard et al., 2010; Tilman et al., 2011). Thus, the management of diseases associated with agriculturally important crops has become a key factor in the worldwide crop industry. These various kinds of plant pathogens have given rise to many catastrophic events in history. For instance, the Irish potato famine in the 1840s was driven by the oomycete *Phytophthora infestans,* causing the potato late blight disease and led to 1.5 million deaths (McDonald and McDermott, 1993; Yoshida et al., 2013). Among the various diseases caused by various microorganisms, fungi also play a vital role in plant pathology and have led to massive yield losses in various agricultural crops. Therefore, taking advanced measures in preventing fungal diseases in agriculturally important crops is vital.

This study mainly focused on two major fungal pathogens *F. graminearum* and *L. maculans* that have caused substantial yield losses in Canada's two major crops: wheat and canola respectively. Both of these crops play a vital role in the Canadian economy. The first chapter of this work focused on the biocontrol of FHB disease in wheat. The fungus *T. gamsii* T6085 has been identified as a potential biocontrol agent to prevent the FHB in wheat. However, the non-target effect on the

microbiome associated with the wheat plant due to the application of this biocontrol agent has not been understood yet. Therefore, the work evaluated the microbial community associated with the wheat production environment and their variation due to the *T. gamsii* T6085 application. The second chapter focused on the blackleg disease in canola. The primary causative agent of this disease is *L. maculans*. The study explored a mutant *L. maculans* isolate that has lost its pathogenicity towards the canola plant due to a random mutation. This mutant *L. maculans* is a potential isolate to discover genes essential for the fungus to infect canola plants. Therefore, the objective of the study was to investigate the mutant fungus's infection process phenotypically by labelling it with a green fluorescent protein (GFP) marker. The ultimate target of the work was to expand the understanding of *F. graminearum*-wheat and the *L. maculans*-canola pathosystems to develop proper management strategies in the future.

# 2.0 LITERATURE REVIEW

## 2.1 Plant diseases caused by fungal pathogens

Various diseases caused by different fungal pathogens are prevalent in agricultural fields. The extensive cultivation of different crops has led to the formation of virulent fungal populations worldwide. Due to the increased demand for plant-based foods with the growing population, taking advanced measures to prevent plant diseases has become an essential aspect of the agricultural industry. This work focused on two important fungal pathogens, *F. graminearum*, and *L. maculans* that cause two important diseases, FHB in wheat and blackleg disease in canola respectively. In this review, the interaction between *F. graminearum*-wheat and *L. maculans*-canola has been discussed independently.

## 2.2 Wheat - *Fusarium* interactions and FHB management

*Fusarium* spp. are fungal pathogens that interact with wheat generating several adverse conditions within the plants. The pathogen infects different plant tissues, from root to kernels, and causes various diseases, including crown and foot rot (Scherm et al., 2011), seedling blight (Dal Bello et al., 2002), and FHB (Gilbert and Tekauz, 2000). These *Fusarium* prompted diseases impose significant constraints on wheat production, and thus, effective control of this pathogen is crucial. Biological control is an eco-friendly disease management strategy, and it has been widely used to mitigate numerous diseases in cereal crops. The activity of biocontrol agents can change the microbial community associated with the wheat plant. One part of this study mainly focused on the microbiome associated with the wheat plant and the impact of the biological control agent on the wheat-associated microbiome during the mitigation of FHB disease in wheat.

### 2.2.1 Wheat

Wheat (genus *Triticum*) is a dominant cereal plant in temperate countries. It is primarily grown in the northern hemisphere, while wheat cultivation is comparatively lower in the southern hemisphere. In addition, China is the leading wheat-producing country, followed by India, Russia, the USA, France, Australia, and Canada. Wheat produced in major wheat-growing countries accounts for more than 60% of total wheat production globally (Briggle and Curtis, 2015; Figueroa et al., 2018; Index Mundi, 2015; Shewry, 2009). Additionally, the main application of wheat grains

is the production of human foods and livestock feeds. Due to the presence of the protein named gluten, wheat grain gives softness and unique characteristics to wheat-based food products. Moreover, wheat cereal has a high nutritional value as it contains essential amino acids, minerals, vitamins and dietary fibre. Further, the antioxidants in bran or whole wheat are beneficial for human health and prevent diseases such as cancer (Baublis et al., 2013; Fardet, 2015; Laddomada et al., 2015). The most broadly cultivated wheat species are bread wheat (*Triticum aestivum*) and durum wheat (*Triticum durum*). Bread wheat is mainly employed in producing bread, while the durum wheat is the main ingredient in pasta and noodles (Edwards et al., 2001). Due to the unique characteristics of wheat grain, it has become an essential cereal crop in the agricultural and food industry.

Wheat is the primary staple food in many countries around the world. Therefore, the utilization of wheat cereal in 2020/21 was 761.9 million tonnes while the production was 776.5 million tonnes. Due to increased demand for wheat as a cereal, a contraction in wheat inventories is expected in 2021/22 (Food and Agriculture Organization of the United Nations, 2021). Nevertheless, various wheat-associated diseases have negatively impacted wheat production on both aspects of quality and yield. Diseases caused by different fungal pathogens are frequent in wheat and have made a significant constraint to wheat production. FHB, leaf spot diseases, powdery mildew, and wheat rust are the most important fungal diseases affecting wheat (Aboukhaddour et al., 2020). Further, at least twenty different fungi that are pathogenic to wheat have been identified from the Canadian prairies (Dickson, 1957). Among these various fungal pathogens, *Puccinia* spp. (stem rust), *Fusarium* spp. (FHB) and *Tilletia* sp. (common bunt) are considered the most vital due to the significant economic losses triggered by these pathogens (Aboukhaddour et al., 2020). Hence, wheat-associated disease management has become a primary concern in the cereal industry as supplying a sufficient amount of wheat cereal is becoming a risk with the growing population.

### 2.2.2 The Fusarium head blight disease in wheat

Fusarium head blight is a fungal disease commonly seen in several cereal crops, including wheat, barley, and oat (McMullen et al., 2012; Mesterházy, 1995; Tekauz et al., 2010). The causative agents for this disease are the fungal pathogens belonging to the genus *Fusarium* and the most prevalent species infecting wheat are *F. graminearum* and *F. culmorum* (Walter et al., 2010).

Moreover, the weather is a primary contributing factor for FHB progression. Warm and humid conditions favour FHB infection and development in wheat. Nevertheless, the environmental conditions influence differently on different *Fusarium* species. For instance, warm and humid conditions favour the progression of *F. graminearum*, while cool and moist conditions favour the infection of *F. culmorum* (Xu et al., 2007). In addition, there are weather-based forecasting systems developed by researchers that are used to predict FHB diseases risk in farmers' fields which are helpful for farmers to decide effective management strategies (Prandini et al., 2009).

FHB is a monocyclic disease. The main source of primary inoculum of the disease is crop residue. *Fusarium* spores overwinter within crop residue. *Fusarium* spp. can infect wheat heads from the flowering stage to the hard dough stage of wheat kernels. However, the primary infection occurs during the flowering period and causes more severe damage (Figure 2.1) (Leplat et al., 2013; Trail, 2009). Moreover, fungal growth stimulants like choline and betaine in wheat anthers promote the infection of *Fusarium* spp. Therefore, wheat anthers act as a perfect entry for *Fusarium* to infect. *Fusarium* can invade wheat tissues either passively through natural openings like stomata or actively by the direct penetration of plant tissues. During the invasion of wheat tissues, the fungi initially colonize the outer surfaces of anthers and glumes, followed by an extension towards the sensitive organs like ovaries. Further, the pathogen spreads from one spike to another through rachis. During the infection, the fungal mycelium colonizes the intercellular spaces of the host tissues, disintegrates host organelles, and collapses the cytoplasm using its enzymes and toxins (Alconada et al., 2019; Kang and Buchenauer, 2000; Strange et al., 1974; Walter et al., 2010).

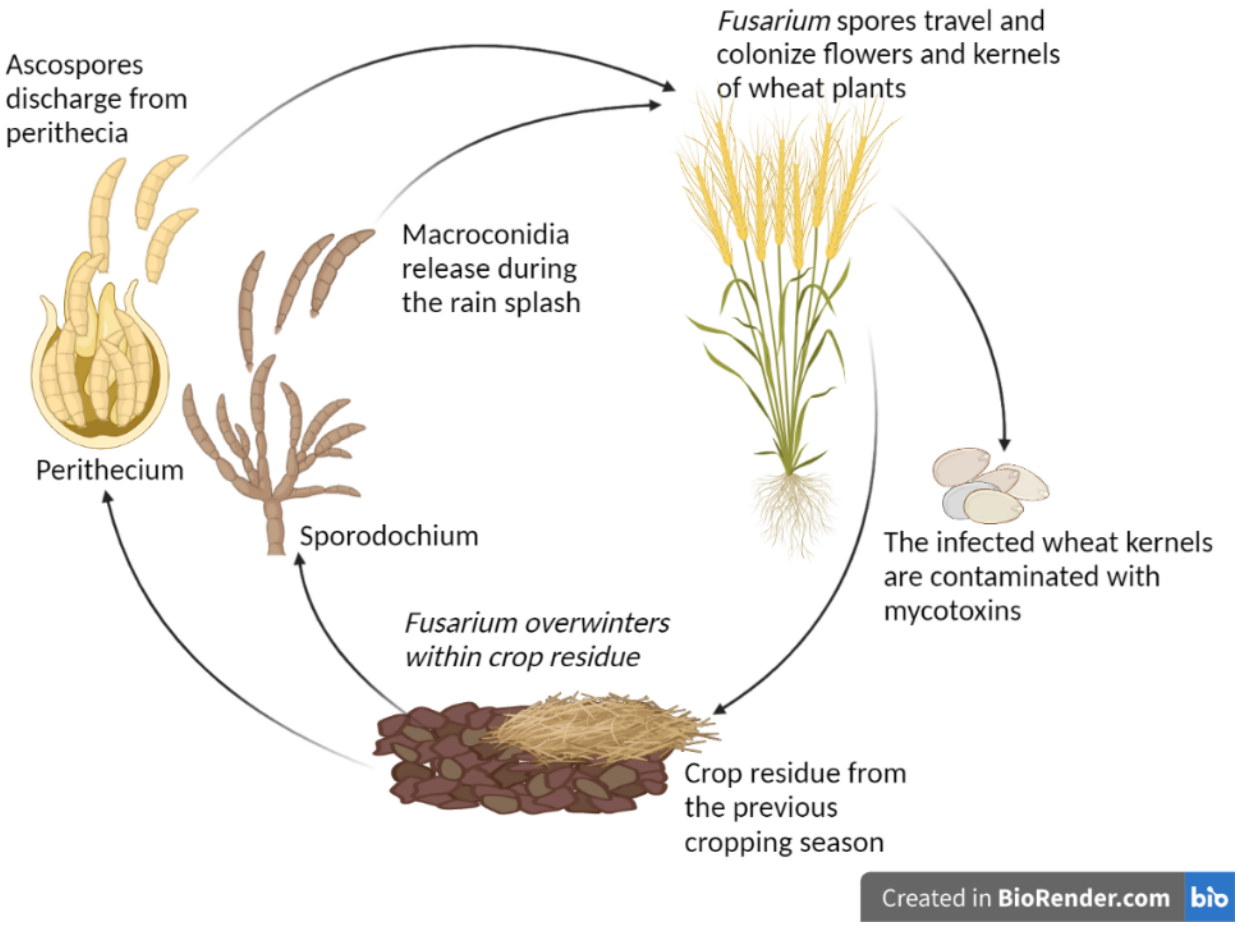



**Figure 2.1.** The life cycle of *F. graminearum*. *F. graminearum* overwinters within crop residue and mainly infects wheat plants during anthesis. *F. graminearum*'s sexual (ascospores) spores are released from perithecia, and the asexual (macroconidia) spores are released from sporodochia. The ascospores and macroconidia infect wheat plants from the flowering stage to the hard dough stage of wheat kernels contaminating them with mycotoxins.

The main symptom of FHB disease is the premature bleaching of wheat heads. The disease severity depends on the time of *Fusarium* infection. For instance, the infection just after the flowers' emergence leads to the kernel's abortion. The infections that occur later in the flowering period give rise to diseased wheat kernels that are shrivelled in appearance. Additionally, *Fusarium* infected wheat kernels are contaminated with the toxins released by the fungus during the infection (Birr et al., 2020). The toxins released by *Fusarium* spp. are fungal secondary metabolites known as mycotoxins. The major classes of mycotoxins released by *Fusarium* species are fumonisin and trichothecene. Members of the *Fusarium fujkuroi* species complex are the major fumonisin producers, while members of the *F. graminearum* species complex are the major trichothecene

producers (Lee et al., 2015). Furthermore, the most important mycotoxins related to FHB are categorized as type B trichothecenes. Type B trichothecenes include deoxynivalenol (DON), nivalenol (NIV) and their derivatives, 3-acetyl deoxynivalenol (3ADON), 15-acetyl deoxynivalenol (15ADON) and 4-acetyl nivalenol (4ANIV). Moreover, DON is the most prevalent mycotoxin associated with FHB in Canada (Oghenekaro et al., 2021). Additionally, the uptake of mycotoxin-contaminated foods can lead to many health risks in humans and animals. For example, these toxic compounds can cause misfunctioning in the immune system, intestine, cell signalling, reproduction, and lead to the development of cancers (Pestka, 2010). Therefore, governments have set standards to minimize the health risk due to mycotoxin contamination in cereals. In Canada, the maximum DON level that can be present in wheat is 2 ppm (Canadian Grain Commission, 2009). Therefore, *Fusarium* infection can cause both quality and yield losses in wheat and a better understanding of the disease progression is crucial to mitigate the disease.

### 2.2.3 Plant microbiome interactions

The plant-associated microbial community is considered the second genome of a plant (Berendsen et al., 2012). Fossil and sequence evidence suggest that the symbiotic association between a phototroph and a fungus may have facilitated the colonization of land by eukaryotes on earth. Even though the periods are hypothetical, it is assumed that these associations could have started 1000 million years ago (Heckman et al., 2001). The plant-associated microbial community has been classified into three categories, which are rhizosphere (microbes associated with plant roots), phyllosphere (microbes associated with aerial surfaces of plants) and endosphere (microbes associated with internal plant tissues) microbial communities (Turner et al., 2013).

The rhizosphere is the soil linked to the plant root system, and it is rich with nutrients due to the root exudates. The rhizosphere is prolific with numerous bacteria, fungi, protists and nematodes, and these microbes can be either beneficial or pathogenic to plants (Ali et al., 2017; Chaparro and Reardon, 2014; Gao et al., 2019). According to Egamberdieva et al., (2008), the rhizosphere can hold up to $10^{11}$ bacteria per gram of root. In the same study, they isolated several plant growth-promoting bacterial strains from wheat rhizosphere. In addition, the phyllosphere microbiome involves the microbes associated with the aerial surfaces of plants. The phyllosphere has lower availability of nutrition for microbes compared to the rhizosphere. However, according to current

studies, there can be $10^7$ cells per $cm^2$ of a leaf. The phyllosphere microbiome also consists of different microbes, including bacteria, fungi, protists, and nematodes, and these microbes interact with plants in various ways. Thus, these interactions can also be either beneficial or pathogenic to plants (Lindow and Brandl, 2003; Turner et al., 2013). Apart from that, the endosphere-associated microbes are referring to the microorganisms that reside within the plant tissues. These microbes are important for plant health and reside within the plant tissues as endophytes (Jia et al., 2016; Podolich et al., 2014). The majority of endophytes are non-pathogenic, but they can occasionally be pathogenic to plants depending on the environmental conditions and plant genotype (Turner et al., 2013).

As introduced above, the microbiome interacting with different parts of the plant can be beneficial, neutral, or detrimental to the plant. Further, beneficial microbes can act in various ways. They can increase plant growth; help in stress tolerance and enhance the nutrient uptake of plants. For instance, *Pseudomonas putida* can enhance the shoot growth, root growth, biomass, and the grain production of wheat plants under heat stress (Ali et al., 2011). In addition, *Trichoderma longibrachiatum* is a plant beneficial fungus that can promote wheat growth and tolerance to salt stress (Zhang et al., 2016). Also, the bacterial species belonging to the genus *Bacillus* can increase the phosphorus and zinc uptake of crops. These bacteria dissolve the insoluble phosphorous and zinc compounds and make them readily available for plants to intake (Ahmad et al., 2019; Glick, 2012). In addition to that, there are numerous bacteria and fungi that increase the resistance of plants towards various pathogens. For example, *Bacillus subtilis*, *Pseudomonas fluorescens*, *Pantoea agglomerans* and *Acinetobacter lwoffi* have efficiently protected the grapevine from the gray mould disease caused by *Botrytis cinerea* by initiating plant defence responses. Further, all these bacterial strains have shown mycoparasitic activity against pathogens (Trotel-Aziz et al., 2008). Hence, these unique beneficial interactions between plants and the different microbes can be useful in agriculture.

### 2.2.4 Biological control for plant disease management

There are various management strategies that are currently used by farmers to control plant diseases. The main strategies used to manage FHB in wheat include crop rotation, using moderately resistant cultivars, timely application of fungicides, risk monitoring and soil tillage.

However, the integrative management approach is the best way to control diseases (Blandino et al., 2012; Shah et al., 2018). Biological control is a promising strategy that can be incorporated into integrated management practices in FHB management. This strategy employs single or multiple beneficial microorganisms for disease control. The microorganism that is used for biocontrol is known as a biocontrol agent. The interactions between biocontrol agents and pathogens occur in natural environments. However, these naturally occurring interactions can be integrated into agricultural practices in more advanced ways. Farmers have been using biological control strategies indirectly since ancient times. For instance, agricultural techniques such as intercropping, fallowing, manure application, and crop rotation, can indirectly influence plant pathogens' survival and disease progression. These techniques change soil conditions such as soil nutrient availability, soil pH, and soil temperature which impact the microbiome residing within the rhizosphere. Without proper soil conditions for survival, pathogens can fail in infecting the host. In addition to that, the microbes antagonistic to the pathogens can be introduced, and these microbes can directly reduce the pathogen inoculum in the soil (Lewis et al., 1991).

Numerous bacterial and fungal species have been identified as biocontrol agents against various plant diseases. These microbes use different mechanisms to inhibit other microorganisms that are living in the same niche as them. These mechanisms include mycoparasitism (John et al., 2010), antibiosis (Leifert et al., 1995), cell wall degradation (Ueki et al., 2017), induced plant resistance (Abo-Zaid et al., 2020), and competition for space and nutrition (Filonow, 2010). These biocontrol mechanisms in fungi and bacteria are their survival mechanisms in nature. Nevertheless, these natural instincts are helpful in agricultural disease management. For instance, *Bacillus amyloliquefaciens* strain FZB42 possesses gene clusters responsible for producing lipopolypeptides and polyketides. These are secondary metabolites, and these compounds have antibacterial, antifungal, and nematocidal properties. Thus, this strain of *B. amyloliquefaciens* has a high potential in the biological control of plant diseases due to the secretion of a wide range of antimicrobial compounds (Chen et al., 2009). In addition, the *Streptomyces* is the most extensive antibiotic-producing genus in the world. This group of bacteria has shown the potential to control different plant pathogens, including *Pythium ultimum*, *Rhizoctonia solani* and *Fusarium oxysporum* (Abd-Allah, 2001; LeBlanc, 2021; Yuan and Crawford, 1995). For instance, *Streptomyces* sp. strain SNL2 is a promising biocontrol agent against the root rot disease in

tomatoes caused by *F. oxysporum*. The bacteria have significantly reduced the disease incidence in tomato plants. Another beneficial role of the SNL2 strain was plant growth promotion (Goudjal et al., 2016). Additionally, several fungal and bacterial species have been identified as potential biocontrol agents to manage FHB in wheat. Some of them includes, *Pseudomonas fluorescens*, *Sarocladium zeae*, *Bacillus amyloliquefaciens* and *T. gamsii*. All these bacterial and fungal species have shown the potential to significantly reduce the FHB disease symptoms caused by *F. graminearum* (Crane et al., 2013; Kemp et al., 2020; Khan and Doohan, 2009; Matarese et al., 2012).

The most crucial aspect of biological control is its potential in replacing chemical pesticides. The use of synthetic fungicides and bactericides is the most effective way of controlling plant diseases caused by pathogenic microorganisms. However, the extensive use of these chemicals leads to pesticide resistance within pathogen populations (Ishii, 2006). In addition to that, the organic and inorganic compounds in these synthetic materials can pollute the environment (Guida et al., 2008). For example, Cu-based contaminations in agricultural fields are a major problem currently. The utilization of fungicides containing Cu can change the microbiome in soil and contaminate the aquatic environment and groundwater. In addition, a high accumulation of Cu can negatively affect both plant and human health (Oliveira-Filho et al., 2004; Michaud et al., 2008; Šantić et al., 2005). Another major drawback of using chemical pesticides is its negative effects on beneficial microorganisms and this impact on non-pathogenic microorganisms from synthetic fungicides could be broad (Yang et al., 2011). The consistency of the microbiota in the natural environment is essential for plant health. Therefore, using alternative methods like biocontrol to mitigate plant diseases is critical for sustainable agriculture.

#### 2.2.4.1 Genus *Trichoderma*

The *Trichoderma* spp. are the most applied biocontrol agents in the world. The genus *Trichoderma* was first reported in 1794 by Christiaan Hendrik Persoon, a botanist, and a mycologist in South Africa (Bisby, 1939). In the past, the *Trichoderma* species had two nomenclatures. The anamorph stage of the fungus was known as *Trichoderma*, while the teleomorph stage was known as *Hypocrea* (Samuels, 2006). However, the use of different names for different morphs of fungi was ended in 2011. Due to the common usage of the *Trichoderma* over *Hypocrea*, the *International*

*Code of Nomenclature for algae, fungi, and plants* (ICN) decided to give priority to *Trichoderma* (Bissett et al., 2015). *Trichoderma* are ubiquitous soil fungi, widely found in soil and decaying wood (Samuels, 1996). In the past, it was believed that *Trichoderma* spp. are non-endophytes, but recent findings showed that some of the *Trichoderma* species are plant endophytes (Samuels, 2006; Rodríguez et al., 2021). For instance, Evans et al., (2003), found several *Trichoderma* species in healthy cocoa stems and pods as endophytes, including *Trichoderma harzianum*, *Trichoderma hamatum*, and *Trichoderma virens*. Interestingly, *T. harzianum* is one of the most commonly isolated *Trichoderma* species as well (Samuels, 2006).

*Trichoderma* spp. can be commonly found in soil and organic matter at any altitude. However, their distribution varies from species to species. While some of the *Trichoderma* species are cosmopolitan, others are restricted to certain areas in the world. For instance, *T. harzianum* and *Trichoderma asperellum* are two examples of *Trichoderma* species showing worldwide distribution (Chaverri et al., 2003; Samuels, 2006). Besides, *T. longibrachiatum* is commonly seen in America, Africa, and Europe but not in Australia and Asian countries except India (Turner et al., 1997). Further, *Trichoderma stromaticum* can be found only in tropical regions of America (Samuels et al., 2021). Moreover, *Trichoderma* species prefer moist and cool temperatures; however, their optimum temperature can also vary among species. For example, *Trichoderma polysporum* and *Trichoderma minutisporum* are widely distributed in cold climate regions. Yet, *Trichoderma viride* and *Trichoderma aureoviride* are limited in cold temperatures (Samuels, 2006). In general, *Trichoderma* spp. are common soil fungi that are widely spread all around the world.

As *Trichoderma* species are non-pathogenic and environmentally friendly organisms, they have various commercial applications. The species of *Trichoderma* have toxin tolerance ability and high biodegradation capability. Hence, *Trichoderma* spp. can be used to biodegrade several chemical compounds, including cyanide (Zhou et al., 2007) and polyphenolic compounds (Harman et al., 2004), polycyclic aromatic hydrocarbons (Zafra and Cortés-Espinosa, 2015), and carbendazim (Sharma et al., 2016). Moreover, *Trichoderma* species are commercially available as bio-fungicides which are alternatives to chemical fungicides. In addition to the fungicidal activity, *Trichoderma* species can promote plant growth and increase crop yield which indirectly benefits

farmers when using the biocontrol agents (Woo et al., 2014). Further, the various enzymes released by *Trichoderma* species are utilized in different industries. For instance, *T. longibrachiatum*-based xylanase production has proven effective during fabric bioprocessing in the textile industry (Abd El Aty et al., 2018). In addition to that, the cellulase enzymes produced by *Trichoderma* spp. are utilized in various industries such as cotton processing in the textile (Heikinheimo, 2002), paper (Dienes et al., 2004), and detergent industries (Iqbal et al., 2011). Due to the vast industrial applications, the genus *Trichoderma* is popular around the world.

#### 2.2.4.1.1 *Trichoderma gamsii* as a potential biocontrol agent

*Trichoderma gamsii* has been known for several years as a promising biocontrol agent. It is a plant growth promoter and a potential biocontrol agent against the FHB disease in wheat (Sarrocco et al., 2021). *T. gamsii* is a non-pathogenic, plant symbiotic fungus. It is an endophyte that colonizes the plant roots. During the colonization, the fungus invades the radial cortex without reaching the vascular system of the plant. The endophytic colonization of plant roots by *T. gamsii* induces the plant's systemic resistance and helps the plant to defend itself against pathogens (Rinu et al., 2014; Sarrocco et al., 2021).

The fungus can grow within the temperature range of 4 ℃ - 30 ℃ while the optimum growth temperature is 25 ℃. Further, it can grow within a pH range of 2.0 - 13.5, and the optimum pH for its growth is 4 – 6 (Rinu et al., 2014). Moreover, *T. gamsii* promotes plant growth by increasing the availability of nutrients in the soil to be taken up by plants. For instance, phosphorous is an essential macronutrient for plant growth and development. However, as phosphorous is highly reactive, it quickly precipitates within the soil, making it unavailable for plants to consume. Interestingly, *T. gamsii* is capable of converting soil insoluble phosphates into a soluble form to facilitate nutrient uptake by plants. The soluble phosphates can be efficiently taken up by plants, consequently enhancing their growth (Bononi et al., 2020; Rinu et al., 2014). Moreover, *T. gamsii* can mycoparasitize other fungi by direct attack. They coil around the hyphae of other fungi and cause physiological disorders. Several researchers have observed these interactions using scanning electron microscopy (Chen et al., 2016; Matarese et al., 2012). Its chitinase activity can effectively inhibit the growth of other pathogenic fungi. When *T. gamsii* is in contact with a pathogen, the chitinase encoding genes are upregulated. This release of chitinase contributes to the mycoparasitic

activity of *T. gamsii*, which helps them to prevent the growth of other fungi that share their environment (Matarese et al., 2012; Rinu et al., 2014). In addition, *T. gamsii* releases different volatile and non-volatile organic compounds, which are fungal secondary metabolites. Some of these compounds have been identified as toxic to other fungi. Some of the volatile organic compounds secreted by *T. gamsii* include methanethiol, dimethyl disulfide, mesitylene, fluorene, and ketones (Chen et al., 2016; Li et al., 2019). Therefore, *T. gamsii* strains are endophytic plant beneficial fungi.

T6085 strain of *T. gamsii* was first selected as a potential biocontrol agent against FHB out of 100 *Trichoderma* isolates (Matarese, 2010). The unique features of this particular strain over the other *Trichoderma* spp. were its ability to grow in the presence of DON and to reduce the DON contaminants produced by *Fusarium* spp. In the work of Matarese et al., (2012), they have co-inoculated *F. graminearum* and *F. culmorum* with *T. gamsii* strain T6085 in separate Petri dishes using rice kernels as the substrate for fungal growth. During this experiment, *T. gamsii* T6085 reduced the amount of DON produced by *F. graminearum* and *F. culmorum* by almost 92% after 14 days of incubation. In addition to that, *T. gamsii* T6085 can endophytically colonize wheat roots without causing any disorders to wheat plants. Further, when applied to wheat residue remaining in wheat fields, *T. gamsii* T6085 strain has significantly reduced *F. graminearum* content and perithecia development within crop residue (Sarrocco et al., 2021). The field trial of the present study also showed a significant reduction in FHB disease index and disease severity when *T. gamsii* T6085 was applied on to wheat spikes during anthesis ($p<0.05$) (Alessandro, 2019). Similarly, when T6085 was applied to the wheat heads, FHB disease severity was reduced by 57% (Sarrocco et al., 2013). Therefore, the *T. gamsii* T6085 strain is a potential biocontrol agent against the FHB in wheat.

### 2.2.5 Impact of biocontrol agents on pathogens

The application of a biocontrol agent can impact plant pathogens in various ways. Due to the extensive growth of the biocontrol agent, there can be a deficiency in nutrients available for the pathogen to consume. Nutrient deficiency can lower the pathogen's activities. For instance, when *T. harzianum* was applied on rhizosphere soil, the chlamydospore germination rate of *F. oxysporum* was lower than the control treatment (Sivan et al., 1989). In addition to that, biocontrol

agents can affect pathogen germination and colonization through competition. This can be seen in an example with cucumber and the pathogenic oomycete *Pythium aphanidermatum* that causes the damping-off disease in cucumber. Extensive prior colonization of cucumber roots by biocontrol bacteria reduces the germination and root colonization of *P. aphanidermatum* (Elad et al., 1987). Some fungal biocontrol agents directly attack other fungi mechanically, and they can degrade the cells of other microbes through chemical reactions. For example, *T. harzianum* can kill the cells of the fungus, *B. cinerea,* within 48 hours of contact. *T. harzianum* penetrates the hyphae of *B. cinerea* through chemical and mechanical disruption, and it can degrade the fungal cells through chitinolytic enzymes. These reactions restrain the pathogen growth (Bélanger et al., 1995). The interactions mentioned above between biocontrol agents and pathogens inhibit pathogen development during crop growth.

### 2.2.6 Impact of biocontrol agents on the broader microbial community

A biocontrol agent is a microbe that has unique characteristics to suppress the growth of specific pathogens. However, similar to other disease management strategies, biological control can also change the natural microbiome associated with plants. The biocontrol agent's mechanism to survive in their environment can be detrimental to numerous fungi and bacteria, including the target pathogen. Therefore, before applying a biocontrol agent in disease management, it is crucial to understand their impact on the microbial community structure. Sometimes, incorporating a biocontrol agent in the field can change the microbial community structure associated with the host plant. Some of these community-level changes are temporal. For example, when *B. amyloliquefaciens* was applied to control *R. solani* in lettuce, there was a shift in the rhizosphere bacterial community. However, this shift was not found to be durable (Chowdhury et al., 2013). Similarly, when *P. fluorescens* was applied to the cucumber rhizosphere, the bacterial community showed a transient change for a short period (Yin et al., 2013). However, sometimes this effect can last long, and there could be a significant change in the abundance of certain non-target microbes. Some biocontrol agents increase the bacterial and fungal diversity of the environments to which they are applied and change the relative abundance of certain organisms (Erlacher et al., 2014; Scherwinski et al., 2007). In addition to that, some biocontrol agents take over the place of the most abundant microbes. For example, *Paenibacillus* spp. are dominant bacteria in wheat roots. The treatment of *Streptomyces* sp. as a biocontrol agent decreased the relative abundance of

*Paenibacillus* in wheat roots (Araujo et al., 2019). In the same study, a shift was seen in several other microbes, including *Actinoplanes*, *Pedobacter*, *Mycoplana*, *Ralstonia*, etc., due to the presence of the biocontrol agent. Thus, there could be non-target effects of the biocontrol agent activity on the microbiome, and these impacts can be either transient or persistent.

However, not all biocontrol agents influence the associated microbial communities. According to current literature, some biocontrol agents did not create measurable changes in the broader microbial community during their biocontrol activity (Perazzolli et al., 2014; Scherwinski et al., 2007; Wei et al., 2016). Sometimes, the activity of a biocontrol agent can compensate for the change in the microbiome due to the growth and infection of the pathogen since the pathogens can similarly alter the rhizosphere, endosphere, and phyllosphere microbial communities. For example, *R. solani* is a phytopathogenic fungus in lettuce. The invasion of *R. solani* in lettuce shifted the microbial community associated with lettuce. However, the introduction of *B. amyloliquefaciens* as a biocontrol agent compensated for the alterations to the pathogen activity (Erlacher et al., 2014). The microbiome associated with different parts of the plant is crucial for plant health and productivity. Therefore, a biocontrol agent that shows a minor impact on these natural microbial communities is appropriate in disease management.

### 2.3 Canola – *Leptosphaeria* interaction

*Leptosphaeria maculans* is an Ascomycete fungus that infects canola plants causing blackleg disease. The fungus infects the stem of the canola plants and forms the stem cankers. The stem cankers prevent water and nutrient transport of the plant leading to plant death. The blackleg is reported worldwide and has caused significant yield losses in Canada, Australia, and Europe. The economic losses due to blackleg disease are more than $900 million per growing season globally (Zhang and Fernando, 2017). Different strategies for disease management are utilized, including tillage practices, fungicide treatment, and crop rotation. Nevertheless, employing resistant canola varieties is the most promising way to mitigate the blackleg disease. Therefore, understanding the gene for gene interaction between pathogen and canola varieties, and applying this knowledge in canola production is essential for managing the blackleg disease with efficiency (Fitt et al., 2008; Zhang and Fernando, 2017).

### 2.3.1 Canola

*Brassica* spp. belong to the family Brassicaceae, known as the family Crucifer in the past. The Crucifer family contains various species and varieties that are used as vegetables, condiments, and oil production. *Brassica carinata*, *Brassica juncea*, and *Brassica nigra* are known as mustard crops while *Brassica oleracea* is extensively used as a vegetable (Kale, Cabbage, and Cauliflower), and *Brassica napus* and *Brassica rapa* are known as rapeseed (McVetty and Duncan, 2015). Three out of six of the above-mentioned *Brassica* species are diploid, while *B. carinata*, *B. juncea*, and *B. napus* are amphidiploid (McVetty and Duncan, 2015; Raymer, 2002). All these *Brassica* species produce seeds that contain a significant amount of oil. Rapeseed was firstly identified as a crop containing a high level of erucic acid and plant secondary metabolites known as glucosinolates in their oil. Hence, in the 1960s and 1970s, Canadian plant breeders developed rapeseed varieties with low erucic acid and low glucosinolates. The name 'canola' is a trademark of the Canadian Canola Association for the rapeseed cultivars they developed in the 1970s. Canola produces seeds that have less than 2% of erucic acid in oil and less than 30 µmol/g of aliphatic glucosinolates in oil-free solid. In addition, canola includes three *Brassica* varieties which are *B. napus*, *B. rapa* and *B. juncea*. *B. napus* is the most common oilseed crop in Europe, China, Australia, and Canada. Moreover, *B. napus* is a natural hybrid between *B. rapa* (n= 10 chromosomes) and *B. oleracea* (n=9 chromosomes), and it contains combined chromosome sets from both species (n=19 chromosomes) (Figure 2.2). The development of Canola caught worldwide attention and became popular around the world due to its health benefits over other rapeseed varieties (Good As Gold. Celebrating 50 Years of Canola, 2021; Raymer, 2002; McVetty and Duncan, 2015).

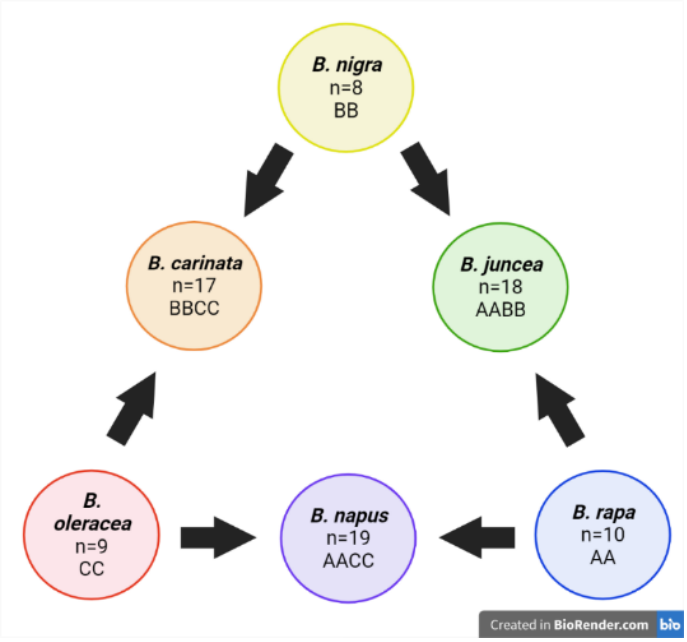



**Figure 2.2.** The genetic relationship among six natural *Brassica* spp. A, B, and C represent three major genomes shared by each other. These three major genomes are present within diploid (AA, BB, and CC) and allotetraploid (AABB, BBCC, and AACC) *Brassica* species.

Canola crops are mainly used for the production of edible oil using seeds. Canola oil has high nutritional value, and the saturated fatty acid content in canola oil is lower than other cooking oils, including olive, coconut, and soybean. In addition, canola oil contains 8-10% omega-3-fatty acids, an essential fatty acid to overcome many diseases, including heart diseases, cancer, and bowel diseases (Simopoulos, 2008.). Furthermore, the consumption of canola oil is beneficial to blood lipids. It decreases the low-density lipoproteins and reduces the risk of heart diseases (Lin et al., 2013). Besides the direct consumption as an edible oil, canola oil is also employed to produce biodiesel, which is eco-friendly, but not cost-effective (Issariyakul et al., 2008). Another primary application of canola is as a livestock feed. After the production of oil from canola seeds, the leftovers are known as the de-oiled meal. This meal is used to feed poultry, ruminants, swine, and in aquaculture. Further, canola meals have a high nutritional value because the canola seeds contain 17-26 % protein including essential amino acids. Even though canola meal is not currently used for human consumption, it is considered a good source of protein for humans as well (Chmielewska et al., 2020). Since canola has a variety of applications in different fields, it has become a popular crop worldwide.

### 2.3.2 Blackleg disease in canola

The blackleg disease is devastating in canola, leading to significant yield losses in many countries, including Canada. The first blackleg outbreak in Canada was reported in 1980, causing more than 50% yield losses in western Canadian canola fields. The reason for this outbreak was the cultivation of susceptible canola variety Westar (Juska et al., 1997). However, the blackleg disease was controlled for several years by introducing blackleg resistant canola varieties and incorporating four-year crop rotation in the early 1990s. However, later on, the four-year crop rotation was commonly neglected by farmers due to the high economic value of canola cultivation. Instead, they began to grow canola every two years and even in successive years. This lower attention to disease management led to blackleg disease outbreaks in some of the Canadian canola fields since 2002. Along with the continuous growth of resistant varieties containing the same R gene, the *L. maculans* population became insensitive to the R gene and imposed a high pressure on canola production again since 2012 (Zhang and Fernando, 2017). In 2016, the blackleg disease was reported in more than 80% of Manitoba canola fields, more than 71% of Alberta canola fields, and more than 59% of Saskatchewan canola fields ("Blackleg survey results from 2016 | The Canola Council of Canada," 2021.). Further, in 2020, Manitoba reported the highest blackleg disease incidence in Canada, reporting blackleg disease infection in 15% of canola plants in their fields (Figure 2.3) (The Canola Council of Canada, 2021). Therefore, the blackleg disease has become a vital disease in Canada.

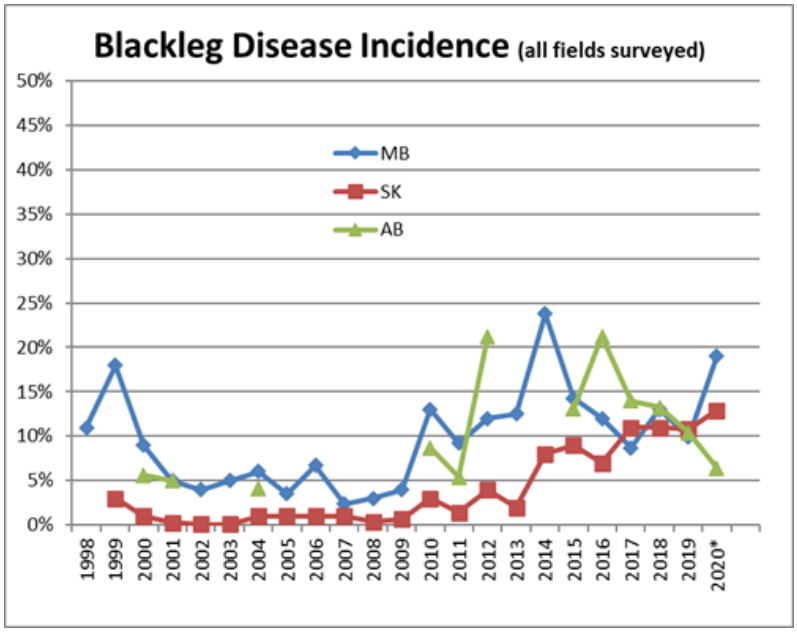



**Figure 2.3**. The blackleg disease incidence over 22 years from 1998 to 2020 in western Canadian canola fields. Manitoba shows the highest blackleg incidences, and in Manitoba, more than 15% of canola plants were infected with the blackleg disease in 2020 (The Canola Council of Canada, 2021).

### 2.3.3 *Leptosphaeria* spp.

*Leptosphaeria* is a genus of fungi that belongs to the phylum Ascomycota. Earlier, the genus was categorized into two main pathotypes. The aggressive strains that cause significant damages were classified as 'pathotype A,' and the less aggressive strains that are less damaging were classified as 'pathotype B.' The fungal strains that belong to 'pathotype A' produce a phytotoxin named Sirodesmin PL, while fungi of 'pathotype B' do not produce this phytotoxin by which they can be easily distinguished (Koch et al., 1989). However, as the interspecific mating between these two pathotypes was incompatible, they were later identified as two separate species. Thus, strains of 'pathotype A' were named *L. maculans*, and the strains of 'pathotype B' were named *Leptosphaeria biglobosa* (Shoemaker and Brun, 2001; Somda et al., 1997). Moreover, the molecular phylogenetic study of the internal transcribed spacer (ITS) region of *Leptosphaeria* spp. revealed that seven subgroups belong to the *L. maculans-L. biglobosa* species complex. These seven subgroups correspond to two main phylogenetic clades: the *L. maculans* and *L. biglobosa*. Further, the subgroups of this species complex have been identified based on their current geographic origin or their host plant. For instance, the two subgroups of *L. maculans* are *L. maculans* 'Brassicae'

from *Brassica* spp. and *L. maculans* 'lepidii' from *Lepidium* spp. The other five subgroups of the *L. maculans*-*L. biglobosa* species complex are *L. biglobosa* strains (Mendes-Pereira et al., 2003). However, *L. maculans* is the primary causal agent of blackleg disease in canola.

*Leptosphaeria maculans* is a bipolar heterothallic fungus and produces both sexual (ascospores) and asexual (pycnidiospores) spores (Venn, 1979). The primary source of the inoculum of the blackleg disease is the airborne ascospores released from the infected stubble from the previous cropping season (Bousset et al., 2015). When the ascospores land on the canola cotyledons or leaves, the hyphae germinate and invade the plant tissue through stomatal openings or natural wounds (Howlett et al., 2001; Li et al., 2004). The fungus then colonizes the extracellular spaces of plant leaf tissues biotrophically and later turns into a necrotrophic phase. During the necrotrophic phase, the fungus produces pycnidiospores, the asexual spores of the fungus (Howlett et al., 2001; Sonah et al., 2016). The pycnidiospores are the secondary inoculum of the blackleg disease (Figure 2.4). The pycnidiospores are less effective during the canola infection compared to ascospores, and a comparatively higher concentration of pycnidiospores is required to develop the disease. When pycnidiospores are inoculated into canola cotyledons, the disease symptoms are delayed for two days, compared to the rate of development when inoculated with ascospores (Hua et al., 2007; Li et al., 2004). After colonizing leaf tissues, the fungal hyphae grow through the petiole through the xylem vessels into the stem base. Then the fungus colonizes and kills the epidermis, cortical cells, vascular tissues, and pith of the stem base, forming stem cankers (Howlett, 2004). The formation of stem cankers is detrimental to canola plants. Therefore, *L. maculans* infections lead to enormous destruction in canola fields.

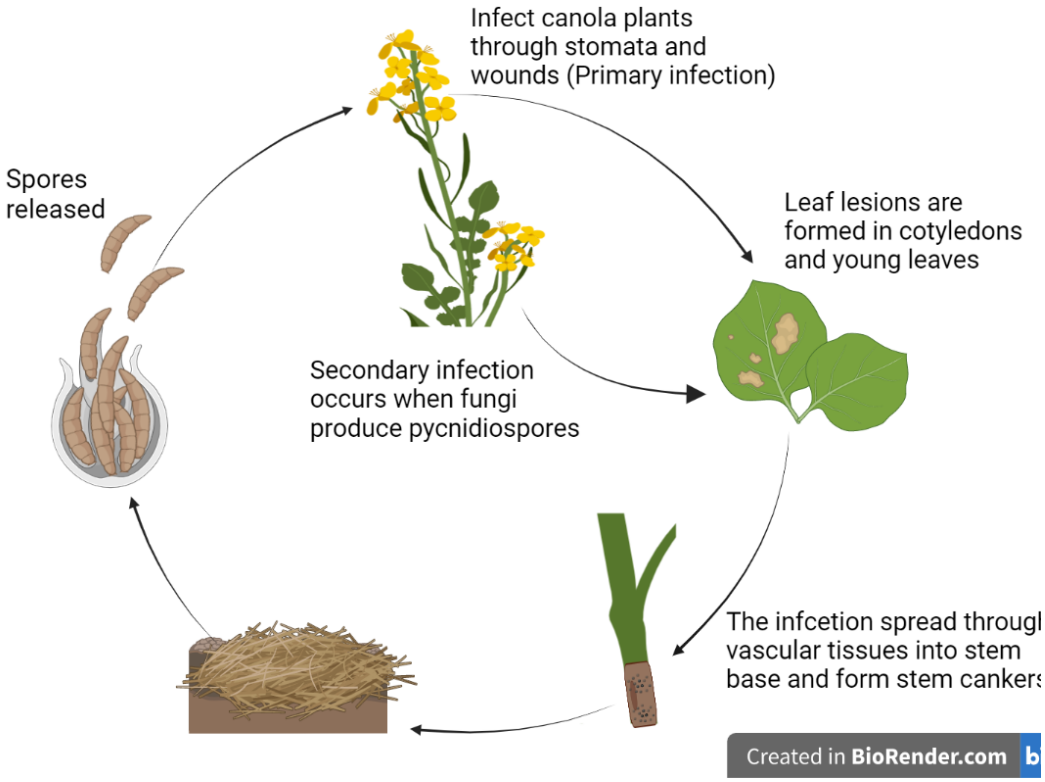



**Figure 2.4**. The life cycle of the blackleg pathogen. The *L. maculans* overwinters within crop residue and infects canola plants during spring, forming leaf lesions and stem cankers. Stem cankers are detrimental to canola plants.

### 2.3.4 Blackleg resistance in *Brassica napus*

Like the human immune system, plants utilize their defence system to protect themselves from pathogenic microbes. When the plant confers the successful defence responses against a pathogen, the plant is considered a resistant plant. *B. napus* possesses two types of resistance against the blackleg disease. These are seedling resistance and adult plant resistance. Seedling resistance, also known as qualitative resistance, is specific to the race of the pathogens and is governed by a single resistance gene (*R* gene) (Rimmer, 2006). The *R* genes initiate the plant defence-related responses and prevent the pathogen from spreading from leaves to stem through a hypersensitive reaction (HR). This HR induces plant cell death within the tissues surrounding the infection site by necrotizing them and inhibits the pathogen's development (Keen, 1990). So far, 18 major *R* genes have been identified in *B. napus*, which are *Rlm1-13*, *RlmS*, *LepR1-4*, *BLMR1*, and *BLMR2* (Raman et al., 2021, 2016; Zhai et al., 2021), and three of them have been cloned (*Rlm2*, *LepR3*, and *Rlm9*). According to current research on *LepR3* (Larkan et al., 2013) and *Rlm2* (Larkan et al., 2015) genes in *B. napus*, *LepR3* encodes a Leucine-rich repeat receptor-like protein (LRR-RLP),

and *Rlm2* is an allelic variant of the same gene. Further, the *Rlm9* gene encodes a wall-associated kinase-like (WAKL) protein, and its functions are less understood (Larkan et al., 2020).

The adult plant resistance (APR) or the quantitative resistance is race-nonspecific. The APR is governed by multiple genes, and environmental conditions influence APR (Li et al., 2006; Rimmer, 2006). The infections that occur at later growth stages of canola plants are controlled mainly through this polygene resistance (Dandena et al., 2019; Li et al., 2006). Compared to the seedling resistance, the durability of APR is longer, and APR resistance increases the durability of *R* gene resistance (Brun et al., 2010). The combination of both types of resistance is more durable and more robust when fighting against the infection of *L. maculans* in canola (Brun et al., 2010).

#### 2.3.4.1 Gene for gene interaction between host and the pathogen

The gene for gene interaction between plants and pathogens has developed during their co-evolution (Thompson and Burdon, 1992). The gene for gene model was discovered by Harold Henry Flor (Flor, 1956). According to Flor's gene for gene model, for every *R* gene in the host plant, there is a corresponding avirulence gene (*Avr* gene) within the pathogen genome. Plant's *R* genes encode for the protein receptors, and the pathogens *Avr* genes encode for the elicitor molecules, which act as ligands. If the plant *R* gene and the pathogen *Avr* gene match, receptor-ligand interaction occurs between the plant receptor proteins and pathogen elicitor molecules. Through this reaction, the plant identifies the pathogen, creates plant defence-related responses, and triggers a local HR within the site of infection. Plants use these protein interactions to resist microbial infections and protect themselves from diseases (Keen, 1990).

The *B. napus*-*L. maculans* pathosystem shows the gene for gene interaction between the *R* and the matching *Avr* genes. So far, at least 17 *Avr* genes have been identified in *L. maculans* population, and 10 of them have been cloned. The identified *Avr* genes include *AvrLm1-11*, *AvrLepR1-3*, *AvrLms*, *AvrLmj* (Liban et al., 2016; Liu et al., 2021), and *AvrLm14,* which is the most recently reported *Avr* gene (Degrave et al., 2021). As mentioned before, for all the plant *R* genes in canola, there is a corresponding *Avr* gene in *L. maculans*. For instance, the *AvrLm1* gene in *L. maculans* interacts with the *Rlm1* gene in *B. napus*. Similarly, *AvrLm2-Rlm2*, *AvrLm3-Rlm3*, *AvrLepR1-LepR1* genes are pairs of genes that interact with each other (Ansan-Melayah et al., 1998a, 1998b;

Zhai et al., 2021). However, current studies on the canola-blackleg pathosystem have revealed some deviations from the gene for gene model described by Flor. For instance, the *AvrLm1* gene in *L. maculans* is recognized by both *Rlm1* and *LepR3* genes. Interestingly, these two genes are independent of each other and located in two different chromosomes, which are A10 (*LepR3*) and A07 (*Rlm1*) in the *B. napus* genome (Larkan et al., 2013). In addition, the *Avrlm4* and *Avrlm7* are two alleles of a single *Avr* gene and are recognized by both the *Rlm4* and *Rlm7* genes in *B. napus*. Therefore, this gene was later named *AvrLm4-7* (Parlange et al., 2008). Further, *AvrLm5* and *AvrLm9* are two alleles of the same gene and are recognized by both *Rlm5* and *Rlm9* genes in *B. napus*. Therefore, this *Avr* gene is now termed *AvrLm5-9*. Furthermore, the presence of the *AvrLm4-7* gene masked the recognition of *Avrlm5-9* by the *Rlm9* gene and the recognition of the *AvrLm3* gene by the *Rlm3* gene in *B. napus* (Ghanbarnia et al., 2018; Plissonneau et al., 2016). The underlying mechanisms are still mysterious; thus, understanding these interactions between *R* genes and the matching *Avr* genes is crucial for blackleg disease management in canola.

### 2.3.5 Fungal transformation

One of the most effective ways of studying underlying mechanisms that fungi use to create numerous disorders in plants is to inhibit the expression of target genes of interest by fungal transformation. Through fungal transformation, we can either inactivate a target gene with a recognizable phenotype (Katayama et al., 2019) or integrate a piece of foreign DNA into the fungal genome, like a reporter gene (Buron-Moles et al., 2012). *Neurospora crassa* and *Aspergillus nidulans* are two model organisms, which have brought enormous support for advancing filamentous fungal transformation (Davis, 2000; Goldman and Kafer, 2004; MacCabe et al., 2001; Riquelme and Martínez-Nñez, 2016). Moreover, the first fungal transformation was reported in the fungus *N. crassa* in 1973 (Mishra and Tatum, 1973).

The fungal transformation can be accomplished by either random gene integration or target gene mutagenesis. During the random integration, a random gene disruption can be achieved by inserting DNA sequence cassettes with a selectable market into the fungal genome. This approach can be used to disrupt genes or tag reporter genes (Mullins and Kang, 2001; Sugui et al., 2005; Takahara et al., 2004; Zhong et al., 2010). Further, targeted gene mutagenesis can be achieved through homologous recombination. First, a cassette of DNA sequences consisting of homologous

sequences to the target gene's flanking sequences is transferred into the host cells. The transferred sequence is then integrated into the host genome through homologous recombination (Weld et al., 2006). In addition, the small genome size and the low genetic redundancy in filamentous fungi make it easier for genetic engineering. However, as some fungal mycelium contains multiple nuclei, it is more challenging to isolate homokaryotic transformants after the transformation (Bashi et al., 2018; Olmedo-Monfil et al., 2004). Nevertheless, the fungal transformation is one of the most effective techniques in studying diverse molecular mechanisms, including gene expressions, host-pathogen interactions, molecular dynamics, and localizations.

#### 2.3.5.1 *Agrobacterium tumefaciens*-mediated transformation

*Agrobacterium tumefaciens* is a gram-negative plant pathogenic bacterium that causes crown gall disease in plants (Escobar et al., 2003). The natural mechanism of *A. tumefaciens* in infecting plants is used under laboratory conditions for the transformation, known as *Agrobacterium tumefaciens* mediated transformation (ATMT). The *Agrobacterium* cells contain a tumour-inducing (Ti) plasmid. The *Agrobacterium* transfers part of its DNA (T-DNA) via the Ti plasmid to the host and integrates it into the host genome. Moreover, the T-DNA region of *A. tumefaciens* naturally consists of genes encoding for plant growth regulators. The integration of T-DNA into plant cells induces plant growth and the formation of tumours within the host plant. The transfer of T-DNA into the host cells is aided by the virulence genes located within the Ti plasmid. The virulence genes are responsible for identifying, preparing, transporting, and integrating T-DNA into the host genome. The mechanism of *A. tumefaciens* T-DNA transfer is used for the genetic transformation of filamentous fungi. However, a modified vector has been developed to use in the fungal transformation by replacing virulence genes of the natural Ti plasmid into a separate plasmid known as the helper plasmid. The modified plasmid with the T-DNA region is known as the binary vector. The smaller binary vector is easier to manipulate compared to the Ti plasmid during the transformation. In addition to that, the gene of interest is placed between the T-DNA region's left and right borders, which integrates into the host genome during the transformation (Figure 2.5) (Hooykaas et al., 2018; Idnurm et al., 2017; Michielse et al., 2005).

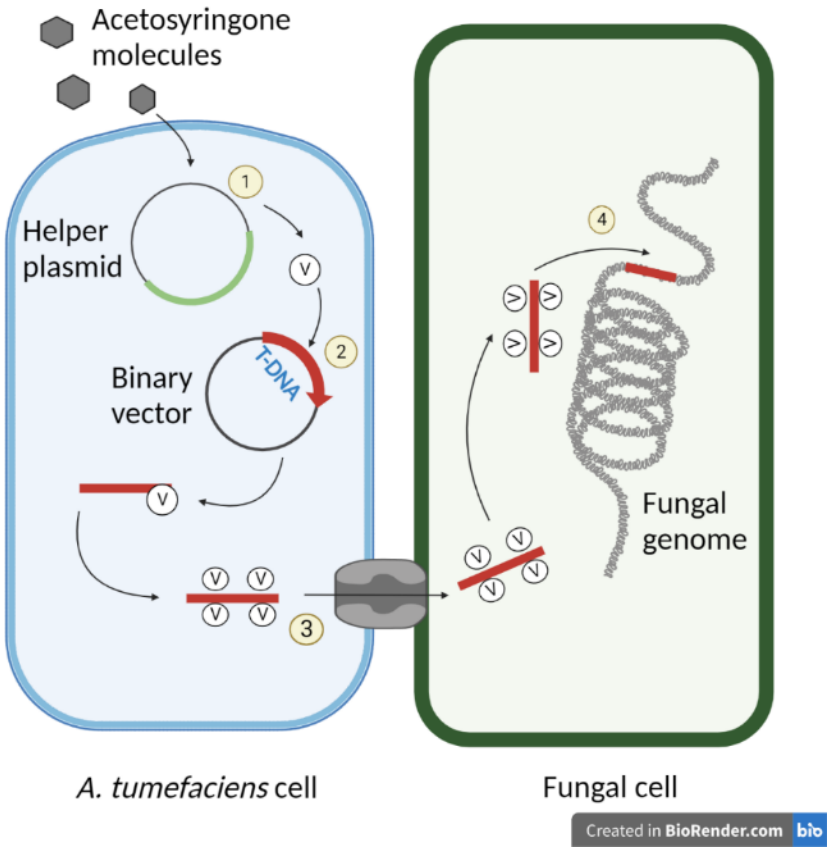



**Figure 2.5**. A summary of *A. tumefaciens* mediated transformation of fungi. 1: Acetosyringone in the culture media triggers the expression of virulence genes. 2: The virulence genes expressed, and virulence proteins cut the T-DNA region. 3: The virulence proteins transfer the T-DNA region through the type IV secretion system. At this point, the virulence proteins are bound to the T- DNA region. The T-DNA with virulence proteins enter the host nucleus with the help of nuclear localization signals. 4: The T-DNA integrates into the host genome.

Over several other methods, including the protoplast mediated transformation, electroporation, shockwave mediated transformation, and biolistics, the ATMT is considered the most effective fungal transformation method (Idnurm et al., 2017; Li et al., 2017). In addition, compared to the conventional methods, the ATMT is cost and labour effective and the transformation efficiency is higher. Moreover, the ATMT transformation can be performed using any vegetative parts of the fungi as the starting materials (Michielse et al., 2005). However, the selection of the starting material for the transformation can vary from species to species. For instance, in *Mortierella alpina,* the fresh spores, the germinated spores, or mycelia can be used during the transformation. However, the number of transformants obtained is lower when using the fresh spores due to the low sporulation rate of this fungus. Moreover, the transformation efficiency of *M. alpina* is 50%

higher for germinated spores than fresh spores (Wang et al., 2018). In addition, the basidiospores of *Agaricus bisporus* are ineffectual as the fungal starting material during co-culture. However, the vegetative mycelium of the *A. bisporus* has been successfully employed to transform the fungal genome (Mikosch et al., 2001). Furthermore, the acetosyringone concentration in the culture media and the co-cultivation conditions are two other major factors that influenced the fungal transformation efficiency. The acetosyringone is required to induce the activity of virulence genes in *A. tumefaciens* cells. However, based on the current literature, acetosyringone is not necessary for a successful transformation, but the presence enhances the transformation efficiency. When considering the co-cultivation conditions, the ratio between the bacterial and fungal concentration in the co-culture plate, temperature, pH of the media, and the co-cultivation period are the factors that impact transformation (Michielse et al., 2005). Therefore, ATMT is an efficient method for fungal transformation. However, the protocol must be optimized based on the fungal strain that is to be transformed.

### 2.3.6 CRISPR for gene editing

Ishino et al., (1987), discovered an obscure finding in 1987 in a research paper about an uncommon DNA fragment in the *E. coli* genome. This DNA fragment consists of short repetitive DNA flanked with a unique sequence. Later, this finding led to the discovery of the remarkable gene-editing tool CRISPR/Cas9 system. The clustered regularly interspaced short palindromic repeats (CRISPR) are related to the archaeal and bacterial adaptive immune systems, and these organisms utilized CRISPR for the identification and degradation of viral and plasmid DNA. Moreover, the CRISPR sequence segment can be found in almost 90% of archaea and 40% of bacteria (Horvath, 2010). In addition, the spacers that separate the repetitive DNA sequences in CRISPR are extrachromosomal DNA resembling the DNA segments of invasive viruses or plasmids and initiate a DNA encoded adaptive immune system in host organisms. Furthermore, the CRISPR-associated (Cas) genes are located close to the CRISPR sequences, and these genes encode for a family of proteins that includes helicases, polymerases, nucleases, and polynucleotide-binding proteins. Thus, CRISPR and Cas proteins are together named the CRISPR/Cas system (Charpentier and Doudna, 2013; Cong et al., 2013; Doudna and Charpentier, 2014; Garneau et al., 2010; Horvath, 2010).

The CRISPR/Cas system is involved in a DNA encoded immunization system in archaea and bacteria. When a bacterial cell encounters an infection, the spacer sequences in CRISPR are transcribed into a long RNA segment called precursor CRISPR RNA (pre-crRNA). The Cas protein complex cleaves and processes the pre-crRNA into small crRNA segments, which consist of genetic materials resembling viruses or plasmids. Subsequently, the crRNA guides the Cas proteins to the foreign DNA/RNA molecules, and the Cas proteins cleave and degrade the foreign nucleic acids (Deltcheva et al., 2011; Horvath, 2010). Even though some CRISPR/Cas systems require several Cas proteins for their function, the type II CRISPR/Cas system in *Streptococcus pyogene* needs only a single protein called Cas9 (Charpentier and Doudna, 2013) and two RNA molecules, trans-activating crRNA (tracrRNA) and crRNA to target foreign DNA. Later the tracrRNA and the crRNA are assembled into a single RNA named the single guide RNA (sgRNA) (Jinek et al., 2012; Mali et al., 2013). Thus, the type II CRISPR/Cas9 system comprises two main components: the Cas9 endonuclease protein and the sgRNA (Charpentier and Doudna, 2013). The sgRNA guides the Cas9 proteins to the target DNA, and the cleavage of the Cas9 needs a protospacer adjacent motif (PAM) adjacent to the complementary sequence (Heler et al., 2015).

CRISPR/Cas9 is an affordable and straightforward method of gene editing compared to the other methods. Therefore, CRISPR/Cas9 has been widely utilized in fungal genetic engineering. Further, CRISPR/Cas9 technology has been used to edit genes in different fungal pathogens. For instance, CRISPR/Cas9 mediated gene engineering has been successfully performed in *L. maculans* to knockout the *AvrLm7* resistance gene through a point mutation (Zou et al., 2020). In addition to that, the rice blast fungus *Magnaporthe oryzae* genome has been edited through the CRISPR/Cas9 technology by incorporating several modifications (Foster et al., 2018). As suggested in this study, the continuous expression of the Cas9 protein is harmful to the rice blast fungus. Therefore, they have created a ribonucleoprotein (RNPs) combining a purified Cas9 protein and the guide RNA to generate a higher rate of mutations in the *M. oryzae.* This modified CRISPR/Cas9 system is termed the RNP-CRISPR-Cas9 system (Foster et al., 2018). Moreover, the techniques have been used to study the virulence factors in *Sclerotinia sclerotiorum* through insertional mutations in the oxalic acid biosynthesis gene (*Ssoah1*) (Li et al., 2018). The first report in CRISPR/Cas9 based gene editing in *Trichoderma* was reported in 2021. The deletion of genes in *Trichoderma* species is difficult using conventional techniques due to the low rate of homologous recombination.

Therefore, they have used CRISPR/Cas9 to delete the auxotrophic marker, Orotidine 5'-phosphate decarboxylase (*pyr*) gene, in *T. harzianum*. Importantly, this is the first genetic engineering of a biocontrol agent using CRISPR/Cas9 technology (Vieira et al., 2021). Thus, the discovery of CRISPR/Cas9 gene-editing system revolutionized the research in various research areas in agriculture and health sciences. Therefore, the pioneers, Emmanuelle Charpentier and Jennifer Doudna were awarded the Nobel prize in chemistry in 2020 (Strzyz, 2020) for their findings in CRISPR/Cas9 (Charpentier and Doudna, 2013; Jinek et al., 2012).

### 2.3.7 Fluorescent proteins

In 1852, George S. Stroke discovered the fluorescent emissions from mineral fluorites when they were excited with UV radiation. This discovery led to the creation of fluorescent probes by scientists later (Sample et al., 2009). In 1961 Osamu Shimomura, isolated the green fluorescent protein (GFP) from the Jellyfish *Aequorea victoria* (Shimomura et al., 1962). The discovery of the genetically encoded fluorescent proteins initiated a massive breakthrough in live-cell imagining in science, and this discovery led to a revolution in cell biology. Therefore, in 2008, Martin Chalfie, Osamu Shimomura, and Roger Tsien were awarded the Nobel prize in chemistry for the discovery and the isolation of GFP from jellyfish (Weiss, 2008).

Various fluorescent proteins (FPs) emit radiation covering most of the visible spectrum. These FPs include the FPs developed through GFP modification and the FPs isolated from various marine animals, including the bioluminescent Hydrozoa and Anthozoa (Chudakov et al., 2010). Furthermore, the FPs are divided into seven classes of emission spectra. These classes are blue, cyan, green, yellow, orange, red, and far-red. Through mutations in the GFP from *A. victoria,* the FPs within the range of blue to yellow in the visible spectrum can be obtained. In contrast, FPs with orange to red emissions have been acquired from organisms in the ocean (Sample et al., 2009) including, the mushroom anemone *Discoma* (Davidson and Campbell, 2009), the stony coral *Fungia concinna* (Karasawa et al., 2004), the copepod *Chiridius poppei* (Masuda et al., 2006) and the sea anemone *Entacmaea quadricolor* (Petersen et al., 2003). The discovery of genetically encoded FPs and the development of multi-colour FPs have hugely impacted medical and agricultural research.

#### 2.3.7.1 Green fluorescent protein as a marker

The wild-type GFP in *A. victoria* is a 27kDa protein that is made up of 238 amino acids. It emits green fluorescent light from an energy transaction reaction. The GFP has an 11 stranded β-barrel protein structure with a single α-helix in the middle of the barrel. The α-helix contains the chromophore, which is responsible for the green colour emission. When the GFP is excited with blue light, it emits green fluorescent light (~ 510nm) through a photon transfer reaction within the chromophore (Remington, 2011; Sample et al., 2009). One limitation of the GFP as a reporter is the disruption of the protein at higher temperatures (37 ℃). Nevertheless, it is still greater than other conventional fungal markers like β-galactosidase and β-glucuronidase as the *gfp* gene expression does not rely on an external substrate. In addition, the GFP reporter is stable and easy to visualize (Lorang et al., 2001; Pöggeler et al., 2003). The reporter can be used in-vivo to study the movement, propagation, and dynamics of fungi in plant tissues in real-time. Thus, the GFP has been used to illuminate the different agriculturally important bacteria and fungi to visualize them in live tissue and understand host-pathogen interactions (Buron-Moles et al., 2012; Carvalho et al., 2016; Spellig et al., 1996).

The GFP marker has had a considerable influence on plant pathological research. The first report on the expression of the *gfp* gene in *L. maculans* was reported in 2001 (Sexton and Howlett, 2001). Until that time, the GUS marker that relies on treatment with a substrate was used to study the progression of the fungus in plant tissues. However, the GFP tagged *L. maculans* has led to understanding the disease progression in live tissues. Nevertheless, strong constitutive expression of the *gfp* gene is essential to label the whole fungal body with GFP. The *A. nidulans gpdA* promoter is commonly used for the constitutive expression of the *gfp* gene (Sexton and Howlett, 2001). In addition to *L. maculans,* several other plant pathogenic fungi have been transformed to express the *gfp* gene to study the disease progression. For instance, the fungus *Ustilago maydis*, which causes the smut disease in corn, was transformed with the *gfp* gene to understand the infection process of the fungus and the proliferation and spore production within the plant tissues (Spellig et al., 1996). In another study, GFP expressing bacterial strains were used to investigate the association between bacteria and arbuscular mycorrhizal fungi. Researchers evaluated the proximity between each bacterial strain with the fungal hyphae (Toljander et al., 2006). Moreover, some studies have used the GFP marker to understand the biocontrol mechanisms of fungi. For

instance, *Acremonium implicatum* is a potential biocontrol agent against the root-knot nematode *Meloidogyne incognita*. In addition to that, this biocontrol agent is a plant endophyte. Further, the GFP marker has been employed to discover the egg-parasitic activity of *A. implicatum* towards *M. incognita* and the endophytic nature of the fungus in plants (Yao et al., 2015). Thus, GFP transformation of microbes is an effective way to study the microbial interactions with plants, soil, and other animals in-vivo.

### 2.4. Research questions

Biological control has gained attention worldwide due to its eco-friendly nature. Several biocontrol agents have shown potential to reduce the FHB in wheat. *T. gamsii* strain T6085 is one of the possible biocontrol agents against FHB in wheat and it has shown a significant reduction in FHB disease severity and DON released by *F. graminearum*. However, it is necessary to take advanced measures when introducing a fungal biocontrol agent into the wheat field as there can be off-target effects on other microbes associated with different wheat tissues. Therefore, the first chapter of the current work was performed to address the question of how the application of *T. gamsii* T6085 as a biocontrol agent into wheat fields affects the natural fungal and bacterial community associated with wheat plants. On the other hand, the *L. maculans* and canola plants show molecular interactions with each during the formation of blackleg disease in canola. Even though, current research has focussed on the interaction between various plant resistance genes and pathogen avirulence genes during the development of blackleg disease in canola, there can be many other genes that are important for the *L. maculans* to infect the canola plants. CRISPR/Cas9 based gene editing has been used to identify various genes that are responsible for important traits in different microbes. Therefore, the second chapter of the current work was performed to phenotypically track a mutant *L. maculans* isolate during its infection of canola leaf tissues. The mutant *L. maculans* isolate contains a genetic mutation in one of its gene that are responsible for disease formation. The mutation is unknown, and this mutant strain is currently being studied to identify this gene that is essential for the *L. maculans* to form blackleg disease in canola.

# 3.0 CHAPTER 1

## Wheat-associated bacterial and fungal communities during the interaction of *Fusarium graminearum* and *Trichoderma gamsii* T6085

## 3.1 ABSTRACT

Alukumbura, Arshani. M.Sc., The University of Manitoba, December, 2021. Wheat-associated bacterial and fungal communities during the interaction of *Fusarium graminearum* and *Trichoderma gamsii* T6085. Major professors: Dr. Dilantha Fernando and Dr. Matthew Bakker.

Fusarium head blight (FHB) is a major fungal disease that has led to extensive yield and quality losses in wheat. The primary causative agents of the disease are *F. graminearum* and *F. culmorum.* Biological control is a promising strategy that can be incorporated into current management practices to increase efficiency. Existing literature has identified *T. gamsii* strain T6085 as a potential biocontrol agent to restrain the infection of *F. graminearum* and *F. culmorum* in wheat. However, the impact of *T. gamsii* T6085 on the microbiome dynamics associated with the wheat plant is not understood well. Therefore, the study evaluated the bacterial and fungal communities associated with different wheat tissues and their variations in response to the addition of *T. gamsii* T6085. The field experimental design was a randomized complete block design with four treatments and five replicates. Crop residue, wheat spike, and kernel samples were collected at different time points. DNA was extracted from the collected wheat tissues, and amplicon sequencing was performed to identify different bacteria using the *16S rRNA* V4 region and different fungi using the *ITS2* region. Quantitative PCR was performed from extracted DNA to evaluate the absolute abundance of *F. graminearum* and *T. gamsii* in different wheat tissues. Abundance of *F. graminearum* in crop residue was significantly higher at the initial time point and declined over time. In wheat spikes, the *F. graminearum* abundance was lower at initial time points, but it increased over time, reaching to a significantly higher amount at harvest. However, the *F. graminearum* abundance did not change significantly due to the *T. gamsii* T6085 treatment. The predominant bacterial groups in wheat spikes and kernels were *Pseudomonas*, *Enterobacter*, and *Pantoea*, while *Alternaria* and *Fusarium* were the dominant fungal groups. Alterations to microbial community structure associated with *T. gamsii* T6085 addition were minimal. However, there were substantial changes in microbial community structure over time. In this experiment colonization of wheat plants by *T. gamsii* T6085 was limited.

## 3.2 INTRODUCTION

Fusarium head blight (FHB) is a prominent disease commonly occurring in wheat fields worldwide. The disease leads to the reduction of wheat yield and contamination of wheat grains with toxins affecting both the quality and the quantity of wheat products (Gilbert et al., 2000.; McMullen et al., 2012). Fusarium head blight is caused by fungal pathogens belonging to the genus *Fusarium*, and the primary causative agents are *F. graminearum* and *F. culmorum* (Walter et al., 2010). The *Fusarium* infection leads to the premature bleaching of wheat spikes. However, the disease symptoms in wheat spikes can be varied depending on the time the infection occurs. The wheat anthers provide a perfect place for the *Fusarium* spp. to infect. Therefore, the disease mainly occurs during the flowering period of the wheat plant. If *Fusarium* spp. infect a wheat plant just after the emergence of flowers; it leads to kernel abortion. However, later infection gives rise to diseased wheat kernels with shrivelled and wilted appearances. In addition, *Fusarium* infections can also arise after the development of wheat kernels. The *Fusarium* infected wheat kernels are commonly contaminated with toxins released by the fungus (Birr et al., 2020; Kang and Buchenauer, 2000; Strange et al., 1974).

*Fusarium graminearum* overwinters within the crop residue. The fungus acquires nutrients from decaying plant materials and lives saprotrophically during the fall, winter, and spring seasons (Sutton, 1982). Different *Fusarium* spp. are favoured by various environmental conditions. Therefore, their abundance varies with the climatic conditions in different locations. However, *F. graminearum* can survive and develop within a wide range of temperatures (10 ℃ – 30 ℃). Nevertheless, warm, and humid environmental conditions favour spore production and infection by *F. graminearum* (Osborne and Stein, 2007). Moreover, *F. graminearum* produces two types of spores. They are ascospores and macroconidia. The airborne ascospores are derived from perithecia, and these are the fungal sexual spores. Ascospores can travel long distances through the wind. The splash-borne macroconidia are asexual spores and travel short distances. The macroconidia are released with the rain splash (Fernando et al., 1997; Gilbert and Fernando, 2004). Upon the infection of wheat kernels, *Fusarium* releases mycotoxins. Type B trichothecenes are the major mycotoxins associated with FHB in wheat. The DON and NIV are the main groups included in Type B trichothecenes. Mycotoxin can not be eliminated during food processing due to its heat

stability and therefore contaminated grain leads to contaminated final food products (Gärtner et al., 2008; Pestka, 2010). Therefore, *F. graminearum* is a pathogen that can cause significant damage to wheat plants and wheat-based food products.

The consumption of *Fusarium*-damaged wheat kernels can cause adverse health effects in humans and animals. Therefore, it is crucial to take preventive measures to minimize disease incidence. Farmers utilize different management strategies to mitigate FHB in wheat. These strategies include using moderately resistant cultivars, timely application of fungicides, risk monitoring, cultural practices such as crop rotation, soil tillage, and application of biocontrol agents. However, the integrative disease management approach, which involves several or all above-mentioned strategies, is more successful during the FHB management (Blandino et al., 2012; Shah et al., 2018). Extensive use of fungicide can lead to the development of fungicide resistance within pathogen populations. Due to the development of fungicide resistance within pathogen populations and public health concerns due to the chemical fungicides, biological control has become an interest to many researchers. Biological control is a cost-effective and environmentally friendly approach. However, the selected biocontrol agent must not be a risk to the environment, consumers, or growers (Köhl et al., 2011).

The genus *Trichoderma* consists of the most widely used biocontrol agents in the world, and their ability to biocontrol different plant diseases has been investigated for an extended period (Amin et al., 2010; Monte, 2001). Among various *Trichoderma* species, *T. gamsii* has been shown to effectively mitigate FHB in wheat. *T. gamsii* is a plant endophyte that colonizes the plant roots without adversely affecting plant health. Endophytic colonization by *T. gamsii* induces plant systemic resistance (Rinu et al., 2014; Sarrocco et al., 2021). Furthermore, the *T. gamsii* T6085 strain has been identified as a promising biocontrol agent to mitigate the growth and development of *F. graminearum* and *F. culmorum* in wheat fields. According to current studies, *T. gamsii* T6085 strain directly attacks *F. graminearum* and *F. culmorum* through hyphal interactions and causes defects and prevents pathogen growth. In addition, *T. gamsii* T6085 strain has reduced the amount of DON release by *F. graminearum* and *F. culmorum* by almost 92% (Matarese et al., 2012). The *T. gamsii* T6085 strain has significantly reduced the *F. graminearum* development in crop residue in wheat fields (Sarrocco et al., 2021) and has reduced the FHB severity by 57% when applied on

wheat heads (Sarrocco et al., 2013.). Therefore, the *T. gamsii* T6085 strain has been identified as a potential biocontrol agent against FHB in wheat.

Wheat plants are associated with numerous fungi and bacteria in addition to the target pathogen. The microbiome associated with plants can be classified into three main categories. These are the rhizosphere, phyllosphere, and endosphere microbial communities (Turner et al., 2013). The association of plants and beneficial microbiome gives various advantages to plants in terms of health and productivity, by facilitating plant nutrient uptake, inducing plant growth and development, inducing plant resistance, and fixing atmospheric nitrogen (Smith and Goodman, 1999). The symbiotic association between plants and microbes is essential to maintain plant health and a balanced eco-system. Like other disease management strategies, biological control can also change the natural microbial community within the wheat production environment. The biocontrol mechanisms shown by *T. gamsii* can be harmful to the target pathogen, but also other non-pathogenic fungi and bacteria associated with the wheat plant. Therefore, it is crucial to understand how *T. gamsii* T6085 impacts the microbial community structure.

This study aimed to evaluate the influence on wheat-associated microbial communities when *T. gamsii* T6085 strain was applied as a biocontrol agent to mitigate FHB in wheat. *T. gamsii* T6085 was applied on crop residue at the beginning of the stem elongation of the wheat plant, and on spikes at anthesis. Crop residue, wheat spikes, and kernels tissues were collected at different time points to identify the bacterial and fungal communities residing within these tissues. The variations in bacterial and fungal communities in response to *T. gamsii* T6085 application were assessed using different analysis methods. In this experiment, the impact of *T. gamsii* T6085 on the microbial communities, including *F. graminearum*, was limited. This study provides information on the microbial community structure of different wheat tissues and possible biocontrol agents to be utilized in FHB management in the future.

## 3.3 MATERIALS AND METHODS

### 3.3.1 The field experimental setup

The field experiment was performed at "Centro Enrico Avanzi," San Piero a Grado, Pisa (University of Pisa, Italy) in a field with a previous history of organic wheat cultivation during the cropping season of 2018-2019 using durum wheat (*Triticum durum* cv Tirex). The disease developed by the natural inoculum of *F. graminearum* was assessed during the experiment. A randomized block experimental design was arranged by using Random.org. Five randomized blocks of plots of 6 m x 9 m were used to evaluate four treatments: 1) control (non-inoculated); 2) *T. gamsii* T6085 applied onto wheat spikes at anthesis; 3) *T. gamsii* T6085 applied onto crop residue at the soil surface (residue was wheat from the previous cropping season); 4) *T. gamsii* T6085 applied onto both crop residue at the soil surface and onto wheat spikes at anthesis.

For the inoculation of crop residue, *T. gamsii* T6085 colonized millet seeds were distributed by hand across the field at the beginning of stem extension (Feekes stage 6). Crop residue samples were collected at three different time points: a day before the treatment ($T_{cr}0$), after 1 month ($T_{cr}1$), and before the harvest ($T_{cr}2$) (three and half months after the treatment). For the inoculation of wheat heads, a conidial suspension of *T. gamsii* T6085 ($10^6$ spore $mL^{-1}$) was sprayed at anthesis. Wheat spikes were sampled at four different time points: a day before *T. gamsii* T6085 application on spikes ($T_{sp}0$), 14 days post-inoculation ($T_{sp}1$), 28 days post-inoculation ($T_{sp}2$), and at harvest ($T_{sp}3$) (two and half months after the treatment). The wheat kernels were collected at harvest (Table 3.1). Tissue samples were received from the University of Pisa as ground material, stored in a nucleic acid preservation solution (DNA/RNA Shield, ZymoResearch).

**Table 3.1.** Number of wheat tissue samples collected at different time points for the microbiome analysis

| Type of tissue | Collected time point | Number of replicates | Number of treatments | Number of samples |
|---|---|---|---|---|
| Crop residue | $T_{cr}0$ | 5 | 4 | 20 |
| | $T_{cr}1$ | 5 | 4 | 20 |
| | $T_{cr}2$ | 5 | 4 | 20 |
| Wheat spikes | $T_{sp}0$ | 5 | 4 | 20 |
| | $T_{sp}1$ | 5 | 4 | 20 |
| | $T_{sp}2$ | 5 | 4 | 20 |

| | | | | |
|---|---|---|---|---|
| | $T_{sp}3$ | 5 | 4 | 20 |
| Wheat kernels | Harvest | 5 | 4 | 20 |

### 3.3.2 Quantitative PCR

The DNA was extracted from 0.1 g of ground crop residue, wheat spikes, and wheat kernel tissues using the GeneJet plant genomic DNA extraction kit (Thermo Fisher Scientific) according to the manufacturer's protocol. Quantitative PCR (qPCR) was performed to calculate the abundances of *T. gamsii* and *F. graminearum* within samples. For the amplification of *F. graminearum* DNA, *Fus.GRA* forward (5′ TCTGCTCTTCCATCTCGTCGG-3′) and *Fus.GRA* reverse (5′-CGTGGCAGTAGTGACTGAACAAACC 3′) primers were used. For the amplification of *T. gamsii* T6085 DNA, *Tgam* forward (5′ AACAACCTCCAAAAGTCCGCC 3′) and *Tgam* reverse (5′ CGGAAGAGCCGTTGTAGATACC 3′) primers were used (both assays from Sarrocco et al., 2019) (Table 3.2). The 20 µL qPCR mixture was comprised of 10 µL of 2X SYBR Green Master Mixture (Bio-Rad, Canada), 0.5 µM forward primer, 0.5 µM reverse primer, 2 ng/µL of template DNA, and nuclease-free water. Standard curves were developed using genomic DNA from *T. gamsii* and from *F. graminearum* to test the efficiency of primers before proceeding with the experimental samples. Efficiencies when amplifying genomic DNA were 94.06% for the *Fusa.GRA* assay and 92.95% for the *Tgam* assay.

**Table 3.2.** The PCR programs for each PCR reaction performed during amplicon generation, addition of indices, and for qPCR

| Reaction | Primers | PCR program |
|---|---|---|
| Amplicon PCR | *ITS2* | Initial denaturation at 98 ℃ for 3 mins, denaturation at 98 ℃ for 15 secs, annealing 57 ℃ for 10 secs, extension 72 ℃ for 1 min, final extension 72 ℃ for 10 min (25 cycles) |
| | *16S rRNA* | Initial denaturation at 98 ℃ for 3 mins, denaturation at 98 ℃ for 15 secs, annealing 57 ℃ for 10 secs, PNA clamping 75 ℃ 10 secs, extension 72 ℃ for 1 min, final extension 72 ℃ for 10 min (25 cycles) |
| Index PCR | Nextera XT index kit | Initial denaturation at 98 ℃ for 3 mins, denaturation at 98 ℃ for 30 secs, annealing 55 ℃ for 30 secs, extension 72 ℃ for 30 secs, final extension 72 ℃ for 5 min (8 cycles) |
| qPCR | *Fus.GRA* | Initial denaturation at 98 ℃ for 3 mins, denaturation at 98 ℃ for 15 secs, annealing/ extension + plate read at 58 ℃ for 30 secs (40 cycles), melt curve analysis at 65-95 ℃ at 3 secs/step increment |
| | *Tgam* | Initial denaturation at 98 ℃ for 3 mins, denaturation at 98 ℃ for 15 secs, annealing/ extension + plate read at 56 ℃ for 30 secs (40 cycles), melt curve analysis at 65-95 ℃ at 3 secs/step increment |

### 3.3.3 Amplicon sequencing

The DNA that was extracted from 0.1 g of ground crop residue, wheat spikes and wheat kernel tissues using the GeneJet plant genomic DNA extraction kit was used for the microbiome analysis. The concentration of extracted DNA was quantified using a spectrophotometer (NanoDrop™ One, Thermofisher), and each DNA sample was normalized to a concentration of 2 ng/µL and used for the library preparation. The *ITS2* region of the fungi and *16S rRNA* v4 region of bacteria were amplified (Caporaso et al., 2011; Toju et al., 2012). Primers with variable length spacers were employed during the amplicon PCR to increase the signal diversity when sequencing through the primer region. The 20 µL PCR mixtures consisted of Kapa Hifi HotStart master mixture (Roche Sequencing Solutions, Canada), 0.8 ng/µL template DNA, 0.5 µM forward primer, 0.5 µM reverse primer, and nuclease-free water. To inhibit the amplification of *16S rRNA* v4 sequences of mitochondrial and plastid DNA in plant tissues, 0.25 µM of mPNA blocker and 0.25 µM of pPNA blocker (PNA Bio Inc.) were added during the amplification of *16S rRNA* v4 region (Table 3.2). The amplified PCR products were purified using KAPA HyperPure beads (Roche Sequencing Solutions, Canada) according to the user guide. Dual indices and adapters were attached to the amplicon PCR products using the Nextera XT Index Kit (Illumina). The PCR reaction mixture for the index PCR consisted of KAPA HiFi HotStart master mixture, 1 µM forward primer, 1 µM reverse primer, template DNA, and nuclease-free water (Table 3.2). The indexed PCR products were purified using KAPA HyperPure beads. The PCR products were quantified using the Quant-iT™ dsDNA Assay Kit, high sensitivity (Thermo Fisher Scientific). Samples were pooled together to make a final pooled library consisting of 40 ng of DNA from each sample in the final solution. Because some smaller than expected fragments (likely primer dimers) were present in the library, the pooled library was run in a Flashgel system (Lonza, Switzerland), and the band with the correct size was recovered using FlashGel recovery buffer. The pooled library with the correct size recovered from the flash gel was run through a purification using KAPA HyperPure beads. The amplicon size distribution of the final library was visualized using the TapeStation system (Agilent, USA), and the concentration was quantified using the KAPA Library Quantification Kit for Illumina® Platforms (Roche Sequencing Solutions, Canada). The samples were split across four libraries. To serve as an internal control, PhiX was spiked into each library at a rate of 7.5 %. The v2 Miseq reagent kit and v3 Miseq reagent kits were used during the sequencing of *16S rRNA* libraries and *ITS2* libraries, respectively. Paired-end sequencing was performed for each final

denatured library according to the manufacturer's guidelines for the sequencing instrument (MiSeq system, Illumina). For each library, negative controls (PCR reactions without template DNA), and mock communities were included. For the bacterial libraries, the mock community was MSA-3002 from the American Type Culture Collection and for the fungal libraries, a mock community from (Bakker, 2018) was used.

### 3.3.4 Data analysis

The sequence data were processed, and taxonomic identification was performed using CLC Genomics Workbench version 20.0.4 (Qiagen). The low-quality sequences (limit 0.05) were trimmed off and, ends with ambiguous nucleotides (maximum 2) were trimmed. The adapter sequences were trimmed off, and the reads below the length of 15 were discarded. Reference-based operational taxonomic unit (OTU) clustering was performed at a 99% similarity percentage. For the identification of different fungi using *ITS2* sequences, the UNITE database (v7.2, 99% with singletons, developer) was used (Abarenkov et al., 2010). For the identification of different bacteria using *16S rRNA* v4 sequences, SILVA 16S v132 99% database was used (Quast et al., 2013). Subsequent analyses were performed using R Studio. The Bray-Curtis dissimilarity analysis and differential expression analysis were done using phyloseq and DEseq packages (Anders and Huber, 2010; McMurdie and Holmes, 2013). The variations in bacterial and fungal communities due to *T. gamsii* T6085 treatment were evaluated. The diversity statistics, including richness and Shannon index, were calculated using packages phyloseq, DECIPHER, phangorn, vegan, and picante in R Studio (Dixon, 2003; Kembel et al., 2010; McMurdie and Holmes, 2013; Schliep, 2011; Wright et al., 2016). The results were subjected to ANOVA, and the Tukey HSD test was performed for the multiple comparisons of diversity indices. The abundances of *T. gamsii* T6085 and *F. graminearum* were calculated using the standard curve method. The significant changes in *F. graminearum* densities due to the activity of *T. gamsii* T6085 and over time were analyzed by ANOVA and Tukey HSD multiple testing correction.

## 3.4 RESULTS

### 3.4.1 The variation in *T. gamsii* T6085 abundance in different wheat tissues

The qPCR data were used to calculate the absolute abundance of *T. gamsii* T6085 on treated and untreated wheat tissue samples. The *T. gamsii* abundance was lower and no significant changes in *T. gamsii* abundance across different treatments were observed in crop residue, wheat spikes, and in wheat kernel tissues (ANOVA, $p>0.05$) (Figure 3.1).

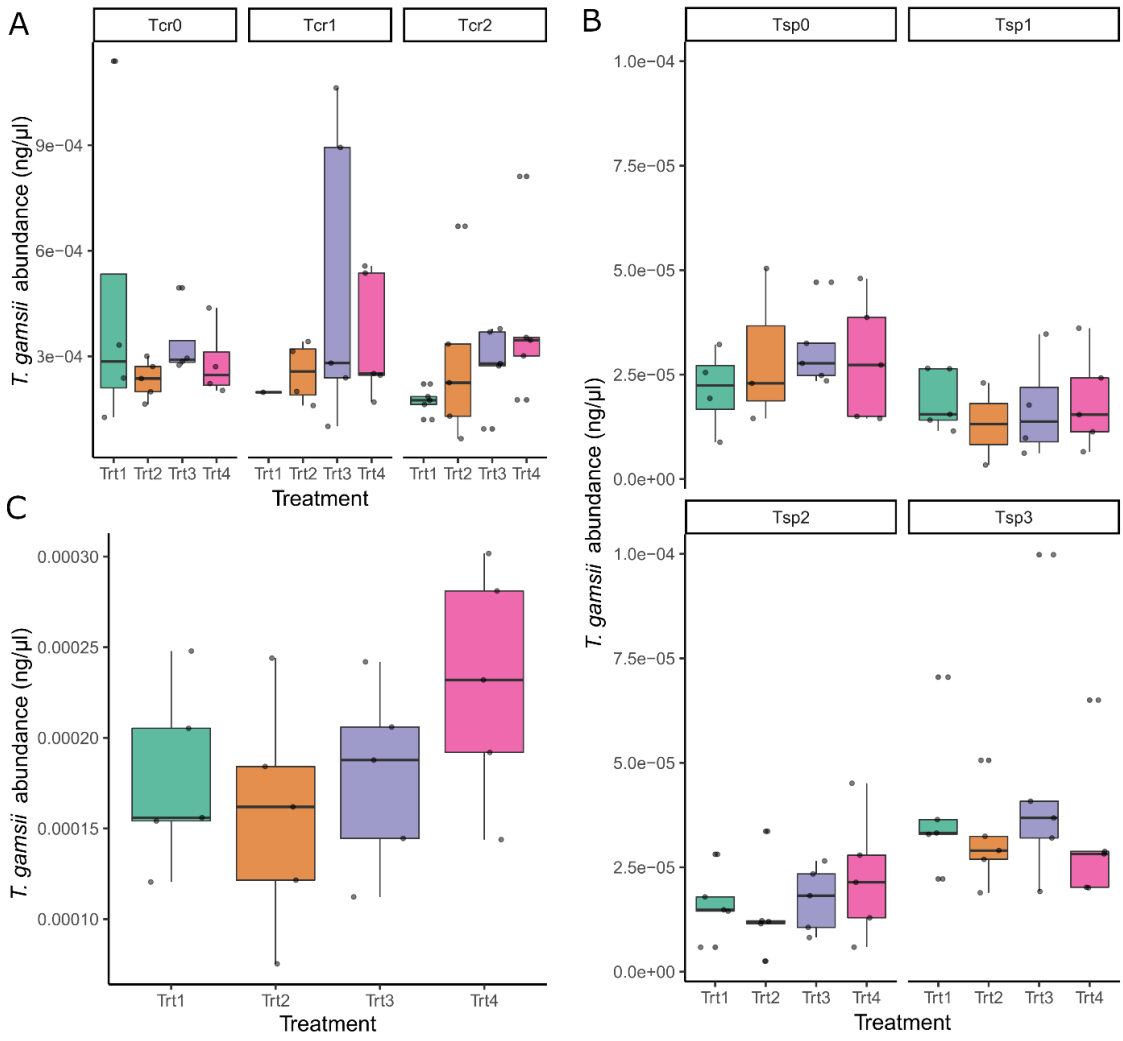



**Figure 3.1.** Variation in *T. gamsii* abundance in A: crop residue; B: wheat spikes; C: wheat kernels across different treatments. $T_{cr}0$, $T_{cr}1$ and $T_{cr}2$ indicate the different time points at which the crop residue samples were collected, while $T_{sp}0$, $T_{sp}1$, $T_{sp}2$, and $T_{sp}3$ indicate the various time points at which the wheat spikes samples were collected. The x-axis labels Trt1 (Control), Trt2 (*T. gamsii* T6085 applied on spikes at anthesis), Trt3 (*T. gamsii* T6085 applied in soil on crop residue), and

Trt4 (*T. gamsii* T6085 applied both in soil on crop residue and on spikes at anthesis) indicates the four different treatments we used in the experiment. The box plots show the 1st quartile, median 3rd quartile, and data set outliers. The changes in *T. gamsii* abundance across different treatments were not significant in crop residue, wheat spikes, and wheat kernels (ANOVA with Tukey HSD, $p>0.05$).

### 3.4.2 The variation in *F. graminearum* abundance due to *T. gamsii* T6085 treatment

The qPCR data were used to calculate the impact of *T. gamsii* T6085 application on the growth of *F. graminearum* in residue, wheat spikes and kernels. No significant changes in *F. graminearum* abundance due to the *T. gamsii* T6085 treatment were evident in crop residue, wheat spikes, or wheat kernels (ANOVA, $p>0.05$) (Figure 3.2).

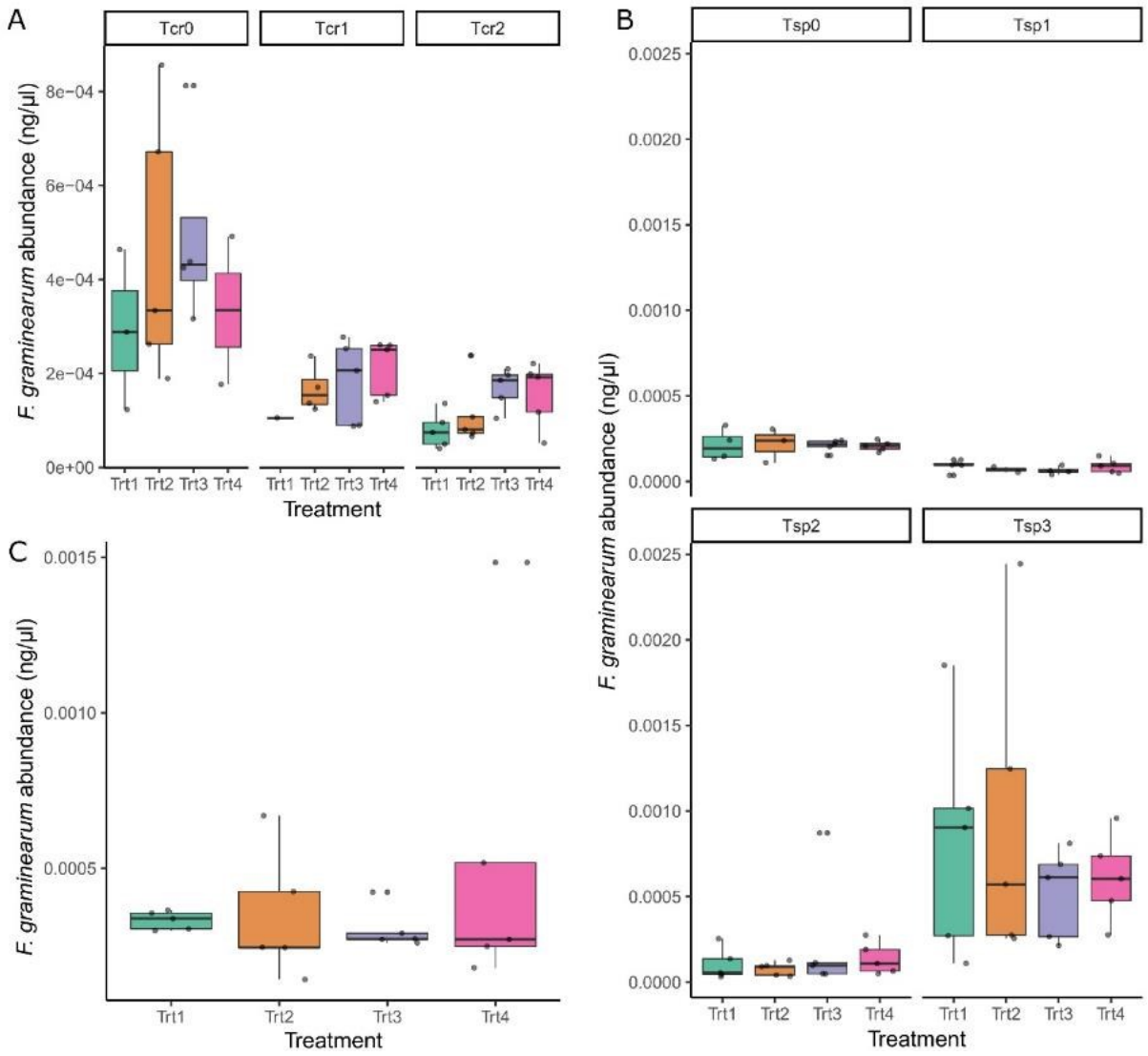



**Figure 3.2.** The impact of *T. gamsii* T6085 application on *F. graminearum* abundance. A: *F. graminearum* abundance in crop residue; B: *F. graminearum* abundance in wheat spikes; C: *F. graminearum* abundance in wheat kernels. $T_{cr}0$, $T_{cr}1$, and $T_{cr}2$ indicate the different time points at which the crop residue samples were collected, while $T_{sp}0$, $T_{sp}1$, $T_{sp}2$, and $T_{sp}3$ indicate the various time points at which the wheat spikes samples were collected. The x-axis labels Trt1 (Control), Trt2 (*T. gamsii* T6085 applied on spikes at anthesis), Trt3 (*T. gamsii* T6085 applied in soil on crop residue), and Trt4 (*T. gamsii* T6085 applied both in soil on crop residue and on spikes at anthesis) indicates the four different treatments we used in the experiment. The box plots show the 1st quartile, median 3rd quartile, and data set outliers. The changes in *F. graminearum* abundance due to *T. gamsii* T6085 treatment was not significant in crop residue, wheat spikes, and wheat kernels (ANOVA with Tukey HSD, $p>0.05$).

### 3.4.3 Variations in *F. graminearum* abundance in different wheat tissues over time

There was an apparent variation in *F. graminearum* abundance over time in wheat spikes and crop residues. The *F. graminearum* abundance in crop residues was within the range of $4.03\times10^{-5}$ - $8.57\times10^{-5}$ ng/µL of DNA, while *F. graminearum* abundance in wheat spikes was within the range of $3.11\times10^{-5}$ - $2.44\times10^{-3}$ ng/µL of DNA. In crop residue, the *F. graminearum* density was significantly higher at the initial time point ($T_{cr}0$), and it decreased over time (ANOVA with Tukey HSD, $p<0.05$). The deviations in *F. graminearum* density in wheat spikes showed an opposite trend to the residue; in wheat spikes, the *F. graminearum* density was significantly higher at harvest, and it had increased significantly over time showing lower densities at initial time points (ANOVA with Tukey HSD, $p < 0.05$) (Figure 3.3).

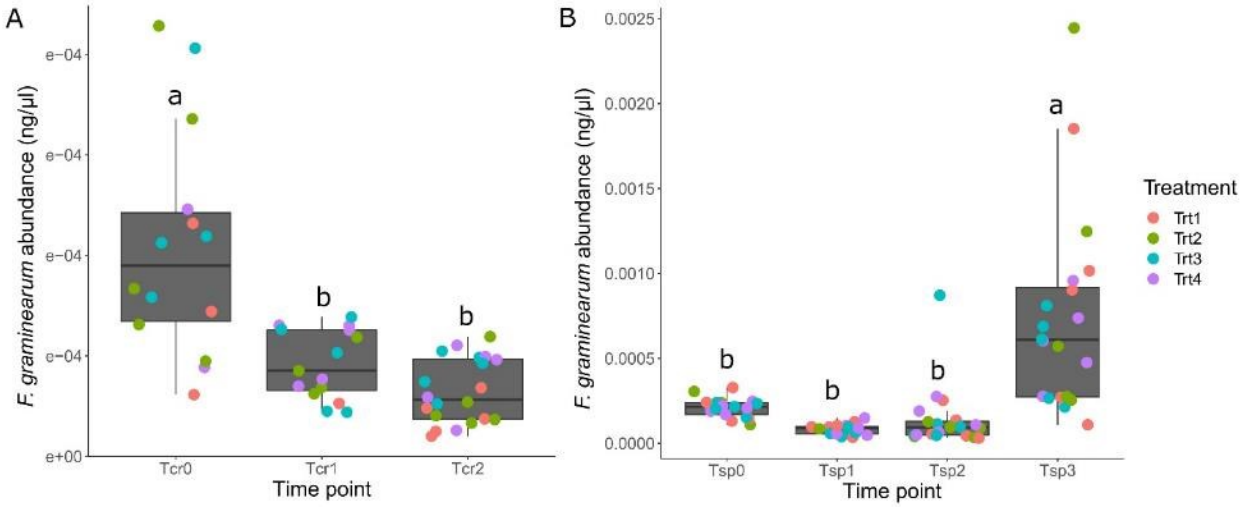



**Figure 3.3.** Variation of *F. graminearum* abundance over time in A: crop residue ($nT_{cr}0=14$, $nT_{cr}1=15$, $nT_{cr}2=20$) and B: wheat spikes ($nT_{sp}0=17$, $nT_{sp}1=16$, $nT_{sp}2=20$, $nT_{sp}3=20$) tissues. $T_{cr}0$, $T_{cr}1$, and $T_{cr}2$ indicate the different time points at which the crop residue samples were collected, while $T_{sp}0$, $T_{sp}1$, $T_{sp}2$, and $T_{sp}3$ indicate the different time points at which the wheat spikes samples were collected. Different colors of the legends represent different treatments including Trt1 (Control), Trt2 (*T. gamsii* T6085 applied on spikes at anthesis), Trt3 (*T. gamsii* T6085 applied onto crop residue at the soil surface), and Trt4 (*T. gamsii* T6085 applied onto both crop residue at the soil surface and onto spikes at anthesis). The box plot shows the 1st quartile, median, and the 3rd quartile of the data set. Different letters indicate a statistically significant difference ($p<0.05$). The *F. graminearum* abundance was significantly higher at the $T_{cr}0$ time point in the residue (Tukey HSD, $p<0.05$), and it decreased over time. The *F. graminearum* abundance is lower during $T_{sp}0$ to $T_{sp}2$ time points in wheat spikes and it reaches a significantly higher abundance at $T_{sp}3$ time point (ANOVA with Tukey HSD, $p<0.05$).

### 3.4.4 Relative abundances of different bacteria and fungi associated with different tissues.

The *ITS2* sequences and *16S rRNA* sequences were used to generate OTU tables, by which the relative abundances of different fungi and bacteria were evaluated. Crop residue showed a comparatively different microbial community composition compared to wheat spikes and kernels (Figure 3.4). Several bacterial genera were dominant in residue. These include *Sphingomonas, Allorhizobium-Neorhizobium-Pararhizobium-Rhizobium, Methylobacterium*, and *Tychonema*. The two most abundant fungi in the residue were unidentified taxa within the phylum Ascomycota. The highest abundance taxa belonged to the class Dothideomycetes and order Pleosporales. However, the second most abundant taxon was only identified up to the phylum level. In addition to these two taxa, *Cyphellophora* and *Alternaria* showed higher relative abundances in crop residue. In addition, *Pseudomonas*, *Enterobacter*, and *Pantoea* were the highly dominant bacterial genera in wheat spikes and kernels. These genera represented more than 60% of the bacterial *16S rRNA* sequences observed. The predominant fungal genera in wheat spikes were *Alternaria* and *Fusarium*, and these two fungal genera accounted for more than 60% of the observed fungal *ITS* sequences from wheat spikes. Similarly, wheat kernels were highly dominated by *Alternaria* and *Fusarium*, which together accounted for more than 70% of the observed fungal sequences from wheat kernels (Figure 3.4).

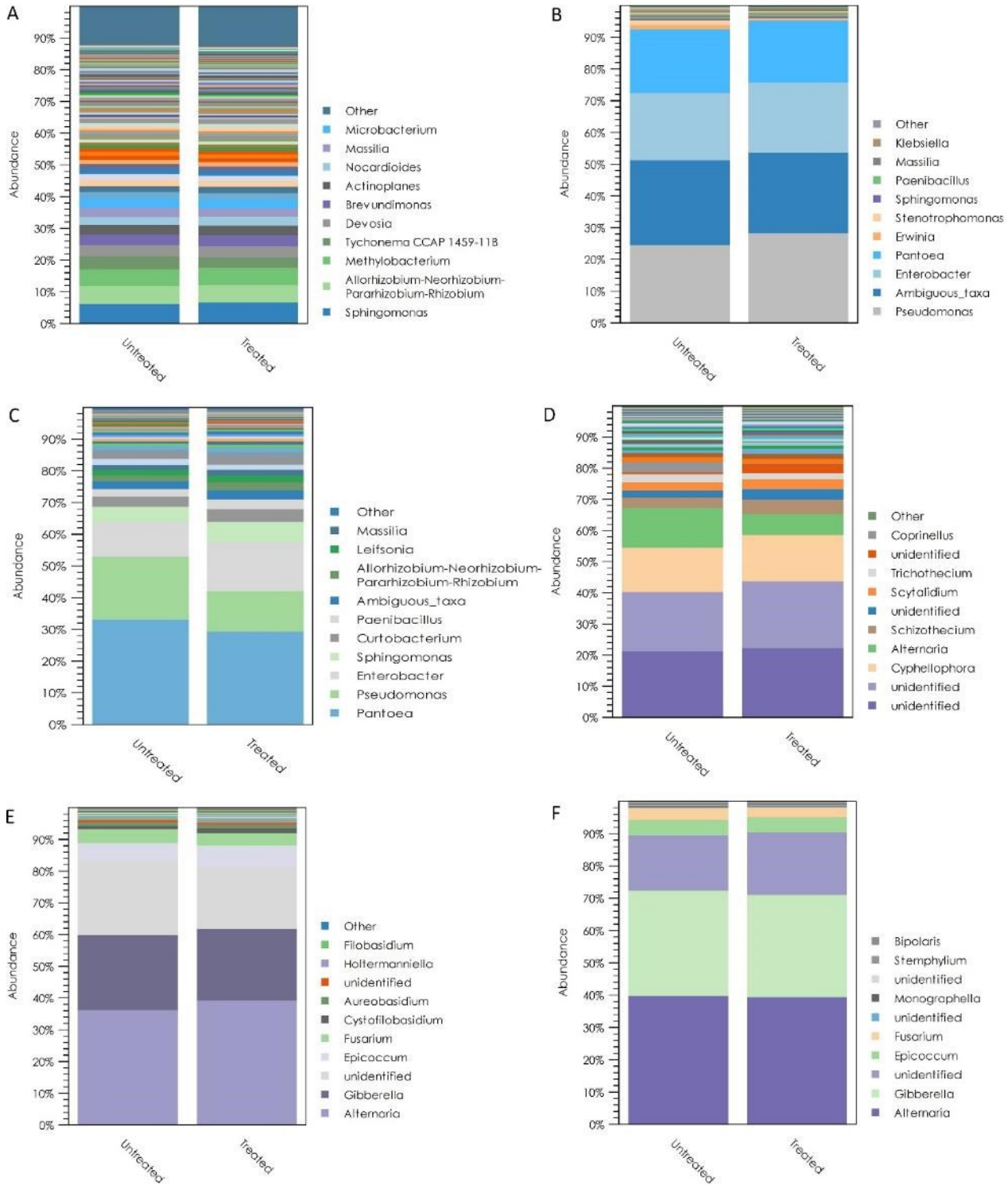



**Figure 3.4**. The relative abundances of different bacteria and fungi present in different samples. A: bacteria in residue B: bacteria in spikes C: bacteria in kernels D: fungi in residue E: fungi in spikes F: fungi in kernels. The legends show the ten most abundant bacterial and fungal genera in each tissue, and different colors represent different genera.

### 3.4.5 Variations in the microbial community due to treatment and over time

The changes in the microbial community due to the *T. gamsii* T6085 treatment were assessed using Bray-Curtis dissimilarities with principal coordinate analysis. Neither bacterial nor fungal community structures were appreciably changed due to the *T. gamsii* T6085 treatment (Figure 3.5).

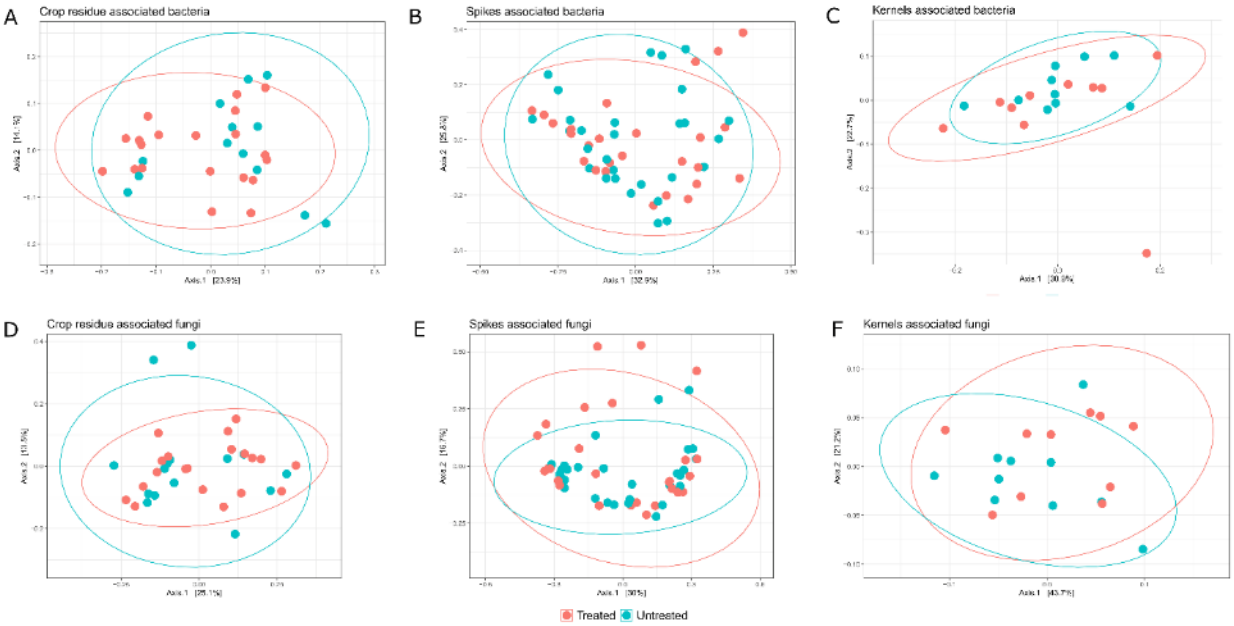



**Figure 3.5**. The variation in the microbial communities associated with crop residue, wheat spikes, and kernels due to the application of *T. gamsii* T6085 was minimal. The plots are principal coordinates ordinations derived from pairwise community dissimilarity values (Bray-Curtis index). A: crop residue-associated bacteria; B: wheat spikes-associated bacteria; C: wheat kernels-associated bacteria; D: crop residue-associated fungi; E: wheat spikes-associated fungi; F: wheat kernels-associated fungi. The red colour indicates the *T. gamsii* T6085 treated samples while the blue colour indicates the untreated samples. The ellipses represent 95% confidence level.

Even though there were not whole community rearrangements in response to the application of *T. gamsii* T6085, some individual taxa showed differential abundance due to the treatments (DEseq2, $p<0.05$). These differentially abundant bacterial taxa included different strains of *Caulobacter* and *Actinoplanes* in crop residue, *Pseudomonas*, *Massilia*, and *Erwinia*, in wheat spikes, and *Stenotrophomonas* in wheat kernels. Meanwhile, the differentially abundant fungal taxa included *Coprinellus*, *Agrocybe*, *Coniophora*, and *Nigrospora* in crop residue, *Fusarium*, and *Alternaria* in wheat spikes (Table 3.3).

**Table 3.3**. Differentially abundant bacterial and fungal taxa compared to Treatment 1 (control treatment) in crop residue, wheat spikes, and kernel samples

| Group | Tissue type | Time point | Treatment 2 | Treatment 3 | Treatment 4 |
|---|---|---|---|---|---|
| Bacteria | Crop residue | $T_{cr}2$ | *Caulobacter* sp. (-) | *Caulobacter* sp. (-)<br>*Actinoplanes* sp. (+) | *Caulobacter* sp. (-)<br>*Actinoplanes* sp. (+) |
| | Wheat spikes | $T_{sp}1$ | *Pseudomonas* sp. (-)<br>*Pseudomonas* sp. (-)<br>*Pseudomonas* sp. (-)<br>*Pseudomonas* sp. (-)<br>*Pseudomonas* sp. (-)<br>*Massilia* sp. (-) | *Pseudomonas* sp. (-) | |
| | Wheat spikes | $T_{sp}2$ | | | *Erwinia* sp. (+) |
| | Wheat spikes | $T_{sp}3$ | | | *Pseudomonas* sp. (-) |
| | Kernels | Harvest | | | *Stenotrophomonas* sp. (-) |
| Fungi | Crop residue | $T_{cr}2$ | *Coprinellus* sp. (-)<br>*Agrocybe* sp. (-) | *Coniophora* sp. (-)<br>*Coprinellus* sp. (-)<br>*Nigrospora* sp. (-) | *Coprinellus* sp. (-) |
| | Wheat spikes | $T_{sp}2$ | *Fusarium* sp. (+) | | |
| | Wheat spikes | $T_{sp}3$ | *Fusarium* sp. (-)<br>*Alternaria* sp. (+) | *Fusarium* sp. (-) | |

(-) indicate taxa that showed decreased abundance compared to treatment 1 (control treatment)
(+) indicate taxa that showed increased abundance compared to treatment 1 (control treatment)

Despite the minimal variations in fungal and bacterial community structures due to the application of *T. gamsii* T6085, there were clear changes in fungal and bacterial community composition over time in crop residue and wheat spikes (Figure 3.6). In crop residue samples, differentially abundant OTUs numbered 446 for the contrast between $T_{cr}0$ and $T_{cr}1$, 1 040 between $T_{cr}0$ and $T_{cr}2$, and 589 between $T_{cr}1$ and $T_{cr}2$. In wheat spike samples, differentially abundant OTUs numbered 76 between $T_{sp}0$ and $T_{sp}1$, 120 between $T_{sp}0$ and $T_{sp}2$, 111 between $T_{sp}0$ to $T_{sp}3$, 44 between $T_{sp}1$ and $T_{sp}2$, 68 between $T_{sp1}$ to $T_{sp}3$ and 69 between $T_{sp}2$ and $T_{sp}3$.

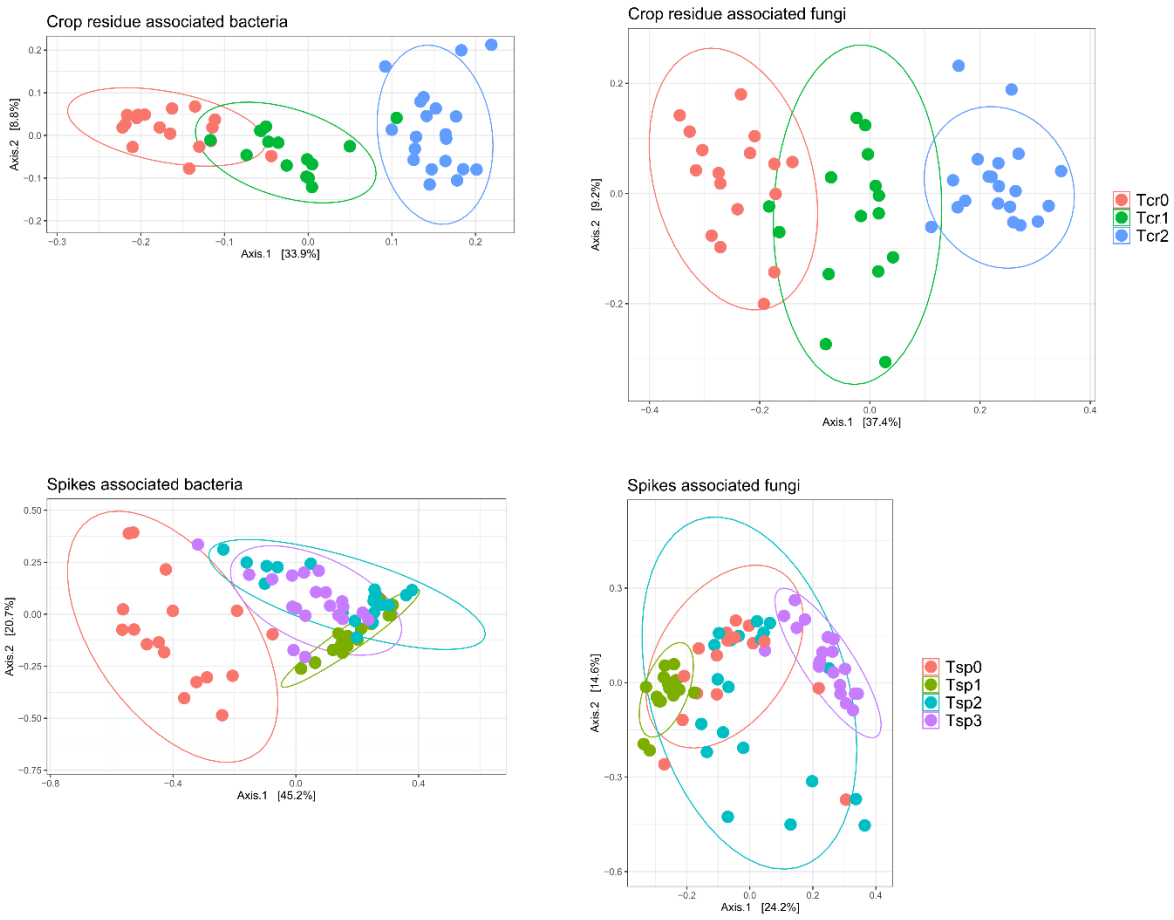



**Figure 3.6**. There was a progressive change in bacterial and fungal communities over time. The variations were more prominent in crop residue-associated microbial communities, compared to wheat spikes-associated microbial communities. The plots are principal coordinates ordinations derived from pairwise community dissimilarity values (Bray-Curtis index). A: crop residue-associated bacteria; B: crop residue-associated fungi; C: wheat spikes-associated bacteria; D: wheat spikes-associated fungi. $T_{cr}0$, $T_{cr}1$, and $T_{cr}2$ indicate the different time points at which the crop residue samples were collected, while $T_{sp}0$, $T_{sp}1$, $T_{sp}2$, and $T_{sp}3$ indicate the various time points at which the wheat spikes samples were collected.

### 3.4.6 Variation in microbial diversity

OTU richness and Shannon diversity index were calculated to further understand the dynamics in the microbial community in different tissues due to the *T. gamsii* T6085 treatment and over time. Crop residue had fungal and bacterial OTU richness within the range between 100-200 OTUs and 2000-3000 OTUs respectively. In both wheat spikes and kernels, fungal OTU richness was less than 200 OTUs while bacterial OTU richness was comparatively higher, within the range of 100-600 OTUs. The OTU richness values did not change in response to the treatments. However, there was a significant variation in the OTU richness over time in fungi in crop residue and both bacteria

and fungi in wheat spikes (ANOVA with Tukey HSD, $p<0.05$). In crop residue, the bacterial OTU richness did not significantly change over time while fungal OTU richness was significantly higher at $T_{cr}2$ compared to earlier time points (ANOVA with Tukey HSD, $p<0.05$). In wheat spikes, the bacterial OTU richness was significantly lower at $T_{cr}0$ time point compared to other time points while the fungal OTU richness significantly increased from $T_{cr}0$ to $T_{cr}1$ and again from $T_{cr}2$ to $T_{cr}3$ time points (ANOVA with Tukey HSD, $p<0.05$) (Figure 3.7).

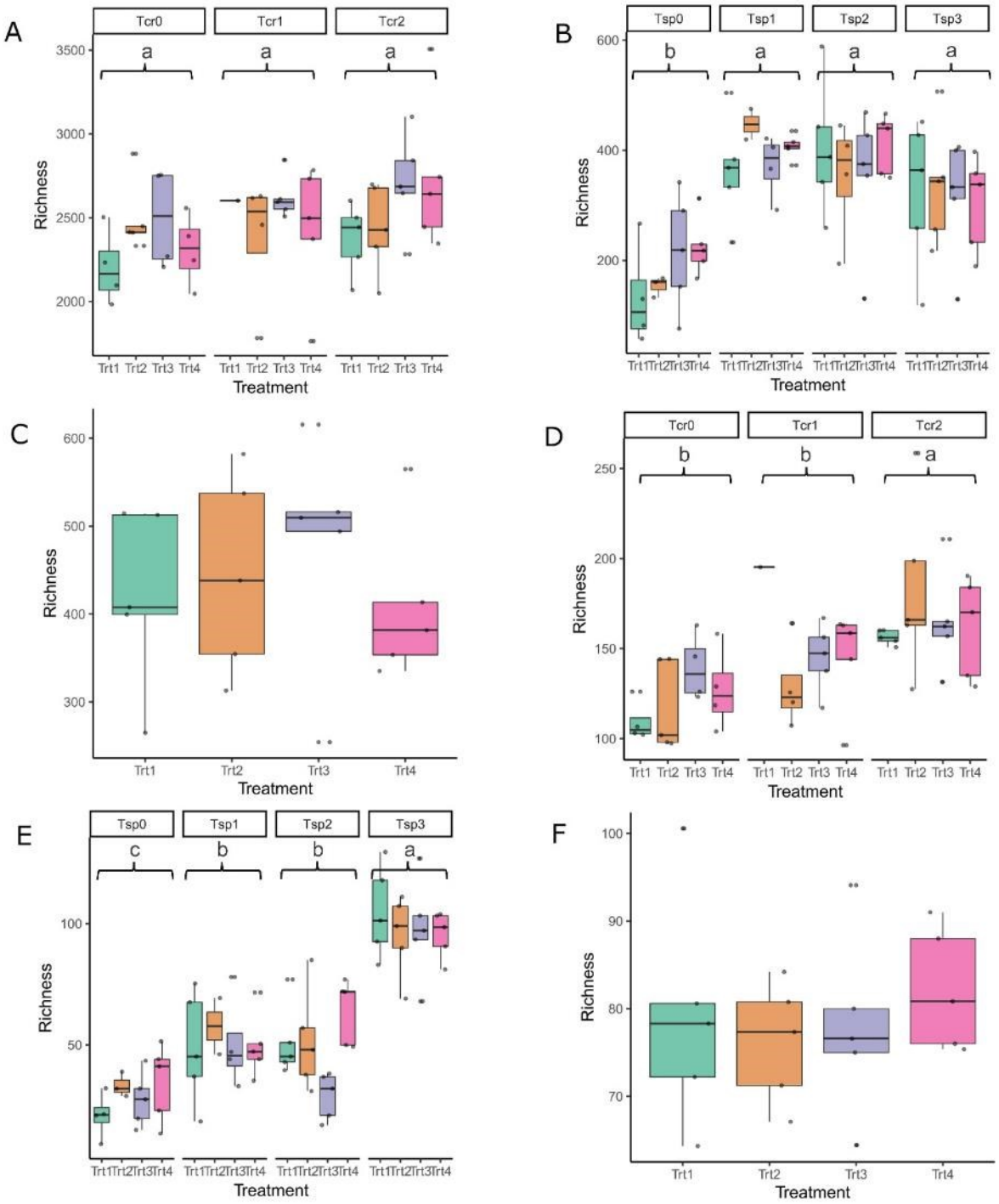



**Figure 3.7**. OTU richness in different tissues, among treatments and over time. A: bacteria in residue; B: bacteria in wheat spikes; C: bacteria in wheat kernels; D: fungi in crop residue; E: fungi in wheat spikes; F: fungi in wheat kernels. $T_{cr}0$, $T_{cr}1$, and $T_{cr}2$ indicate the different time points at which the crop residue samples were collected, while $T_{sp}0$, $T_{sp}1$, $T_{sp}2$, and $T_{sp}3$ indicate the various time points at which the wheat spikes samples were collected. The Trt1 (Control), Trt2 (*T. gamsii* T6085 applied on spikes at anthesis), Trt3 (*T. gamsii* T6085 applied in soil on crop residue), and Trt4 (*T. gamsii* T6085 applied both in soil on crop residue and on spikes at anthesis) indicates the

four different treatments we used in the experiment. The box plots demonstrate the 1st quartile, median, 3rd quartile and the outliers of the data set. Different letters indicate a statistically significant difference ($p<0.05$). The OTU richness values were not significantly different among different treatments in crop residue, wheat spikes, and wheat kernels. However, there were significant changes in species richness between different time points in some tissues (ANOVA with Tukey HSD, $p<0.05$).

Similarly, the Shannon index of bacterial and fungal OTU diversity was not significantly changed by the *T. gamsii* T6085 treatment. However, there was a significant variation in the Shannon index over time in microbes associated with wheat spikes and crop residue (Figure 3.8). The bacteria associated with crop residue had a significantly higher Shannon index at $T_{cr}2$ compared to initial time points (ANOVA with Tukey HSD, $p<0.05$). The fungi associated with crop residue had a significantly lower Shannon index at $T_{cr}0$ time point, which then shifted to a higher value over time (ANOVA with Tukey HSD, $p<0.05$). Further, there was a significant change in the Shannon index in the bacterial community at each time point except between $T_{sp}1$ and $T_{sp}2$ in spikes (ANOVA with Tukey HSD, $p<0.05$). The fungal community associated with wheat spikes showed a significant change in Shannon index between all time points except $T_{sp}1$ - $T_{sp}0$ and $T_{sp}2$ - $T_{sp}3$ (ANOVA with Tukey HSD, $p>0.05$).

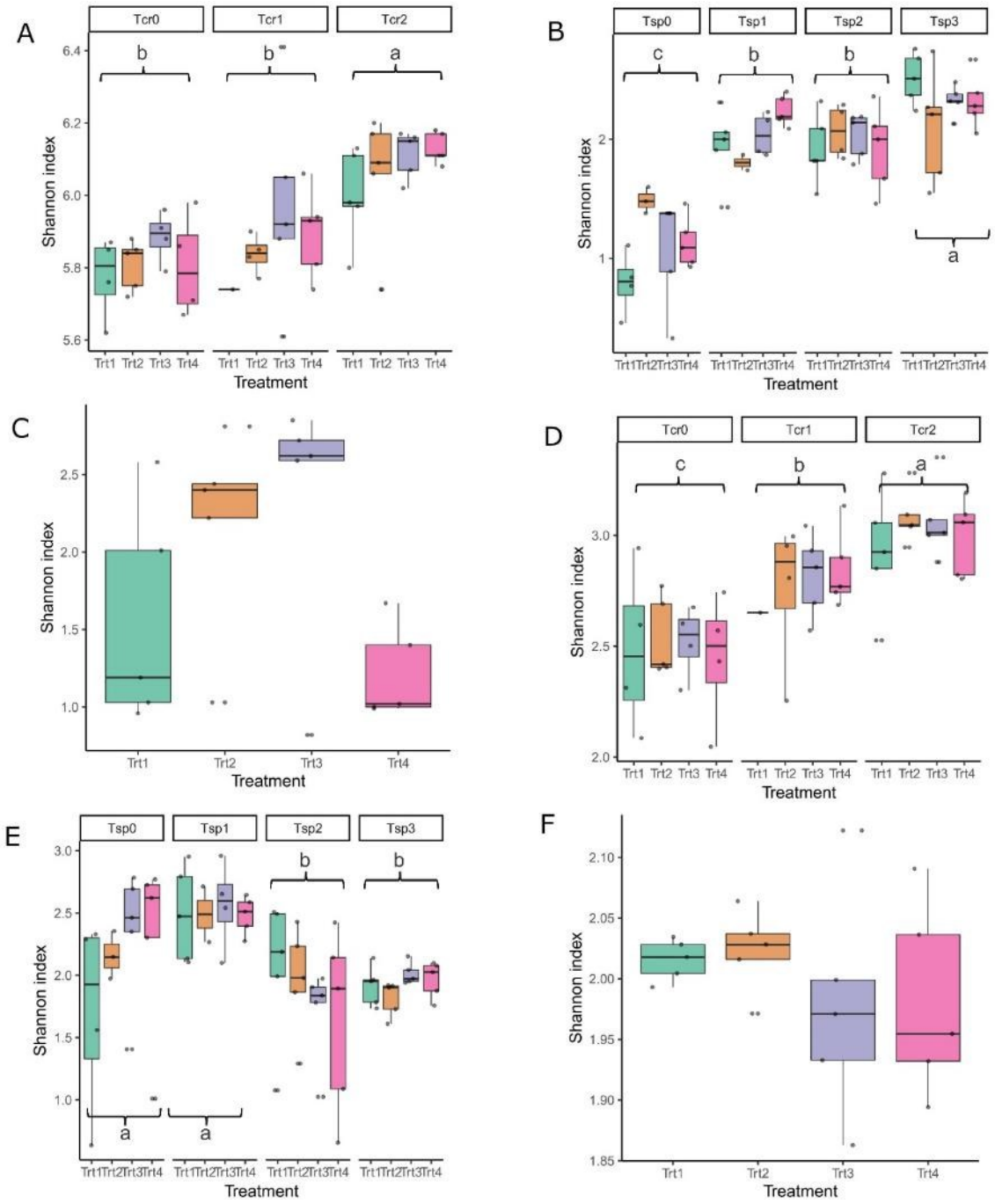



**Figure 3.8**. Shannon diversity index for microbial communities associated with different tissues, among treatments, and over time. A: bacteria in residue; B: bacteria in wheat spikes; C: bacteria in kernels; D: fungi in residue; E: fungi in wheat spikes; F: fungi in kernels. $T_{cr}0$, $T_{cr}1$, and $T_{cr}2$ indicate the different time points at which the crop residue samples were collected, while $T_{sp}0$, $T_{sp}1$, $T_{sp}2$, and $T_{sp}3$ indicate the various time points at which the wheat spikes samples were collected. The Trt1 (Control), Trt2 (*T. gamsii* T6085 applied on spikes at anthesis), Trt3 (*T. gamsii* T6085 applied in soil on crop residue), and Trt4 (*T. gamsii* T6085 applied both in soil on crop residue and on spikes at anthesis) indicates the four different treatments we used in the experiment. The box plots demonstrate the 1$^{st}$ quartile, median, 3$^{rd}$ quartile, and the outliers of the data set.

Different letters indicate a statistically significant difference ($p<0.05$). The Shannon index values did not change due to the treatments but did change over time (ANOVA with Tukey HSD, $p<0.05$).

## 3.5 DISCUSSION

Fusarium head blight (FHB) is an important fungal disease in wheat worldwide. An integrated management strategy is the most effective way of controlling the disease. Biological control is another method that can be combined into integrated management practices to enhance the outcome of disease management. *Trichoderma gamsii* T6085 has been identified as a potential biocontrol agent to manage FHB in wheat (Matarese et al., 2012). However, before employing *T. gamsii* T6085 in wheat fields, it is crucial to understand the non-target effects of the biocontrol agent on the natural microbial community associated with wheat. Therefore, this study's main objective was to evaluate the impact of *T. gamsii* T6085 application on *F. graminearum*, and on other bacteria and fungi associated with wheat tissues. In addition to that, we examined the microbial community composition in crop residue, wheat spikes, and kernels, and the microbial community changes over time.

The presence of *T. gamsii* T6085 was confirmed by qPCR data. However, *T. gamsii* T6085 showed a low abundance in all wheat tissues tested during the experiment. Additionally, the variation of *T. gamsii* T6085 in treated and untreated samples was not significant (Figure 3.1). The *T. gamsii* T6085 treatment had a minimal impact on the abundance of *F. graminearum* in crop residue, wheat spikes and kernels (Figure 3.2). The method we used to inoculate *T. gamsii* T6085 in wheat spikes may not be sufficient for the successful establishment of the fungus in wheat tissues, or *T. gamsii* T6085 may have colonized different portions of wheat spikes compared to *F. graminearum*. Non-uniform colonization of *T. gamsii* T6085 in wheat spikes was observed by Sarrocco et al., (2013) when they performed a similar field experiment in 2011 and 2012 growing seasons. According to their results, *T. gamsii* T6085 colonized lower spikelets more efficiently compared to upper spikelets of a wheat spike. This non-uniform colonization of wheat spikes by the fungus could be due to the falling of spores to the bottom with gravity when applying it as a spore suspension. The modifications that can be incorporated for an effective establishment of *T. gamsii* T6085 would be applying a higher amount of fungal inoculum onto crop residue, increasing the concentration of spore suspension, adding an adhesive compound to the spore suspension, and spraying it uniformly throughout the spikes (Sarrocco et al., 2013). Moreover, weather conditions also play an essential role. If the weather conditions are more favourable for the pathogen over the biocontrol agent, the

biocontrol agent may not form enough population to inhibit the pathogen. During a similar field experiment in the 2011 growing season, a significant reduction in FHB disease severity (DS: % of affected spikelets within the spike) was observed when *T. gamsii T6085* was applied on wheat spikes at anthesis. However, when they performed the same field experiment in the following year, they did not observe a significant reduction in FHB DS (Sarrocco et al., 2013). Therefore, the results can depend on the variations in weather conditions during the growing season.

We observed that *F. graminearum* abundance in crop residue and wheat spikes changed significantly throughout the period during which data were collected (Figure 3.3). There was a significantly higher amount of *F. graminearum* in crop residue initially. However, the *F. graminearum* density decreased over time in crop residue. *Fusarium* spp. grow well in nutrient-rich residue. They can use residues from wheat, maize or rape for their survival. However, *Fusarium* spp. are poor competitors among the crop residue-associated microbiome (Leplat et al., 2016, 2013). According to Leplat et al., (2016), *F. graminearum* growth rate is higher within sterile soil compared to non-sterilized soil. In presence of an antagonist their abundance can be decreased over time (Leplat et al., 2013). In addition to that, the weather can also influence the *Fusarium* abundance in crop residue over time. For instance, during dry weather conditions perithecia development is lower (Manstretta and Rossi, 2016). Therefore, the amount of *F. graminearum* present in soil can also vary with the humidity. However, the *F. graminearum* abundance in wheat spikes showed an opposite trend, where at the initial time points, the *F. graminearum* abundance was significantly lower in wheat spikes, and it was significantly higher during the harvest. The growth and development of *F. graminearum* have been enhanced during the seed maturation. This could be due to *F. graminearum* having more time to proliferate during the Maturation of wheat spikes.

The microbiome associated with the wheat plant is essential for its health. Different fungal and bacterial genera dominate in various types of plant tissues. Therefore, it is interesting to see the changes in the microbiome according to the niche in which they reside. Our results showed that wheat residue were primarily dominated by *Alternaria* and *Cyphellophora,* two unidentified fungi*,* and several bacterial genera with higher diversity. *Alternaria* and *Fusarium* were the dominant fungal genera in wheat spikes and kernels*,* while *Pseudomonas*, *Enterobacter*, and *Pantoea* were

the predominant bacterial species (Figure 3.4). The dominancy of *Fusarium* and *Alternaria* in wheat phyllosphere has been previously observed in several studies (González et al., 2008; Hertz et al., 2016; Schiro et al., 2018). According to Hertz et al., (2016), the dominant pathogen may depend on the climatic conditions. In the same study, they sparsely observed *F. graminearum* in wheat due to the dry climatic conditions during anthesis. Both *Fusarium* and *Alternaria* are pathogenic to wheat plants and contaminate the seeds with toxic compounds harmful to the consumers. The presence of the two primary pathogens may have reduced the colonization of other fungi in the wheat plant through competition (Hoffmann et al., 2021; Müller et al., 2018). However, the predominant bacterial species, including *Pseudomonas*, *Enterobacter*, and *Pantoea,* have overcome the competition from the two fungal pathogens and have well colonized the wheat spikes and kernels.

Interestingly, all these predominant bacterial genera include plant-beneficial and potential biocontrol agents (Chen et al., 2017; Kumar et al., 2017; Müller et al., 2018). According to Müller et al., (2018), *Pseudomonas* species have shown potential biocontrol ability against *F. graminearum*. Yet, the naturally occurring *Pseudomonas* spp. are unlikely to reduce FHB in wheat. Even though the natural populations of these bacteria do not inhibit FHB, artificial inoculation or combining with another biocontrol agent like *T. gamsii* may increase the chance of mitigating the *F. graminearum* infection in wheat. Bakker and McCormick, (2019), also observed similar bacterial and fungal compositions in wheat kernels. Their study showed more than 100 bacterial taxa and several dozens of fungal taxa in an individual wheat kernel and more significant microbial composition changes over the years. They found a negative correlation between *Fusarium* load and the *Sphingomonas* abundance in wheat kernels. Our results also showed a higher relative abundance in *Sphingomonas* in wheat kernels. Therefore, *Sphingomonas* could be another potential biocontrol agent to be used in fighting against FHB in wheat (Bakker and McCormick, 2019).

One drawback we encountered in this study is not identifying *Trichoderma* sequences within the microbiome profiles by the workflow we used; given that *T. gamsii* T6085 was applied to the plots, we expected to observe this taxon in our microbiome profiles. The mock community control samples we used contained *Trichoderma reesei* sequences. However, the *ITS* sequence reads of

*Trichoderma reesei* could not be classified further than the family Hypocreaceae. Similarly, in our OTU table, we encountered OTUs classified under family Hypocreaceae. Therefore, it appears that the method we used for fungal community profiling does not provide good discrimination among genera or species within this family. In addition, even though the *ITS* is considered a superior marker in species identification across the Kingdom fungi, the discriminatory power of *ITS* in Ascomycota is lower (Schoch et al., 2012).

The Bray-Curtis dissimilarity is a multivariate analysis method that can be used to perform pairwise comparisons across different treatment levels (Qian et al., 2020). We used this analysis method to compare the microbial community composition among other treatments and among different time points. The results suggested that there were not any microbial community-scale differences when *T. gamsii* T6085 was applied as a biocontrol agent (Figure 3.5). Nevertheless, several fungal and bacterial taxa were differentially abundant in *T. gamsii* T6085 treated samples compared to control samples (Table 3.3). Yet, the impact of plant tissue type and the plant development stage was more apparent than the impact of *T. gamsii* T6085 colonization on the variations in microbial community structure (Figure 3.6). Similar results were observed in several other studies when biocontrol agents were applied for the prevention of other pathogens, including *R. solani* (Grosch et al., 2006; Kröb, *Phytophthora capsici* (Cucu et al., 2020) and *Verticillium dahlia* (Scherwinski et al., 2007). These studies have also encountered a more significant effect on the microbial communities in response to the plant growth stage than the treatments. However, there could be an effect of environmental changes on the microbial community-scale differences other than the plant development stage (Araujo et al., 2019; Latz et al., 2021; Lauber et al., 2013; Massart et al., 2015).

The operational taxonomic unit richness and the Shannon diversity index are commonly used estimates to measure the biodiversity of microbial communities. Therefore, it is crucial to calculate the diversity indices to see the alteration made by the *T. gamsii* T6085 (Brown et al., 2007; Spellerberg and Fedor, 2003). However, the impacts of *T. gamsii* T6085 on OTU richness and Shannon index of the microbial community associated with crop residue, wheat spikes, and kernels were minimal. Yet, there was an apparent variation in OTU richness and Shannon index over time (Figure 3.7 and Figure 3.8). Our results indicated the critical role of the plant development stage,

tissue type, and environmental conditions in maintaining the microbial community structure. However, the application of the *T. gamsii* T6085 has a limited impact on the changes in the microbial populations associated with wheat plants. Having a minimal effect on the natural microbial community from a biocontrol agent is essential for a sustainable agricultural system.

# 4.0 CHAPTER 2

## Infection of a CRISPR/Cas9 derived green-fluorescent protein labeled *Leptosphaeria maculans* strain on *Brassica napus*

## 4.1 ABSTRACT

Alukumbura, Arshani. M.Sc., The University of Manitoba, December, 2021. Infection of a CRISPR/Cas9 derived green-fluorescent protein labeled *Leptosphaeria maculans* strain on *Brassica napus*. Major professors: Dr. Dilantha Fernando and Dr. Matthew Bakker.

*Leptosphaeria maculans* is a pathogenic fungus that causes the blackleg disease in canola plants. The CRISPR/Cas9 system is used in genetic engineering to knock out genes for the identification of their function. However, this technology sometimes gives rise to non-target mutations. The mutant JN3 isolate (mJN3) of *L. maculans* includes an unknown mutation in its genome created by the CRISPR/Cas9 system. Due to the random mutation, the mJN3 has defects in infecting the susceptible *B. napus* variety, Westar. The objective of this study was to tag the mJN3 and its wild-type strain JN3 with the GFP reporter to observe their changes during the invasion of canola leaf tissues. The pRM-eGFP vector with the *egfp* gene and the *ble* antibiotic resistance gene was transferred into *A. tumefaciens* cells by electroporation. The transformed *A. tumefaciens* cells were co-cultured with fresh spores of mJN3 and JN3 to transfer its T-DNA region into the fungal cells. The transformed *L. maculans* isolates that contain the *egfp* gene were selected using fluorescent microscopic observations and by PCR amplification of the *egfp* gene. Two isolates were selected from mJN3gfp and JN3gfp transformants (mJN3gfp2 and JN3gfp2) to analyze tissue colonization. The strain LmGFP (a pre-existing GFP expressing *L. maculans* strain) was used as the positive control. The transformed *L. maculans* isolates of mJN3gfp and JN3gfp showed reduced pathogenicity compared to untransformed *L. maculans* strains when inoculated into cotyledons of Westar. When inoculated into the cotyledons, the mycelial growth of mJN3gfp2 and JN3gfp2 was similar. Further, the colonization of the mJN3gfp2 isolate was compared with the LmGFP isolate. The results indicated that both isolates colonized the intercellular spaces of the canola tissue similarly. However, the difference was that extension of the hyphae of mJN3gfp2 was restricted to the area around the inoculation site but the hyphae of LmGFP extended toward the leaf petiole. The results indicated that the plant defence responses restrain the growth of mJN3gfp2. Therefore, mJN3 should have altered the expression of an important pathogenicity gene which would otherwise help them to overcome the plant defence responses.

## 4.2 INTRODUCTION

Blackleg is a devastating fungal disease in canola (*Brassica napus*) which is a major agricultural crop in Canada. The first blackleg disease outbreak in Canada was reported in 1980, causing more than 50% yield losses all over the country (Juska et al., 1997). However, the disease was controlled over several years using resistant canola varieties and crop rotation. However, disease resistance in canola plants was overcome by the pathogen population over time through evolutionary changes. Therefore, the blackleg disease again turned into a critical issue in Canadian canola fields since 2012 (Zhang and Fernando, 2017).

The plant pathogenic fungus *L. maculans* is the primary causative agent of the disease. The *L. maculans* is an Ascomycetes fungus that overwinters in crop residue and infects the canola plants during spring. The fungus produces two types of spores: air-borne ascospores (sexual spores) and splash-borne pycnidiospores (asexual spores). The ascospores travel long distances over the wind, while the pycnidiospores travel short distances (Bousset et al., 2015; Koch et al., 1989; Venn, 1979). When the *L. maculans* spores are in direct contact with canola leaves, they germinate, and the fungal hyphae extend towards the intercellular spaces of the plant tissue through the natural openings (stomata) or wounds. The fungi colonize the intercellular spaces of the leaf tissue necrotizing the surrounding tissues causing the brown-colored leaf lesions on canola leaves. Later, *L. maculans* extend towards the stem base through the vascular tissues. When the fungi reach the stem base, they leave the vascular tissues and necrotize the surrounding tissues causing the stem cankers. The stem cankers block the plant's water and nutrient uptake and kill the plant eventually (Howlett, 2004; Howlett et al., 2001; Sonah et al., 2016).

Various methods are being used to control the blackleg disease in canola including, crop rotation, tillage practices, and fungicide application. Among these different strategies in blackleg disease management, the most promising method is the utilization of blackleg-resistant canola varieties in the field (Dolatabadian et al., 2021; Zhang and Fernando, 2017). *B. napus* has two main types of resistance against *the L. maculans* infection: major gene resistance (qualitative/ seedling resistance) and minor gene resistance (quantitative/ adult plant resistance). The seedling resistance is governed by a single *R* gene. The proteins encoded by the *R* genes interact with the *L. maculans*

elicitor molecules and initiate plant defence responses. The genes encoding for pathogen elicitor molecules are *Avr* genes (Keen, 1990; Rimmer, 2006). So far, at least 18 *R* genes have been identified in *B. napus*, while at least 17 *Avr* genes have been identified within *L. maculans* population (Degrave et al., 2021; Liban et al., 2016; Liu et al., 2021; Raman et al., 2021; Zhai et al., 2021). On the other hand, multiple resistant genes govern the adult plant resistance. The adult plant resistance has higher durability compared to seedling resistance, and the presence of both types of resistance is more favourable when overcoming the blackleg disease development (Brun et al., 2010).

Understanding the interaction between the host and the pathogen is vital in discovering promising disease management strategies. GFP is a marker that can be expressed in plant pathogens to visualize them in live plant tissues. GFP was first discovered from the jellyfish *A. victoria* in 1961 (Shimomura et al., 1962). The discovery led to a revolution in live-cell imaging. This gene encoded fluorescent marker emits green fluorescent light when excited with blue light, and the illumination can be visualized using a fluorescent microscope. GFP has been expressed in various animals, plants and microbes. *Ustilago maydis* was the first filamentous fungus to be labelled with GFP (Spellig et al., 1996). GFP has been successfully expressed in many other filamentous fungi such as *Cochliobolus heterostrophus* (Maor et al., 1998), *F. oxysporum* (Lagopodi et al., 2002), *Aspergillus nidulans* (Yang et al., 2004), and *Colletotrichum destructivum* (Chen et al., 2003). A GFP-tagged *L. maculans* strain was first reported in 2001 (Sexton and Howlett, 2001). Compared to traditional markers used to examine fungi, the GFP is stable and easy to use as it does not rely on external substrates. In addition, the visualization of GFP-tagged fungi in plant tissues does not involve destructive sample preparation, which is time-consuming. It allows for a continuous study of fungal propagation in real-time. Due to these properties, the GFP has become one of the most convenient strategies to observe plant-pathogen interactions in living tissues (Lorang et al., 2001; Valdivia et al., 1996).

The engineering of the fungal genome is complicated due to the complex cell wall structure of filamentous fungi. Several methods are available for genetic transformation of fungi, including protoplast mediated transformation, shock-wave transformation, biolistic transformation and electroporation (Li et al., 2017). Among these various methods, the *Agrobacterium*-mediated

transformation (ATMT) is considered the most efficient fungal transformation method. It is simple, and the transformation efficiency is higher than the conventional methods (Hooykaas et al., 2018; Li et al., 2017). The ATMT method relies on the soil bacterium *A. tumefaciens*'s ability to transfer part of its DNA of the tumour-inducing plasmid (Ti plasmid) into the host genome during the infection. The DNA sequence that is transferred is known as the T-DNA region. The ATMT method needs two plasmids, which are binary vector and helper plasmids. The binary vector was designed to facilitate an easy transfer of the T-DNA into the fungal cells. The helper plasmid includes virulence genes that encode proteins that enable T-DNA transfer and integration. The primary model of integrating the T-DNA with the desired gene expression cassette into the host genome is the non-homologous end-joining pathway. Thus, the ATMT is a convenient method for filamentous fungal transformation (Hooykaas et al., 2018; Li et al., 2017; Park et al., 2015).

The interaction between plants and pathogens is complex and yet more remains to be discovered. CRISPR/Cas9 mediated gene editing is an effective method to find the function of different proteins encoded by various genes. This study incorporated a CRISPR/Cas9 based mutant *L. maculans* fungus named mJN3 and its wild-type isolate JN3. The mJN3 isolate includes an unknown mutation in its genome created by the CRISPR/Cas9 system. Due to the random mutation, the mJN3 has lost its pathogenicity towards the susceptible *B. napus* variety Westar. This study aimed to develop GFP-tagged mJN3 and JN3 isolates and observe their ability to invade plant tissues under the fluorescent microscope.

## 4.3 MATERIALS AND METHODS

### 4.3.1 Fungal material and inoculum preparation

The *L. maculans* strain JN3 and its mutant mJN3 from the Fernando laboratory culture collection were used for the experiment. The fungi were grown in V8 media with 0.35% (w/v) streptomycin sulphate under fluorescent lights at room temperature. The culture plates were flooded with sterilized distilled water to prepare the fungal inoculum, and the mycelia were scraped gently using a sterilized metal spatula to dislodge the pycnidiospores. The spore suspension was filtered using a sterilized Miracloth and stored at -20 ℃ for future use (Liban et al., 2016). The remaining mycelia on the plates were scraped and collected into 1.5 mL Eppendorf tubes and used for fungal DNA extraction.

### 4.3.2 Fungal DNA extraction

Fungal DNA was extracted using a modified CTAB (Cetyl Trimethyl Ammonium Bromide) fungal DNA extraction protocol (Lee and Taylor, 1990). The fungal mycelia collected into 1.5 mL Eppendorf tubes were lysed with 2×CTAB DNA extraction buffer. Sterilized ceramic beads (0.2 mm, 6-8 beads per tube) were added into the tubes for mechanical disruption. The mixture was homogenized at 5 000 rpm for 45 secs and incubated for 20 – 30 mins at 65 ℃ in a water bath. The Phenol: Chloroform extraction was performed twice using the 300 µL of Phenol: Chloroform: Isoamyl alcohol (25: 24: 1) solution. The DNA was precipitated using 80 µL of 5 M NaCl and 1 mL of 95% ethyl alcohol and washed twice with 200 µL of 70% alcohol. The DNA pellet was air-dried and dissolved in 100 µL of nuclease-free water and 1 µL of RNase. The DNA extracts were stored at -20 ℃ until used.

### 4.3.3 Characterization of the avirulence gene profile

The avirulence gene profile of the JN3 isolates was examined by genotypic and phenotypic methods. For the genotypic identification of the *R* genes, gene-targeted PCR assays were performed. For the phenotypic identification, a cotyledon inoculation assay was carried out in the greenhouse, using a set of differential canola lines. The *Avrlm1*, *2*, *3*, *4*, *6*, *7*, and *9* genes were identified employing both genotypic and phenotypic methods. The *AvrLm5*, *10*, *11* genes were assessed only using the genotypic method due to the unavailability of the differential lines

containing *Rlm5*, *10*, and *11* genes. In addition, the *AvrLepR1*, *LepR2*, and *LepR3* genes were tested only via the phenotypic method due to the lack of primers to target these genes.

#### 4.3.3.1 Genotypic identification

The extracted fungal DNA was amplified using the target-specific primers (Table 4.1). The 20 µL PCR mixture was comprised of 10 µL of 2X FroggaMix plus master mixture (FroggaBio, Canada), 0.2 µM forward primer, 0.2 µM reverse primer, template DNA, and nuclease-free water. The PCR program consisted of initial denaturation at 95 ℃ for 3 mins, denaturation at 95 ℃ for 30 secs, annealing at 50 ℃ for 30 secs, extension at 72 ℃ for 1 min (35 cycles), final extension at 72 ℃ for 5 min. The amplified products were visualized using 2% agarose gel in TAE buffer (Tris HCL, EDTA, and glacial acetic acid), stained with red safe nucleic acid visualization solution (FroggaBio, Canada) and sized by comparison with a 100 bp ladder. The PCR banding pattern in the agarose gel was observed using a UV transilluminator.

**Table 4.1**. The nucleotide sequences of each primer pair used to amplify the avirulence genes in *L. maculans* isolates

| Primer pair | Sequence (5' to 3`) | Reference |
|---|---|---|
| *AvrLm1-F* | CTATTTAGGCTAAGCGTATTCATAAG | Gout et al., 2006 |
| *AvrLm1-R* | GCGCTGTAGGCTTCATTGTAC | |
| *AvrLm2-F* | CGTCATCAATGCGTTCGG | Ghanbarnia et al., 2014 |
| *AvrLm2-R* | CTGGATCGTTTGCATGGA | |
| *AvrLm3-F* | GAGAGAACTAGTCTGTTAAATGCCTGCTGT | Plissonneau et al., 2016 |
| *AvrLm3-R* | GAGAGACTCGAGCGCGCTTATGTTAGAATC | |
| *AvrLm4-7-outer-F* | GTAACAAAGTAACGAAGGGCTTAATT | Zou et al., 2018 |
| *AvrLm4-7-outer-R* | GAAAACTCACCTCCGTATCTTTAGTC | |
| *AvrLm4-7-Inner-F* | TCTAAACCAGTCTCCTGCCC | Zou et al., 2018 |
| *AvrLm4-7-Inner-R* | TAG CTCAGC ACCTGG AGTTATATATC | |
| *AvrLm5-9-F* | ACAACCACTCTTCTTCACAGT | Zou et al., 2018 |
| *AvrLm5-9-R* | TGGTTTGGGTAAAGTTGTCCT | |
| *85C-F* | TCCTTCGCTTAGTGATTACCCAATTGAACA | Zou et al., 2018 |
| *85C-R* | CGTTCTTTGTTCTGTAGTGTAACGTCGCG | |
| *AvrLm6-F* | TCAATTTGTCTGTTCAAGTTATGGA | Fudal et al., 2007 |
| *AvrLm6-R* | CCAGTTTTGAACCGTAGTGGTAGCA | |
| *AvrLm10A-F* | TCAAAAAGCGGCCTTCTC | Petit-Houdenot et al., 2019 |
| *AvrLm10A-R* | GAAGTTAAGAGAGCAGGTGAGG | |
| *AvrLm10B-F* | GCGACAGGAATCACAACCTT | Petit-Houdenot et al., 2019 |
| *AvrLm10B-R* | GCCTACGCCAATCTCCAATA | |
| *AvrLm11-F* | TGCGTTTCTTGCTTCCTATATTT | Balesdent et al., 2002 |
| *AvrLm11-R* | CAAGTTGGATCTTTCTCATTCG | |

#### 4.3.3.2 Phenotypic identification

For the phenotypic identification of avirulence genes, the cotyledon inoculation assay was performed using 11 *B. napus* differential lines, including Topas Rlm1, Topas Rlm2, 02-22-2-1, Topaz Rlm4, Forge, 01-23-2, Goeland, 1065, 1135, Surpass400, and Westar (Table 4.2). The seeds of the *B. napus* differential lines were planted and grown for seven days in the greenhouse at 16 ℃ in the night and 21 ℃ in the day with a 16-hour photoperiod. During the inoculation day, the concentration of the fungal inoculum was adjusted to $2\times10^7$ spores/mL using a hemocytometer. The cotyledons of the seven-day-old seedlings were punctured using a tweezer and inoculated with 10 µL droplets of inoculum (4 inoculation sites per plant). For each test, six plants were inoculated. The disease symptoms were evaluated after 14 days post-inoculation (dpi) using the 0 - 9 rating scale according to (Kutcher et al., 2010). The mean disease score (MDS) was used to determine the phenotype of each *L. maculans* isolate. The MDS 0 - 4.9 was considered avirulent, and MDS 5 - 9 was considered virulent. The interaction between each isolate with different *B. napus* lines were used to deduce the avirulence gene profile of the JN3 and mJN3 isolates (Fernando et al., 2018).

**Table 4.2.** The resistance genes present in each differential line of *B. napus* plants are used for phenotypic characterization of *L. maculans* avirulence genes

| ***B. napus* differential line** | ***B. napus* resistance gene** | **Reference** |
|---|---|---|
| Topaz Rlm1 | *Rlm1* | Larkan et al., 2016 |
| Topaz Rlm2 | *Rlm2* | Larkan et al., 2016 |
| 02-22-2-1 | *Rlm3* | Gout et al., 2006 |
| Topaz Rlm4 | *Rlm4* | Larkan et al., 2016 |
| Forge | *Rlm6* | Rashid et al., 2018 |
| 01-23-2-1 | *Rlm7* | Dilmaghani et al., 2013 |
| Goeland | *Rlm9* | Balesdent et al., 2006 |
| 1065 | *LepR1* | Kutcher et al., 2010 |
| 1135 | *LepR2* | Kutcher et al., 2010 |
| Surpass400 | *LepR3* | Larkan et al., 2013 |
| Westar | No R gene | Balesdent et al., 2002 |

### 4.3.4 The examination of the pathogenicity of mJN3 and JN3 isolates

The cotyledon inoculation assay was performed to test the differences in the infection process between the mJN3 and the JN3 strains. For the experiment, 27 randomly selected *B. napus* varieties with different resistance genes, 1 *Brassica juncea* variety, and 2 *Brassica alba*

varieties were used. Four cotyledon sites of six, seven-day-old seedlings for each variety were inoculated with fungal inoculum ($2\times10^7$ spores/mL). The inoculated plants were incubated for 14 days in the greenhouse at 16 ℃ in the night and 21 ℃ in the day with a 16-hour photoperiod. Two trials were performed, and the disease symptoms were evaluated after 14 dpi using the 0 - 9 rating scale according to (Kutcher et al., 2010). The MDS was calculated. To deduce the phenotype of *Brassica* varieties the MDS ≤4.5 was considered as resistant (R), the MDS of 4.6 – 6.0 was considered as the intermediate resistant (IR), and the MDS of 6.1 – 9.0 was considered as the susceptible (S) phenotype. The interactions between either mJN3 or JN3 isolates with different *Brassica* plants were used to differentiate pathogenicity behaviour between the wildtype and mutant strain (Zhang et al., 2016).

### 4.3.5 Development of a transgenic fungus

The ATMT method was used for the development of the transgenic fungi expressing the *egfp* gene. The process consists of a series of steps, including antibiotic sensitivity testing, transfer of the pRM-eGFP vector into *A. tumefaciens* cells, transformation of *L. maculans* isolates, and mitotic stability testing.

#### 4.3.5.1 The pRM-eGFP vector

The pRM-eGFP vector with the *egfp* gene was kindly provided by Dr. Marcelo Fernandez Lahore (University of Jacob, Bremen, Germany). The vector was designed to be transformed through the *Agrobacterium*-mediated transformation method. The T-DNA region of the pRM-eGFP vector consists of the *egfp* reporter gene and the *ble* antibiotic resistance gene, which gives phleomycin resistance. The expression of the *egfp* gene is regulated by the *A. nidulans PgpdA* constitutive promoter, while the expression of the *ble* gene is regulated by the *A. nidulans PtrpC* promoter. The vector backbone consists of the *KanR* gene, which confers resistance to the kanamycin. The vector came in *E. coli* cells (Figure 4.1) (Mora-Lugo et al., 2014).

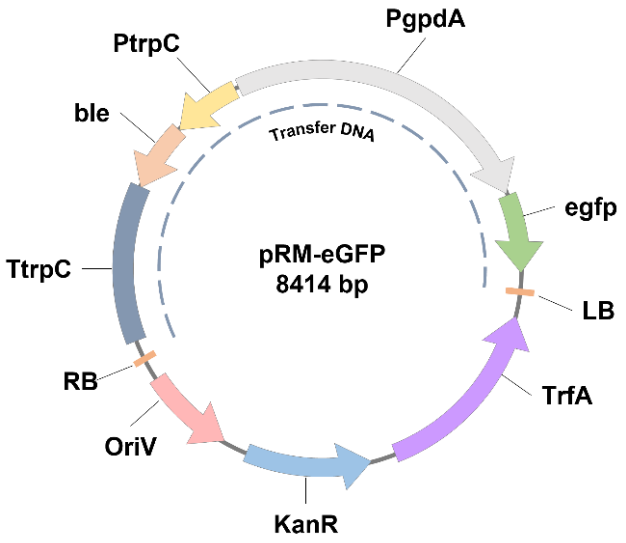



**Figure 4.1**. The pRM-eGFP vector (8414 bp) contains the *egfp* gene that encodes for enhanced GFP and the *ble* gene, which confers the resistance to phleomycin. The constitutive expression of the *egfp* gene is regulated by the *PgpdA* promoter. The *ble* gene is under the control of the *PtrpC* promoter and the *TtrpC* terminator. The vector backbone consists of the Kanamycin resistance gene (*KanR*). The LB and RB indicate the left border and the right border of the T-DNA region, respectively.

#### 4.3.5.2 Plasmid DNA extraction and the transformation of *A. tumefaciens* cells by electroporation

According to the manufacturer's protocol, the plasmid DNA was extracted from the *E. coli* cells using the OMEGA plasmid DNA extraction kit. The electrocompetent *A. tumefaciens* AGL-1 cell line (Gold Biotechnology®, USA) was used for the experiment. The AGL-1 cells carry a carbenicillin resistance gene in their genome. The AGL-1 cells were removed from the -80 ℃ freezer and thawed completely on ice (10-15 mins). Sterile cuvettes and microcentrifuge tubes were placed on ice to be chilled. 15 µL of AGL-1 cells and 1.5 µL of plasmid DNA were mixed in the chilled cuvette. The cuvette with the bacterial cell suspension and plasmid DNA was electroporated using the Gene Pulser Xcell Electroporation System (Biorad, Canada). The electroporated cell suspensions were plated on LB media containing antibiotics, carbenicillin (30 µg/mL), and kanamycin (50 µg/mL) and incubated at 30 ℃ in the dark for 2-3 days. The transformed AGL-1 colonies with the pRM-eGFP vector appeared within 3 days. The individual colonies were picked and transferred into new LB plates.

#### 4.3.5.3 Antibiotic sensitivity test of the JN3 and mJN3 isolates

An antibiotic sensitivity test was performed to decide the appropriate concentration of antibiotics to use for the experiment. Phleomycin was used as the antibiotic for selecting the transformed *L. maculans* isolates as the phleomycin resistance gene (*ble* gene) is present within the T-DNA region of the pRM-eGFP vector. A series of V8 agar plates were prepared with four different concentrations of phleomycin (0 µg/mL, 25 µg/mL, 50 µg/mL and 100 µg/mL) in the presence of the same concentration of cefotaxime (200 µg/µL). Cefotaxime is used to inhibit the growth of *A. tumefaciens* cells during the selection of transformed *L. maculans* isolates. Single pycnidia of mJN3 and JN3 isolates were grown in the prepared V8 plates and incubated under fluorescent light at room temperature for 10 days. After 10 days, the mycelial growth of the culture plates with different phleomycin concentrations was observed.

#### 4.3.5.4 *Agrobacterium tumefaciens*-mediated transformation of *L. maculans* isolates

For the transformation, a modified protocol from Gardiner et al., (2004) was used. The *A. tumefaciens* AGL-1 cells containing the pRM-eGFP vector were incubated overnight (16-18 hrs) in 7 mL of LB media containing kanamycin (50 µg/mL) and carbenicillin (100 µg/mL) at 28 ℃ and 220 rpm until $OD_{600}$ reaches to ~ 1.0. The overnight culture was diluted with ABI media (3.86 mg/mL $K_2HPO_4.3H_2O$, 1 mg/mL $NaH_2PO_4.H_2O$, 1 mg/mL $NH_4Cl$, 2 mg/mL Glucose, 1 M KCl, 200 mM $CaCl_2$, 1 M $MgSO_4.7H_2O$, 0.1 M $FeSO_4.7H_2O$, 4.88 mg/mL MES) containing acetosyringone (40 µM) until $OD_{600}$ = 0.15 and the final volume around 20 mL. The culture was grown in a 250 mL conical flask at 28 ℃ and 220 rpm until $OD_{600}$ reached ~ 0.6. During the incubation of the AGL-1 cells, fresh spores were harvested using 5-7 days old *L. maculans* cultures and the concentration of the spores were adjusted to $1\times10^7$ using sterile distilled water. The log phase ($OD_{600}$ ~ 0.6) *A. tumefaciens* cells (4 mL) and fresh *L. maculans* spores (2 mL) were mixed. The cell suspension was spread on Petri dishes containing solid ABI media and incubated at 22 ℃ for 48 hours in the dark. After 48 hours of incubation, the plates were overlayed with 10% V8 agar containing the antibiotic for selection (phleomycin (100 µg/mL) and cefotaxime (400 µg/mL)). The plates were sealed and incubated at 22 ℃ for 5-10 days until the fugal mycelia appeared on the surface of the overlayed V8 media. The fungal tips and pycnidia of the colonies that appeared on the overlayed V8 media were picked and transferred into new V8 media containing phleomycin (50 µg/mL) and cefotaxime (200 µg/mL).

#### 4.3.5.5 Fluorescence microscopic confirmation of GFP expressing fungi

The individual colonies that grew in the presence of phleomycin were observed under the EVOS M5000 microscope using the objective 1.25× (Thermofisher). The fungal colonies that were visibly expressing the GFP were selected.

#### 4.3.6.6 PCR amplification of *egfp* gene in transformed fungal isolates

The presence of the *egfp* gene in the selected fungal isolates was further confirmed by PCR. The DNA of the selected fungal strains were extracted using the CTAB DNA extraction protocol. The *egfp* gene was amplified using *EGFP-F* (5′-ACCTACGGCAAGCTGACCCTGAAGT-3′) and *EGFP-R* (5′-TGTACAGCTCGTCCATGCCGAGAGT-3′) primers (Mora-Lugo et al., 2014). The non-transformed mJN3 and JN3 DNA were used as the negative control, while the *A. tumefaciens* plasmid DNA was used as the positive control. The 20 µL of PCR reaction mixture was comprised of 10 µL of FroggaMix plus master mixture, 0.2 µM forward primer, 0.2 µM of reverse primer, template DNA, and nuclease-free water. The PCR program consisted of initial denaturation at 94 ℃ for 5 mins, denaturation at 94 ℃ for 15 secs, annealing at 60 ℃ for 15 secs, extension at 68 ℃ for 45 secs for 30 cycles, and final extension at 68 ℃ for 5 min.

#### 4.3.5.7 Mitotic stability test for the fungal transformants

The mitotic stability of the *egfp* gene in the fungal genome was tested. The selected fungal strains were grown in non-selective V8 media for 5 generations and then transferred into a selective media containing phleomycin (50 mg/µL). The ability to grow in the presence of the antibiotic and the ability to express the *egfp* gene were evaluated (Andargie et al., 2015).

#### 4.3.5.8 The disease forming ability of GFP transformants

The pathogenicity of GFP-transformed fungal isolates was tested with the cotyledon inoculation assay. For the experiment, the mJN3 and JN3 isolates were used as the negative controls. The *L. maculans*, strain LmGFP, was used as the positive control. LmGFP is an *L. maculans* strain that has been previously tagged with GFP. The strain was from the laboratory fungal collection.

The susceptible variety Westar (no *R* gene) was grown in the greenhouse at 16 ℃ in the night and 21 ℃ in the day with a 16-hour photoperiod for seven days. Four cotyledon sites on each of twelve

plants were inoculated using 10 µL droplets of inoculum ($2\times10^7$ spores/mL) for each test. Two trials were performed, and the disease symptoms were evaluated after 14 dpi using the 0 - 9 rating scale according to (Kutcher et al., 2010). The MDS was calculated. To deduce the phenotype in Westar, the MDS ≤4.5 was considered as resistant (R), the MDS of 4.6 – 6.0 was considered as the intermediate resistant (IR), and the MDS of 6.1 – 9.0 was considered as the susceptible (S) phenotype (Zhang et al., 2016). The inoculated cotyledons were observed under the EVOS M5000 microscope after 11 dpi. For further study, two fungal transformants were selected based on their ability to form disease in canola cotyledons and the intensity of their fluorescent protein when observed under the fluorescence microscope.

#### 4.3.5.9 Fluorescent microscopic observation of the spores and hyphae of the selected mJN3gfp and JN3gfp isolates

The pycnidiospores and hyphae of the selected mJN3gfp and the JN3gfp isolates were observed under the EVOS M5000 microscope using the 40× objective. The slide culture technique was used to prepare the slides. The fungal mycelium was grown in a square agar block placed on a glass slide covered with a coverslip and incubated for around seven days at room temperature. After the incubation, the coverslip was removed from the agar block and placed on a glass slide containing a drop of water. The mycelia and spores attached to the coverslip were observed under the microscope.

#### 4.3.5.10 Fluorescent microscopic observation of the selected mJN3gfp and JN3gfp isolates in live plant tissues

The fungal inoculum was prepared using the spores of the selected mJN3gfp and JN3gfp isolates. The seven-day-old cotyledons of Westar were inoculated with fungal inoculum ($2\times10^7$ spores/mL) using 10 µL droplets (4 sites were inoculated in each plant). The cotyledons of Westar were observed under the Zeiss Axio Imager Z1 Microscope and the EVOS M5000 microscope after 11, 14, and 17 dpi. The GFP expressing *L. maculans* isolate (LmGFP) from the laboratory was used as the positive control, and non-transformed isolates from each strain were used as negative controls.

## 4.4 RESULTS

### 4.4.1 The avirulence gene profile of the mJN3 and the JN3 isolates

The avirulence gene profiles of the mJN3 and the JN3 isolates were tested using both genotypic and phenotypic methods. Both the mJN3 and JN3 isolates of *L. maculans* contain *AvrLm1*, *AvrLm4*, *AvrLm5*, *AvrLm6*, *AvrLm7*, *AvrLm11*, *AvrLepR1* and *AvrLepR3* genes. In the *B. napus*-*L. maculans* pathosystem, the presence of *AvrLm4-7* masks the activity of *AvrLm3* and *AvrLm9* genes (Ghanbarnia et al., 2018; Plissonneau et al., 2016). However, the absence of the *AvrLm3* and the *AvrLm9* genes in mJN3 and JN3 was not due to the phenotypic interaction as it was confirmed by the genotypic method as well.

### 4.4.2 Pathogenicity of mJN3 and JN3 isolates

The pathogenicity of the mJN3 isolate towards different *Brassica* species was tested and compared with the JN3 isolate. The 0-9 rating scale was used to deduce the phenotype of each plant after the inoculation. All tested *Brassica* plants showed the resistant phenotype in response to infection by mJN3. The disease did not develop even without any resistance genes in the plant (Westar and Topas WT). The *B. alba* and *B. juncea* lines were resistant to both isolates. The JN3 isolate interacted differently in response to the varying *R* genes in different *B. napus* varieties. The interaction between JN3 and each of these *R* genes was following the gene for gene hypothesis (Table 4.3).

**Table 4.3.** The deduced phenotypes of different *Brassica* varieties in response to the infection of mJN3 and JN3 isolates

| ***Brassica* ID** | **Resistance genotype** | **Inferred phenotype** | |
|---|---|---|---|
| | | **mJN3** | **JN3** |
| Topas Rlm1 | *Rlm1* | R | R |
| HP28 | *Rlm1* | R | R |
| MT29 | *Rlm1,9* | R | IR |
| Quinta | *Rlm1,3* | R | R |
| 1056 | *Rlm2,* unknown | R | S |
| 8037 | *Rlm2, Rlm3,* unknown | R | S |
| 1055 | *Rlm2,* unknown | R | IR |
| Glacier | *Rlm2,3* | R | S |
| Bristol | *Rlm2,9* | R | S |

| | | | |
|---|---|---|---|
| Topaz Rlm2 | *Rlm2* | R | S |
| HC1014 | *Rlm3* | R | S |
| 8027 | *Rlm3* | R | IR |
| HC801 | *Rlm3* | R | S |
| 02-22-2-1 | *Rlm3* | R | S |
| 8016 | *Rlm4* | R | R |
| HC1022 | *Rlm4* | R | R |
| CC10 | *Rlm4* | R | R |
| Topas Rlm4 | *Rlm4* | R | R |
| 01-23-2 | *Rlm7* | R | R |
| Goeland | *Rlm9* | R | S |
| 1065 | *LepR1* | R | R |
| 1135 | *LepR2* | R | S |
| Surpass 400 | *LepR3, RlmS* | R | R |
| 8011 | Unknown | R | S |
| *Brassica* juncea (Vattasso) | Unknown | R | R |
| *Brassica* alba (Admiral) | Unknown | R | R |
| *Brassica* alba (Salsa) | Unknown | R | R |
| Westar | None | R | S |
| Topas WT | None | R | S |

### 4.4.3 Transformation of *A. tumefaciens* cells by electroporation

*Agrobacterium tumefaciens* cells were transformed with pRM-eGFP vector by electroporation. The electroporated cells were grown in LB media with antibiotics for selection (kanamycin and carbenicillin). Bacterial colonies appeared within 3 days of incubation at 30 ℃ at dark (Figure 4.2). Individual colonies were picked and transferred onto new media.

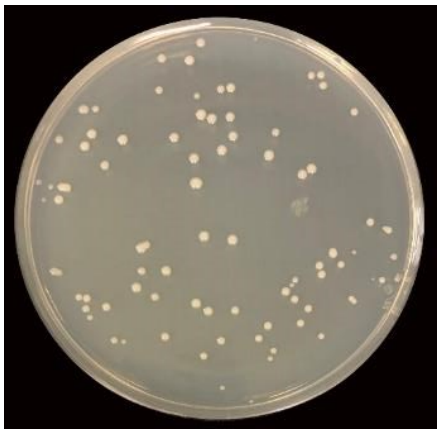


**Figure 4.2.** The growing *Agrobacterium tumefaciens* cells in LB media after transferring the pRM-eGFP vector into the bacterial cells by electroporation. The bacterial colonies appeared within 3 days of incubation at 30 ℃ in the dark.

### 4.4.4 Antibiotic sensitivity testing of the mJN3 and JN3 isolates

The ability of the mJN3 and JN3 isolates to develop at different concentrations of phleomycin was tested. The culture plates were incubated for 10 days, and the results were observed. The response of the mJN3 isolates towards the different antibiotic concentrations was slightly different from the JN3. The mJN3 showed a slow growth at 25 µg/mL concentrations while its development was completely inhibited at 50 µg/ml and 100 µg/mL concentrations for 10 days. However, the JN3 did not grow at any concentration of phleomycin for 10 days. Therefore, 50 µg/mL was chosen as the minimum concentration to select and maintain the fungal transformants (Figure 4.3).

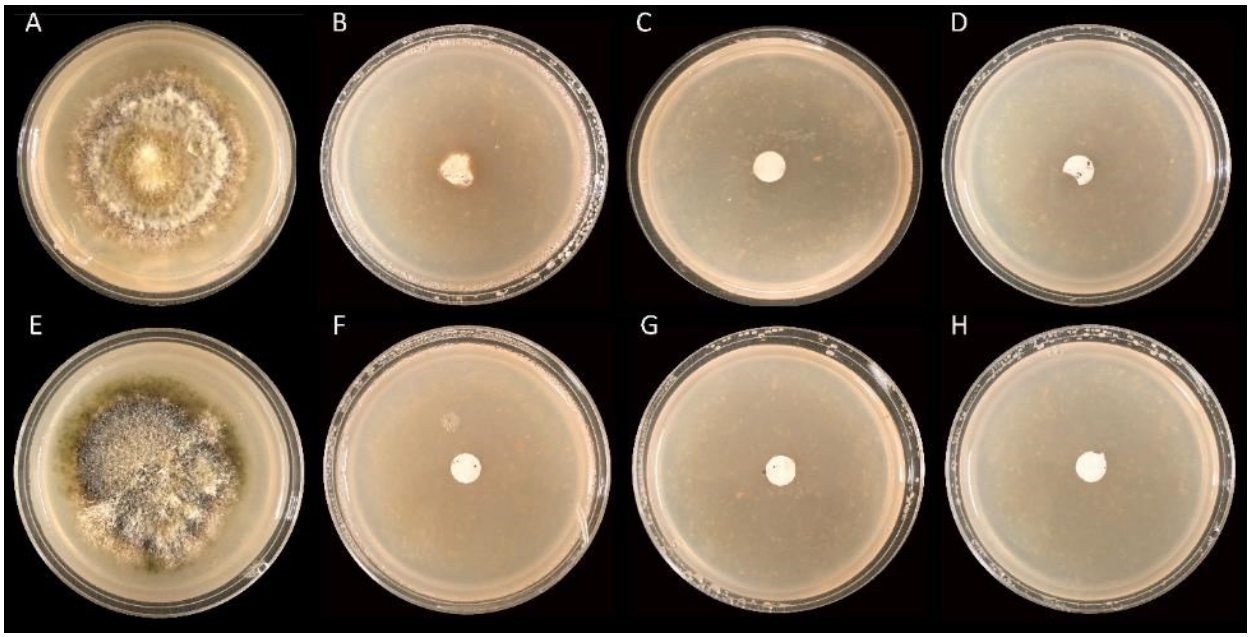



**Figure 4.3**. The growing mJN3 (first row) and JN3 (second row) isolates at 4 different concentrations of phleomycin A and E: 0 µg/mL, B and F: 25 µg/mL, C and G: 50 µg/mL and D and H: 100 µg/mL in V8 media. The cultures were incubated at room temperature for 10 days under fluorescent light. The mJN3 showed a minimal growth at 25 µg/ml, and its development was completely inhibited at 50 µg/ml and 100 µg/ml concentrations. All tested concentrations of phleomycin inhibited the growth of JN3 for 10 days.

### 4.4.5 *A. tumefaciens*-mediated transformation

The *A. tumefaciens* mediated transformation was performed to transform the mJN3 and JN3 *L. maculans* isolates with the *egfp* gene. The fungal mycelia appeared in the overlayed co-culture plates after 10 days of incubation at 22 ℃ under fluorescent light. The pycnidia were observed in some culture plates, and in some areas, only the mycelia were detected. Both pycnidia and hyphal tips from growing mycelia were picked and transferred into new selection media to isolate individual fungal colonies. The newly transformed fungal isolates showed lower growth rates in selection media. Therefore, the cultures were grown for 10-14 days until they produced pycnidia. Then single pycnidia of newly transformed fungal colonies were picked and transferred into new selection media to obtain pure cultures. The subculturing was performed for five generations to obtain pure cultures. After five generations of subculturing, the growing mycelia of the individual colonies were checked under the fluorescent microscope. From the transformed mJN3 isolates (mJN3gfp), 10 out of 72 isolates expressed GFP when observed under the fluorescent microscope.

The isolates were labelled as mJN3gfp1-10. From the transformed JN3 isolates (JN3gfp), 5 out of 20 isolates expressed GFP after the transformation. The isolates were labelled as JN3gfp1-5.

### 4.4.6 Confirmation of the presence of the *egfp* gene within the transformants by PCR

The presence of the *egfp* gene in the transformants was confirmed by PCR amplification. *A. tumefaciens*'s pRM-eGFP plasmid DNA was used as the positive control. All the selected fungal transformants of mJN3gfp and JN3gfp showed a band resembling the positive control within the range of 600bp to 700bp (Figure 4.4). The negative controls (JN3 and mJN3) did not show a band after the PCR amplification.

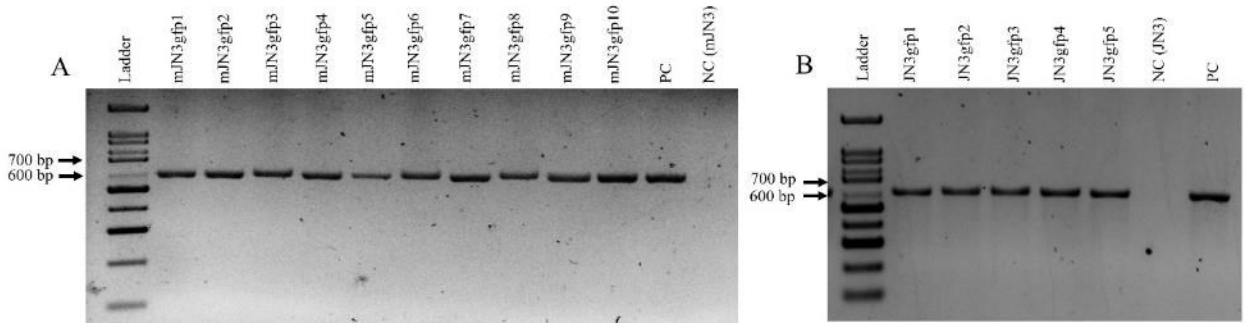



**Figure 4.4**. The gel image demonstrates the PCR amplified product of the *egfp* gene from the extracted DNA of transformed *L. maculans* isolates. A: mJN3gfp isolates; B: JN3gfp isolates. PC: positive control: NC: Negative control. The bands that are similar to the positive control were within the range of 600bp-700bp. A 100-1500 bp ladder was used for reference.

### 4.4.7 The mitotic stability test

The mitotic stability test was performed to test the stability of the *egfp* gene during cell division. All ten mJN3gfp isolates and all five mJN3gfp isolates grew well in the presence of phleomycin after being cultured in non-selective media for five generations. In addition to that, all the selected transformed fungal isolates showed GFP when observed under the fluorescent microscope.

### 4.4.8 The disease forming ability of GFP transformants

The disease forming ability of the isolated mJN3gfp and JN3gfp strains was tested with the cotyledon inoculation assay. The mJN3gfp isolates formed leaf lesions which are similar in size to the leaf lesions formed by mJN3. The MDS in the mJN3gfp and mJN3 inoculated cotyledons were 3, and the inferred phenotype in Westar was resistant. However, the activity of JN3gfp isolates

deviated from the expected results. The JN3gfp transformants showed reduced virulence, and these isolates formed small leaf lesions with an MDS of 3. Therefore, the inferred phenotype in Westar in response to the inoculation of JN3gfp isolates was resistant. However, the JN3 and the LmGFP (Positive control) isolates showed a virulent reaction giving the susceptible phenotype in Westar (Table 4.4).

**Table 4.4.** The disease scores and the inferred phenotypes in Westar after inoculating with different *L. maculans* strains

| Isolate | Mean Disease Score (MDS) | Inferred phonotype |
|---|---|---|
| mJN3gfp1 | 3 | R |
| mJN3gfp2 | 3 | R |
| mJN3gfp3 | 3 | R |
| mJN3gfp4 | 3 | R |
| mJN3gfp5 | 3 | R |
| mJN3gfp6 | 3 | R |
| mJN3gfp7 | 3 | R |
| mJN3gfp8 | 3 | R |
| mJN3gfp9 | 3 | R |
| mJN3gfp10 | 3 | R |
| mJN3 | 3 | R |
| JN3gfp1 | 3 | R |
| JN3gfp2 | 3 | R |
| JN3gfp3 | 3 | R |
| JN3gfp4 | 3 | R |
| JN3gfp5 | 3 | R |
| JN3 | 9 | S |
| LmGFP (Positive control) | 9 | S |

The cotyledons inoculated with the 15 GFP transformants were examined under the fluorescent microscope after 11 dpi. The fungal mycelium and the pycnidiospores were observed around the wounding sites of the cotyledons. The pycnidiospores were almost homogeneously distributed all over the mycelia of the fungi and were well apparent. The progression of fungal mycelia in Westar showed slight differences among various isolates. Among the different mJN3gfp isolates, mJN3gfp4 and mJN3gfp5 were not visible when observed under the fluorescent microscope (Figure 4.5I and J). Only the wound was illuminated under the light. The images of mJN3gfp4 (Figure 4.5I) and mJN3gfp5 (Figure 4.5J) were similar to the negative control (Water) (Figure 4.5P). Among different JN3gfp isolates, the growth of the JN3gfp1 (Figure 4.5A) was restricted around the wounding site, and their projection throughout the leaf was minimal compared to other

JN3gfp isolates. However, the mJN3gfp2 (Figure 4.5G) and the JN3gfp2 (Figure 4.5B) were selected to study them further. The reason for choosing these two isolates was their clear visibility in live tissue when examined under the microscope (Figure 4.5).

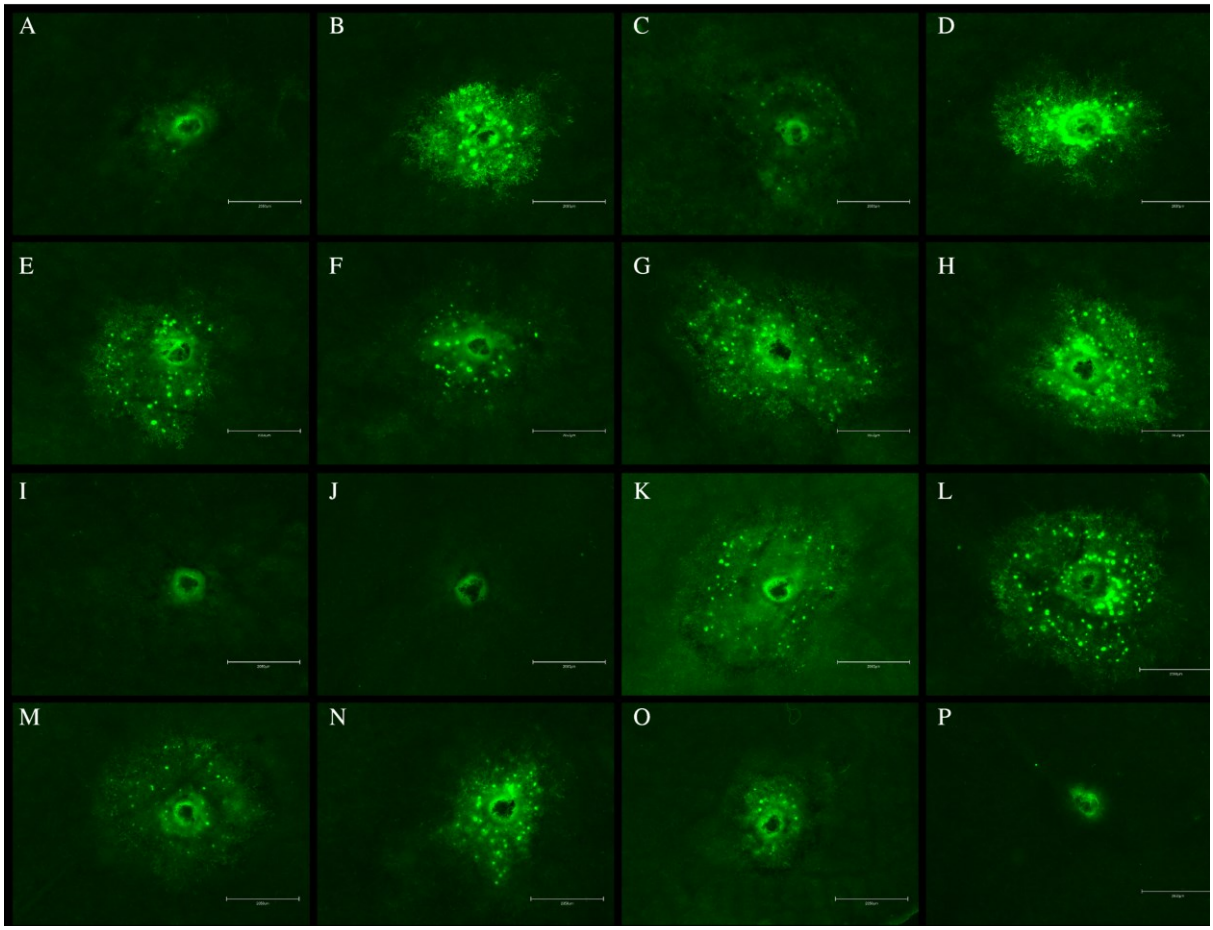



**Figure 4.5**. Fluorescent microscopic images of mycelia of different GFP expressing *L. maculans* transformants after inoculating into cotyledons of Westar under the EVOS M5000 microscope using the 1.25× objective. The images were taken after 11 dpi. A: JN3gfp1; B: JN3gfp2; C: JN3gfp3; D: JN3gfp4; E: JN3gfp5; F: mJN3gfp1; G: mJN3gfp2; H: mJN3gfp3; I: mJN3gfp4; J: mJN3gfp5; K: mJN3gfp6; L: mJN3gfp7; M: mJN3gfp8; N: mJN3gfp9; O: mJN3gfp10; P: Negative control. The scale bar represents 2 050µm.

### 4.4.9 Fluorescent microscopic observation of the selected mJN3gfp and JN3gfp isolates

The mycelia and the spores of the mJN3gfp2 and the JN3gfp2 were further observed under the fluorescent microscope. The slide culture technique was used to prepare the slides containing hyphae and spores. The slides were incubated for 10 days before taking the images. The hyphae and the spores were visible in both isolates (Figure 4.6).

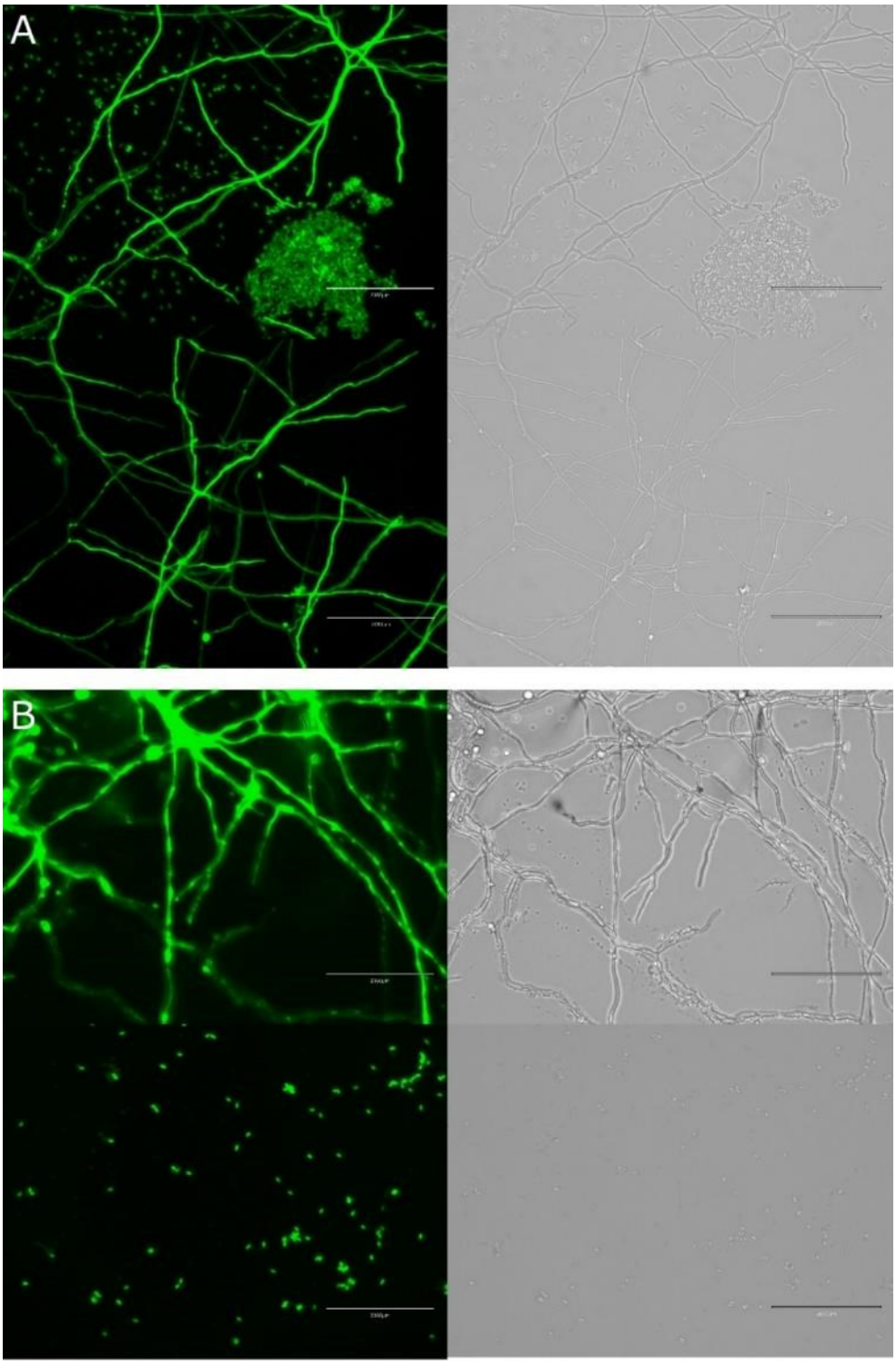



**Figure 4.6**. The mycelia and the pycnidiospores transformed *L. maculans* isolates with *egfp* gene. A: mJN3gfp2 and B: JN3gfp2. The slides were prepared using the slide culture technique. The images were taken after 10 days of incubation of the slide cultures at room temperature under the fluorescent light. The images were taken under the EVOS M5000 microscope using the 40× objective. The images on the left side were taken using the GFP channel, and the right side was taken using the TRANS channel. The scale bar represents 2 050µm.

### 4.4.10 The growth of mJN3gfp in *B. napus* cotyledons comparative to the JN3gfp

The infection processes of the GFP expressing isolates were studied in more depth using the Axio Imager Z1 Microscope with Apotome (Zeiss) after 11 dpi, 14 dpi, and 17 dpi. Both of these isolates showed similar progression in the plant tissue. mJN3gfp2 was able to infect and colonize the plant tissue as same as the JN3gfp2. The extension of the hyphae and the production of pycnidiospores were equivalent to each other. However, the intensity of the JN3gfp2's hyphae was slightly higher compared to the mJN3gfp2 isolate. The expression of GFP of JN3gfp2 mycelium increased over time while it kept consistent in mJN3gfp2 (Figure 4.7).

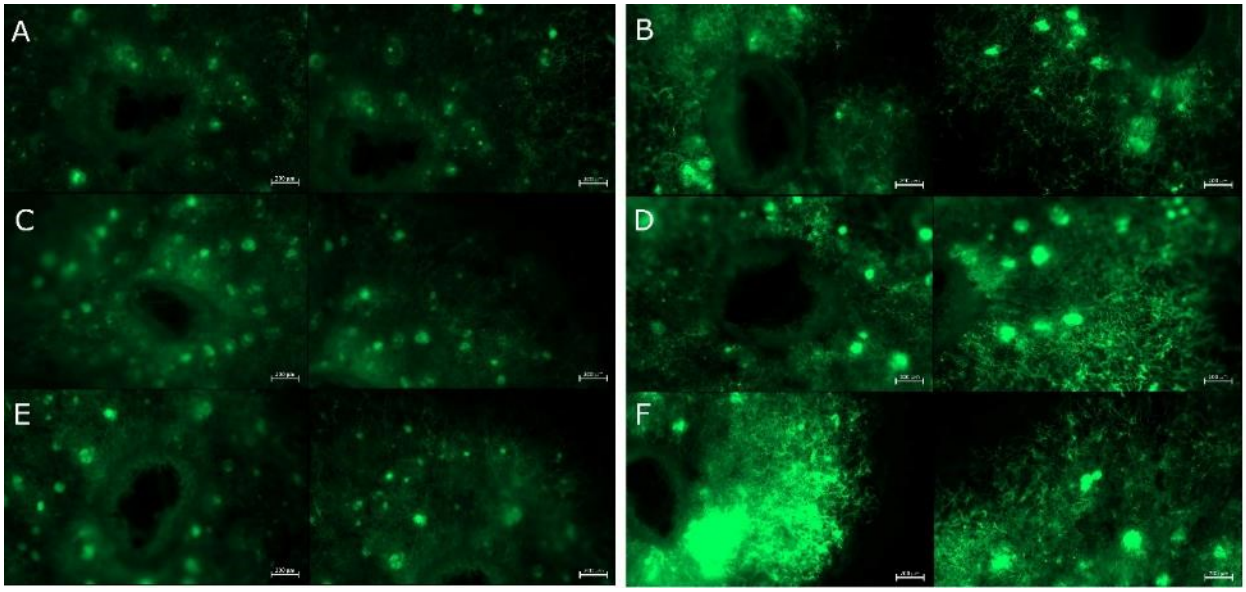



**Figure 4.7**. The mycelial growth of the transformed *L. maculans* isolates with *egfp* gene. A: mJN3gfp2 after 11 dpi; B: JN3gfp2 after 11 dpi; C: mJN3gfp2 after 14 dpi; D: JN3gfp2 after 14 dpi; E: mJN3gfp2 after 17 dpi; F: JN3gfp2 after 17 dpi. The images were taken under the Zeiss Axio Imager Z1 Microscope using the 5× objective. The scale bar represents 200µm.

The LmGFP isolate was used as the positive control for the experiment. The behaviour of the mJN3 isolate was compared with LmGFP. The growth of LmGFP was considerably higher compared to mJN3gfp2. The hyphae of the LmGFP extended towards the petiole, and it colonized the whole plant leaf within 11 dpi (Figure 4.8E and G), while the hyphal extension of mJN3 was restrained around the wounding site (Figure 4.8A and C). The LmGFP produced a vast amount of pycnidia all over the leaf tissue (Figure 4.8F). Even though the growth of the mJN3 was restricted

around the wounding site, the hyphal development and the pycnidiospores production of mJN3 were similar to the LmGFP.

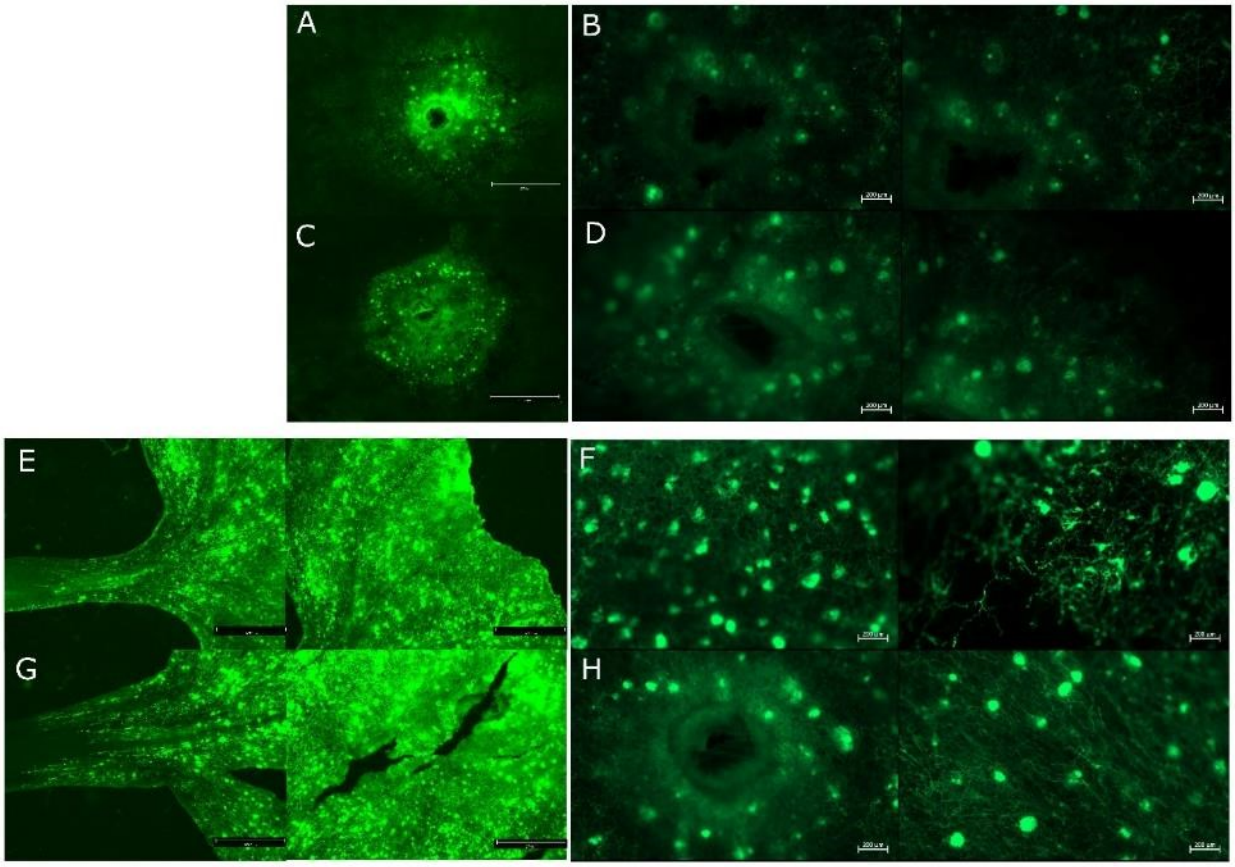



**Figure 4.8**. The mycelial growth of transformed *L. maculans* isolates; mJN3gfp2 and LmGFP isolates in *B. napus* cotyledons after 11 and 14 dpi. A and B: mJN3gfp2 after 11 dpi; C and D: mJN3gfp2 after 14 dpi; E and F: LmGFP after 11 dpi; G and H: LmGFP after 14 dpi. The images were taken using two microscopes: the EVOS M5000 microscope using the 1.25× objective [A, C, E and G (scale bar represent 2 050µm)] and the Zeiss Axio Imager Z1 Microscope using the 5× objective [B, D, F and H (scale bar represent 200µm)].

## 4.5 DISCUSSION

The mJN3 strain of *L. maculans* contains a random mutation generated during the CRISPR/Cas9 gene editing. CRISPR's actual target DNA sequence was the gene encoding region of the α-L-Arabinofuranosidase B protein, which is a plant cell wall degrading enzyme secreted by *L. maculans* and it targets the polysaccharides consisting of L-arabinose (Wu et al., 2016). However, the target gene was not mutated after the CRISPR/Cas9 gene editing. Instead, the mutant has lost its ability to form the blackleg disease in *B. napus* due to an unknown mutation created during the transformation. Therefore, this study was conducted to phenotypically assess the differences in the mutant compared to the wild-type strain during the infection of *B. napus*. Thus, the mutant fungus and its wild-type strain were tagged with the green fluorescent reporter protein for the live imagining of the fungi.

The cotyledon inoculation assay, conducted using different *Brassica* varieties, proved the incompetence of mJN3 to cause the blackleg disease in *B. napus.* The mJN3 strain did not interact with *B. napus* according to the gene for gene interaction (Table 4.3). We identified 8 avirulence genes in the JN3 isolate, including *AvrLm1*, *AvrLm4*, *AvrLm5*, *AvrLm6*, *AvrLm7*, *AvrLm11*, *AvrLepR1*, and *AvrLepR3* genes. According to Zhang et al., 2016, the JN3 strain also possesses another avirulence gene, *AvrLm8*, which we couldn't identify as we do not have access to the differential line containing the *Rlm8* gene or primers to target the *AvrLm8* gene. Since JN3 contains the *AvrLm8* gene, the mJN3 should include the *AvrLm8* gene, as these isolates had the same avirulence gene profiles. According to the gene for gene hypothesis, if the *L. maculans* isolate does not have an *Avr* gene corresponding to the *R* gene present within the *B. napus* plants, the fungus can form the disease in the plant. However, the colonization of mJN3 has been successfully inhibited by all the tested *B. napus*, *B. juncea*, and *B. alba* varieties, even in the absence of the matching *Avr* gene in mJN3.

During this study, a modified protocol of ATMT was used for the fungal transformation (Gardiner et al., 2004). First, the pRM-eGFP vector was transferred into the *A. tumefaciens* AGL-1 electrocompetent cells by electroporation. Then, the electroporated cells were grown in a selective media containing kanamycin to identify the bacterial cells with pRM-eGFP vector (Figure 4.2).

The kanamycin resistance gene in the pRM-eGFP vector created the resistance to the kanamycin in the transformed AGL-1 cells and allows them to grow in the presence of the kanamycin. Besides, the *A. tumefaciens* AGL-1 cells integrated their T-DNA into the *L. maculans* genome during the co-cultivation. The addition of acetosyringone is important to initiate the virulence gene in AGL-1 cells during this time (Sørensen et al., 2014). The transformed fungal isolates were identified using phleomycin, a glycopeptide antibiotic that inhibits microbial growth through DNA cleavage. The phleomycin resistance gene encodes a protein that interacts with the antibiotic by binding and inhibiting its activity (Kross et al., 2002; Punt and van den Hondel, 1992; Stokowa-Sołtys et al., 2019). The fungal transformants that showed resistance to phleomycin appeared on the selection plate within 10 days of incubation at 22 ℃ under the fluorescent light. However, a majority of the transformants were grown in selective media containing phleomycin but failed in expressing the GFP. These transformants that have gained antibiotic resistance but cannot express the GFP are false-positive transformants. Several other studies have similarly observed the formation of false-positive transformants during fungal transformation (Allison et al., 1992; Birch et al., 1998; Takahara et al., 2004). The transformation efficiency for the mJN3 was lower compared to JN3. Ten out of 72 (13.8%) isolates of mJN3 transformants expressed GFP, while 5 out of 20 (25%) JN3 transformants were positive for the GFP expression.

In our study, all the GFP-tagged transformants obtained have shown reduced virulence towards the *B. napus* plants (Table 4.4). The altered pathogenicity in fungal transformants is frequently observed in several studies (Blaise et al., 2007; Meyer et al., 2016; Nakamura et al., 2012). Moreover, the reduced or complete loss of virulence in *L. maculans* after the ATMT has been published by several authors (Blaise et al., 2007; Elliott and Howlett, 2006; van de Wouw et al., 2009). The T-DNA integration of the fungal genome during the ATMT procedure is non-target specific. Therefore, T-DNA can be integrated into the fungal genome randomly (Meyer et al., 2016). Li et al., (2007), have observed that the T-DNA integration of filamentous fungi is more biased towards the non-coding regions, and chromosomal rearrangements are associated with the integration. The study has been performed using the rice blast fungus *Magnaporthe oryzae*. In contrast, Bourras et al., (2012), have identified that the random integration of *L. maculans* is more biased towards the gene-rich regions. The integration of the foreign DNA into a gene regulatory region can alter protein expression in *L. maculans*. Further, a defect in a gene related to

pathogenicity can lead to the formation of less virulence fungal isolates. Moreover, the loss of pathogenicity during the random integration of T-DNA has been observed and has led to the discovery of essential genes responsible for the pathogenicity of *L. maculans*. For example, the 3-ketoacyl-CoA thiolase gene in *L. maculans* has been overexpressed after the ATMT, due to the integration of the T-DNA into its promoter region. Further examination of this gene has revealed that the 3-ketoacyl-CoA thiolase gene is important for the virulence of *L. maculans* and the overexpression of this gene can give rise to the defects in pathogenicity of the fungus towards *B. napus* (Elliott and Howlett, 2006).

The GFP expressing transformants of mJN3 and JN3 were inoculated into canola cotyledons and observed under the fluorescent microscope. There were no apparent changes between the mJN3gfp2 vs JN3gfp2 (Figure 4.7). However, as the JN3gfp2 strain has similarly encountered the problem of the loss of pathogenicity, it was hard to compare these two isolates with each other. Therefore, the LmGFP strain was used to compare the differences in the infection process of the two fungi in *B. napus* plants (Figure 4.8). The mJN3gfp2 strain can extend within the intercellular spaces of the *B. napus* cells. However, their extension rate is lower compared to LmGFP. The plant defence mechanisms successfully inhibited the growth of the fungi restricting the infection within a small leaf area. However, the reason for the inhibition of the mJN3 by the plant defence mechanism is not understood. The loss of a gene associated with pathogenicity or an alteration in gene regulatory region associated with *L. maculans* pathogenicity may have influenced the fungus colonization within the *B. napus* tissue. However, we understood that the ATMT transformation method could similarly cause the defects in other genetic elements of the mJN3 isolates. Therefore, it was hard to reveal the exact underlying phenomenon behind the loss of the pathogenicity of mJN3 through the expression of a reporter gene via the ATMT method.

# 5.0 GENERAL DISCUSSION AND CONCLUSIONS

The diseases caused by pathogenic fungi in various crops have become a significant challenge for farmers worldwide. As fungi can reproduce and disseminate rapidly, it is hard to mitigate the diseases. Due to the sexual reproduction and the high population size of this group of microorganisms, they evolve quickly and overcome plant defence responses making them further hard to manage. Therefore, the work focussed on two major diseases in the Canadian agriculture industry. The first chapter was designed to understand the microbial community structure and the impact of biological control of FHB on the microbiome associated with wheat plant. The second chapter was based on the blackleg disease in canola. The objective of the second chapter was to understand the interaction between the blackleg disease-causing pathogen *L. maculans* and *B. napus* plant using a CRISPR/Cas9 mutant *L. maculans* strain.

Both *F. graminearum* and *L. maculans* are fungal strains belonging to the phylum Ascomycota, and both are hemibiotrophic. However, their disease formation (in wheat and canola, respectively) differs in significant ways. *F. graminearum* infections mainly occur in wheat flowers and lead to the formation of diseased wheat kernels contaminated with mycotoxins released by the fungus. *Fusarium* can infect the wheat plant either passively through natural openings or actively through direct penetration of wheat tissues. However, wheat plants lack qualitative resistance against the FHB disease. Therefore, only quantitative resistance can be used in FHB management. On the other hand, *L. maculans* can only invade canola tissues through natural openings and wounds. *L. maculans* infections mainly occur in canola cotyledons or early true leaves. The fungus infects the stem base of the canola plants, causing stem cankers that eventually lead to the plant's death. Most importantly, canola shows qualitative resistance against the blackleg disease. Therefore, applying qualitative resistance for blackleg disease management has been the most effective management strategy against *L. maculans* infection in the canola plant.

The biological control of plant diseases has been applied for an extended period to manage various fungal infections in plants. The current studies have identified *T. gamsii* T6085 strain as a potential biocontrol agent to manage FHB in wheat. However, the effect of *T. gamsii* T6085 on the other bacteria and fungi associated with wheat plant during the mitigation of FHB has not been

understood well. Therefore, this study evaluated the bacterial and fungal communities associated with crop residue (from previous cropping season), wheat spikes, and kernels and the impact of *T. gamsii* T6085 on their variations. The crop residue in wheat fields were mainly colonized by *Alternaria* and *Cyphellophora* spp., while wheat spikes and kernels were dominated by *Alternaria* and *Fusarium* spp. *Alternaria* and *Fusarium* both include species that cause diseases in wheat. The predominant bacterial groups in wheat spikes and kernels were *Pseudomonas*, *Enterobacter*, and *Pantoea.* All these dominant bacterial groups may consist of potential biocontrol agents to fight against *F. graminearum* since these bacterial groups have overcome the pressure developed by the *Fusarium* during the colonization of wheat spikes and kernels. Therefore, these findings could be beneficial when deciding other potential biocontrol agents against FHB in wheat in the future.

In addition to that, another outcome of the study was the variation in *F. graminearum* abundance over time in crop residue and wheat spikes. We observed a higher abundance of *F. graminearum* in crop residue initially, which then decreased over time, while in wheat spikes, the *F. graminearum* abundance was lower at the beginning, and then it increased rapidly leading up to harvest. The germination and spore production of *F. graminearum* is high when the environmental conditions are warm and humid. Therefore, there can be a high impact from the temperature and humidity variations on their abundance. Additionally, *T. gamsii* is a saprotroph that survives within decaying plant material. It is highly competitive for space and nutrient uptake. During survival, *F. graminearum* needs to compete with other bacterial and fungal groups, including *T. gamsii*, to thrive in its environment. During this competition, the most competitive microorganisms inhibit the growth of others who share the same space. These factors can influence the variations in *F. graminearum* abundance in crop residue over time. In addition, certain bacteria and fungi showed differential abundance in *T. gamsii* T6085 treated samples. However, the microbial community-level changes were not observed in response to *T. gamsii* T6085 treatment. The major outcomes of the study showed that the environmental changes and the plant's developmental stages play an important role in the microbial community dynamics associated with wheat plants, and the impact of the biocontrol agent on these variations is minimal. This is encouraging concerning the potential for using *T. gamsii* T6085 as a biocontrol agent with limited off-target effects on the microbiome.

In conclusion to chapter one, the *F. graminearum* abundance in wheat stubble is reduced over time, reaching a significantly lower concentration during the harvest. Their abundance is significantly higher in wheat spikes during the harvest than other time points. The microbial community associated with wheat is dynamic, and it varies according to the plant's developmental stage. The impact of *T. gamsii* T6085 on the microbial community changes and *F. graminearum* abundance was minimal. The work on FHB disease management using biological control provides possible biocontrol agents that can be used in the future for the biocontrol of FHB in wheat. These potential microbes include bacterial species belonging to *Pseudomonas* and *Sphingomonas* genera. Another possible biocontrol strategy would be the simultaneous integration of *T. gamsii* T6085 with another above-mentioned bacterial species as biocontrol agents. The same experiment can be repeated using a combination of two biocontrol agents to see the efficiency. When designing a similar experiment, a more advanced application method could be used during the application of *T. gamsii* on wheat tissues to obtain a consistent establishment of the biocontrol agent on the field. The work can be redesigned and performed for more than one growing season to observe the growth and establishment of *T. gamsii* T6085 on the field over time. The application of *T. gamsii* T6085 in consecutive years may give the biocontrol agent to establish in the field well. An experiment with more than one growing season would provide more information on the interaction between *T. gamsii* and *F. graminearum* and also the interaction between *T. gamsii* with other microbes over a longer period.

CRISPR/Cas9 is a promising gene-editing technology. The method has attracted huge attention due to its simplicity. Even though the CRISPR/Cas9 system is designed to precisely target a nucleotide sequence, there can be unexpected outcomes like random mutations within the host genome. The study employed an *L. maculans* isolate with a random mutation created by the CRISPR/Cas9 system. The mutation is unknown, yet the isolate has lost its ability to develop the blackleg disease in canola plants due to the mutation. Therefore, the mutant *L. maculans* isolate was tagged with the green fluorescent reporter protein to study their progression microscopically on canola leaf tissues. According to the outcomes of the work, the mutant fungus has not lost its ability to penetrate and colonize the canola cotyledons. But somehow, its growth was inhibited by the *B. napus* through a hypersensitive reaction initiated in response to plant defence mechanisms. Therefore, the gene that has been altered within the host genome should be an essential gene in *L.*

*maculans* to overcome the plant defence system. However, the phenotypic observation enabled by GFP tagging does not help in identifying the specific mutation within the fungus, and I was not able to determine the mechanistic basis for the altered interaction.

The method we developed to express the GFP in *L. maculans* species will benefit future studies. One problem we encountered during the ATMT mediated transformation of *L. maculans* species is that the gene-rich regions of the *L. maculans* genome are sensitive to the integration of the T-DNA. Therefore, integrating the T-DNA into the gene-rich area can lead to the formation of transformed fungi with different defects such as reduced spore production or growth rate, and defects in infection of plants. Therefore, during the ATMT mediated transformation of *L. maculans* species, it is important to isolate many transformants to obtain a fungal transformant without any mutation in their essential genes.

In conclusion to chapter two, the mJN3 isolate has a mutation in its genome, preventing it from growing within the intercellular spaces of the canola cotyledons. However, the expression of GFP in mJN3 did not provide considerable information to determine the underlying mechanism behind the loss of pathogenicity of the mJN3 strains. The ATMT method is sensitive in altering gene-rich regions of *L. maculans*. Therefore, the experiment can be repeated in the future, with some modifications to obtain *L. maculans* strains without alterations in their genes. One possible modification would be isolating many strains after the co-culture step with *A. tumefaciens*. Isolation of many transformants will increase the potential of obtaining an *L. maculans* strain without any gene alterations in its genome. In addition to that, the modified method used in this experiment can be used to tag various *L. maculans* strains with GFP in the future.

## 6.0 REFERENCES


Abarenkov, K., Nilsson, R.H., Larsson, K.H., Alexander, I.J., Eberhardt, U., Erland, S., Høiland, K., Kjøller, R., Larsson, E., Pennanen, T., Sen, R., Taylor, A.F.S., Tedersoo, L., Ursing, B.M., Vrålstad, T., Liimatainen, K., Peintner, U., Kõljalg, U., 2010. The UNITE database for molecular identification of fungi – recent updates and future perspectives. New Phytologist 186, 281–285. https://doi.org/10.1111/J.1469-8137.2009.03160.X

Abd El Aty, A.A., Saleh, S.A.A., Eid, B.M., Ibrahim, N.A., Mostafa, F.A., 2018. Thermodynamics characterization and potential textile applications of *Trichoderma longibrachiatum* KT693225 xylanase. Biocatalysis and Agricultural Biotechnology 14, 129–137. https://doi.org/10.1016/j.bcab.2018.02.011

Abd-Allah, E.F., 2001. *Streptomyces plicatus* as a model biocontrol agent. Folia Microbiologica 46, 309–314. https://doi.org/10.1007/BF02815619

Aboukhaddour, R., Fetch, T., McCallum, B.D., Harding, M.W., Beres, B.L., Graf, R.J., 2020. Wheat diseases on the prairies: A Canadian story. Plant Pathology 69, 418–432. https://doi.org/10.1111/PPA.13147

Abo-Zaid, G.A., Matar, S.M., Abdelkhalek, A., 2020. Induction of plant resistance against tobacco mosaic virus using the biocontrol agent *Streptomyces cellulosae* isolate actino 48. Agronomy 2020, Vol. 10, Page 1620 10, 1620. https://doi.org/10.3390/AGRONOMY10111620

Ahmad, M., Adil, Z., Hussain, A., Mumtaz, M.Z., Nafees, M., Ahmad, I., Jamil, M., 2019. Potential of phosphate solubilizing *Bacillus* strains for improving growth and nutrient uptake in mungbean and maize crops. Pakistan Journal of Agricultural Sciences 56, 283–289. https://doi.org/10.21162/PAKJAS/19.7285

Alconada, T.M., Moure, M.C., Ortega, L.M., 2019. *Fusarium* infection in wheat, aggressiveness and changes in grain quality: a review. Vegetos 32, 441–449. https://doi.org/10.1007/s42535-019-00054-z

Alessandro Bigi, 2019. Field application of *Trichoderma gamsii* T6085 to control FHB in wheat. MSc thesis, University of Pisa, Italy

Ali, M.A., Naveed, M., Mustafa, A., Abbas, A., 2017. The Good, the Bad, and the Ugly of Rhizosphere Microbiome. Probiotics and Plant Health 253–290. https://doi.org/10.1007/978-981-10-3473-2_11

Ali, Shaik.Z., Sandhya, V., Grover, M., Linga, V.R., Bandi, V., 2011. Effect of inoculation with a thermotolerant plant growth promoting *Pseudomonas putida* strain AKMP7 on growth of wheat (*Triticum* spp.) under heat stress. https://doi.org/10.1080/17429145.2010.545147

Allison, D.S., Rey, M.W., Berka, R.M., Armstrong, G., Dunn-Coleman, N.S., 1992. Transformation of the thermophilic fungus *Humicola grisea* vat. thermoidea and overproduction of *Humicola* glucoamylase. Curr Genet 21, 225–229.

Amin, F., Razdan, V.K., Mohiddin, F.A., Bhat, K.A., Banday, S., 2010. Potential of *Trichoderma* species as biocontrol agents of soil borne fungal propagules. Journal of Phytology 2010, 38–41.

Andargie, M., Li, L., Feng, A., Zhu, X., Li, J., 2015. Development of a GFP-expressing *Ustilaginoidea virens* strain to study fungal invasion and colonization in rice spikelets. South African Journal of Botany 97, 16–24. https://doi.org/10.1016/j.sajb.2014.11.013

Anders, S., Huber, W., 2010. Differential expression analysis for sequence count data. Genome Biology 11, 1–12. https://doi.org/10.1186/GB-2010-11-10-R106/COMMENTS

Ansan-Melayah, D., Balesdent, M.H., Delourme, R., Pilet, M.L., Tanguy, X., Renard, M., Rouxel, T., 1998a. Genes for race-specific resistance against blackleg disease in *Brassica napus* L. Plant Breeding 117, 373–378. https://doi.org/10.1111/J.1439-0523.1998.TB01956.X

Ansan-Melayah, D., Balesdent, M.H., Rouxel, T., Delourme, R., Pilet, M.L., Tanguy, X., Renard, M., 1998b. Gene-for-gene interactions in the *Leptosphaeria maculans-Brassica napus* pathosystem. Acta Horticulturae 459, 329–333. https://doi.org/10.17660/ACTAHORTIC.1998.459.38

Araujo, R., Dunlap, C., Barnett, S., Franco, C.M.M., 2019. Decoding wheat endosphere–rhizosphere microbiomes in *Rhizoctonia solani*–infested soils challenged by *Streptomyces* biocontrol agents. Frontiers in Plant Science 10, 1038. https://doi.org/10.3389/fpls.2019.01038

Bakker, M.G., 2018. A fungal mock community control for amplicon sequencing experiments. Molecular ecology resources 18, 541–556. https://doi.org/10.1111/1755-0998.12760

Bakker, M.G., McCormick, S.P., 2019. Microbial correlates of *Fusarium* load and deoxynivalenol content in individual wheat kernels. Phytopathology 109, 993–1002. https://doi.org/10.1094/PHYTO-08-18-0310-R

Balesdent, M.H., Attard, A., Kühn, M.L., Rouxel, T., 2002. New avirulence genes in the phytopathogenic fungus *Leptosphaeria maculans*. Phytopathology 92, 1122–1133. https://doi.org/10.1094/PHYTO.2002.92.10.1122

Balesdent, M.-H., Louvard, K., Pinochet, X., Rouxel, T., 2006. A large-scale survey of races of *Leptosphaeria maculans* occurring on oilseed rape in France. Sustainable strategies for managing *Brassica napus* (oilseed rape) resistance to *Leptosphaeria maculans* (phoma stem canker) 53–65. https://doi.org/10.1007/1-4020-4525-5_5

Bashi, Z.D., Khachatourians, G., Hegedus, D.D., 2018. Isolation of fungal homokaryotic lines from heterokaryotic transformants by sonic disruption of mycelia. https://doi.org/10.2144/000113243 48, 41–46. https://doi.org/10.2144/000113243

Baublis, A.J., Lu, C., Clydesdale, F.M., Decker, E.A., 2000. Potential of wheat-based breakfast cereals as a source of dietary antioxidants. Journal of the American College of Nutrition 19, 308S-311S. https://doi.org/10.1080/07315724.2000.10718965

Bélanger, R.R., Dufour, N., Caron, J., Benhamou, & N., 1995. Chronological events associated with the antagonistic properties of *Trichoderma harzianum* against *Botrytis cinerea*: indirect evidence for sequential role of antibiosis and parasitism. Biocontrol Science and Technology 5, 41–54. https://doi.org/10.1080/09583159550040006

Berendsen, R.L., Pieterse, C.M.J., Bakker, P.A.H.M., 2012. The rhizosphere microbiome and plant health. Trends in Plant Science 17, 478–486. https://doi.org/10.1016/J.TPLANTS.2012.04.001

Birch, P.R.J., Sims, P.F.G., Broda, P., 1998. A reporter system for analysis of regulatable promoter functions in the basidiomycete fungus *Phanerochaete chrysosporium*. Journal of Applied Microbiology 85, 417–424. https://doi.org/10.1046/J.1365-2672.1998.853468.X/FORMAT/PDF

Birr, T., Hasler, M., Verreet, J.A., Klink, H., 2020. Composition and predominance of *Fusarium* species causing Fusarium head blight in winter wheat grain depending on cultivar susceptibility and meteorological factors. Microorganisms 8, 617. https://doi.org/10.3390/microorganisms8040617

Bisby, G.R., 1939. *Trichoderma viride* pers. Ex fries, and notes on Hypocrea. Transactions of the British Mycological Society 23, 149–168. https://doi.org/10.1016/S0007-1536(39)80020-1

Bissett, J., Gams, W., Jaklitsch, W., Samuels, G.J., 2015. Accepted *Trichoderma* names in the year 2015. IMA Fungus 6, 263. https://doi.org/10.5598/IMAFUNGUS.2015.06.02.02

Blackleg survey results from 2016 | The Canola Council of Canada [WWW Document], 2016. URL https://www.canolacouncil.org/canola-watch/2017/02/08/blackleg-survey-results-from-2016/ (accessed 11.7.21).

Blaise, F., Rémy, E., Meyer, M., Zhou, L., Narcy, J.P., Roux, J., Balesdent, M.H., Rouxel, T., 2007. A critical assessment of *Agrobacterium tumefaciens*-mediated transformation as a tool for pathogenicity gene discovery in the phytopathogenic fungus *Leptosphaeria maculans*. Fungal Genetics and Biology 44, 123–138. https://doi.org/10.1016/j.fgb.2006.07.006

Blandino, M., Haidukowski, M., Pascale, M., Plizzari, L., Scudellari, D., Reyneri, A., 2012. Integrated strategies for the control of Fusarium head blight and deoxynivalenol contamination in winter wheat. Field Crops Research 133, 139–149. https://doi.org/10.1016/j.fcr.2012.04.004

Bononi, L., Chiaramonte, J.B., Pansa, C.C., Moitinho, M.A., Melo, I.S., 2020. Phosphorus-solubilizing *Trichoderma* spp. from Amazon soils improve soybean plant growth. Scientific Reports 10, 1–13. https://doi.org/10.1038/s41598-020-59793-8

Bourras, S., Meyer, M., Grandaubert, J., Lapalu, N., Fudal, I., Linglin, J., Ollivier, B., Blaise, F., Balesdent, M.H., Rouxel, T., 2012. Incidence of genome structure, DNA asymmetry, and cell physiology on T-DNA integration in chromosomes of the phytopathogenic fungus *Leptosphaeria maculans*. G3 Genes|Genomes|Genetics 2, 891–904. https://doi.org/10.1534/G3.112.002048

Bousset, L., Jumel, S., Garreta, V., Picault, H., Soubeyrand, S., 2015. Transmission of *Leptosphaeria maculans* from a cropping season to the following one. Annals of Applied Biology 166, 530–543. https://doi.org/10.1111/aab.12205

Briggle, L.W., Curtis, B.C., 2015. Wheat worldwide. Wheat and wheat improvement 13, 1–32. https://doi.org/10.2134/agronmonogr13.2ed.c1

Brown, R.L., Jacobs, L.A., Peet, R.K., 2007. Species richness: small scale. Encyclopedia of Life Sciences. https://doi.org/10.1002/9780470015902.a0020488

Brun, H., Chèvre, A.-M., Fitt, B.D., Powers, S., Besnard, A.-L., Ermel, M., Huteau, V., Marquer, B., Eber, F., Renard, M., Andrivon, D., 2010. Quantitative resistance increases the durability of qualitative resistance to *Leptosphaeria maculans* in *Brassica napus*. New Phytologist 185, 285–299. https://doi.org/10.1111/J.1469-8137.2009.03049.X

Buron-Moles, G., López-Pérez, M., González-Candelas, L., Viñas, I., Teixidó, N., Usall, J., Torres, R., 2012. Use of GFP-tagged strains of *Penicillium digitatum* and *Penicillium expansum* to study host-pathogen interactions in oranges and apples. International Journal of Food Microbiology 160, 162–170. https://doi.org/10.1016/j.ijfoodmicro.2012.10.005

Canadian Grain Commission General Requirements for [WWW Document], 2009. URL https://www.grainscanada.gc.ca/en/index.html (accessed 11.4.21).

Caporaso, J.G., Lauber, C.L., Walters, W.A., Berg-Lyons, D., Lozupone, C.A., Turnbaugh, P.J., Fierer, N., Knight, R., 2011. Global patterns of 16S rRNA diversity at a depth of millions of sequences per sample. Proceedings of the National Academy of Sciences of the United States of America 108, 4516–4522. https://doi.org/10.1073/pnas.1000080107

Carvalho, G., Quecine, M.C., Longatto, D.P., Peters, L.P., Almeida, J.R., Shyton, T.G., Silva, M.M.L., Crestana, G.S., Creste, S., Monteiro-Vitorello, C.B., 2016. *Sporisorium scitamineum* colonisation of sugarcane genotypes susceptible and resistant to smut revealed by GFP-tagged strains. Annals of Applied Biology 169, 329–341. https://doi.org/10.1111/AAB.12304

Chaparro, J.M., Reardon, K.F., 2014. Rhizosphere interactions: Root exudates, microbes, and microbial communities1. https://doi.org/10.1139/cjb-2013-0225

Charpentier, E., Doudna, J.A., 2013. Rewriting a genome. Nature 2013 495:7439 495, 50–51. https://doi.org/10.1038/495050a

Chaverri, P., Castlebury, L.A., Samuels, G.J., Geiser, D.M., 2003. Multilocus phylogenetic structure within the *Trichoderma harzianum*/*Hypocrea lixii* complex. Molecular Phylogenetics and Evolution 27, 302–313. https://doi.org/10.1016/S1055-7903(02)00400-1

Chen, C., Xin, K., Liu, H., Cheng, J., Shen, X., Wang, Y., Zhang, L., 2017. *Pantoea alhagi*, a novel endophytic bacterium with ability to improve growth and drought tolerance in wheat. Scientific Reports 7, 1–14. https://doi.org/10.1038/srep41564

Chen, J.L., Liu, K., Miao, C.P., Sun, S.Z., Chen, Y.W., Xu, L.H., Guan, H.L., Zhao, L.X., 2016. Salt tolerance of endophytic *Trichoderma koningiopsis* YIM PH30002 and its volatile organic

compounds (VOCs) allelopathic activity against phytopathogens associated with *Panax notoginseng*. Annals of Microbiology 66, 981–990. https://doi.org/10.1007/S13213-015-1171-5

Chen, N., Hsiang, T., Goodwin, P.H., 2003. Use of green fluorescent protein to quantify the growth of *Colletotrichum* during infection of tobacco. Journal of Microbiological Methods 53, 113–122. https://doi.org/10.1016/S0167-7012(02)00234-8

Chen, X.H., Koumoutsi, A., Scholz, R., Schneider, K., Vater, J., Süssmuth, R., Piel, J., Borriss, R., 2009. Genome analysis of *Bacillus amyloliquefaciens* FZB42 reveals its potential for biocontrol of plant pathogens. Journal of Biotechnology 140, 27–37. https://doi.org/10.1016/J.JBIOTEC.2008.10.011

Chmielewska, A., Kozłowska, M., Rachwał, D., Wnukowski, P., Amarowicz, R., Nebesny, E., Rosicka-Kaczmarek, J., 2020. Canola/rapeseed protein – nutritional value, functionality and food application: a review. https://doi.org/10.1080/10408398.2020.1809342

Chowdhury, S.P., Dietel, K., Rändler, M., Schmid, M., Junge, H., Borriss, R., Hartmann, A., Grosch, R., 2013. Effects of *Bacillus amyloliquefaciens* FZB42 on lettuce growth and health under pathogen pressure and its impact on the rhizosphere bacterial community. PLoS ONE 8, e68818. https://doi.org/10.1371/journal.pone.0068818

Chudakov, D.M., Matz, M. v., Lukyanov, S., Lukyanov, K.A., 2010. Fluorescent proteins and their applications in imaging living cells and tissues. https://doi.org/10.1152/physrev.00038.2009 90, 1103–1163. https://doi.org/10.1152/PHYSREV.00038.2009

Cong, L., Ran, F.A., Cox, D., Lin, S., Barretto, R., Habib, N., Hsu, P.D., Wu, X., Jiang, W., Marraffini, L.A., Zhang, F., 2013. Multiplex genome engineering using CRISPR/Cas systems. Science 339, 819–823. https://doi.org/10.1126/science.1231143

Crane, J.M., Gibson, D.M., Vaughan, R.H., Bergstrom, G.C., 2013. iturin levels on wheat spikes linked to biological control of Fusarium head blight by *Bacillus amyloliquefaciens*. http://dx.doi.org/10.1094/PHYTO-07-12-0154-R 103, 146–155. https://doi.org/10.1094/PHYTO-07-12-0154-R

Cucu, M.A., Gilardi, G., Pugliese, M., Ferrocino, I., Gullino, M.L., 2020. Effects of biocontrol agents and compost against the *Phytophthora capsici* of zucchini and their impact on the rhizosphere microbiota. Applied Soil Ecology 154, 103659. https://doi.org/10.1016/j.apsoil.2020.103659

Dal Bello, G.M., Mónaco, C.I., Simón, M.R., 2002. Biological control of seedling blight of wheat caused by *Fusarium graminearum* with beneficial rhizosphere microorganisms. World Journal of Microbiology and Biotechnology 2002 18:7 18, 627–636. https://doi.org/10.1023/A:1016898020810

Dandena, H.B., Zhang, Q., Zhou, T., Hirani, A.H., Liu, Z., Fernando, D.W.G., Duncan, R.W., Li, G., 2019. Analysis of quantitative adult plant resistance to blackleg in *Brassica napus*. Molecular Breeding 2019 39:9 39, 1–12. https://doi.org/10.1007/S11032-019-1035-Y

Davidson, M.W., Campbell, R.E., 2009. Engineered fluorescent proteins: innovations and applications. Nature Methods 2009 6:10 6, 713–717. https://doi.org/10.1038/nmeth1009-713

Davis, R., 2000. *Neurospora*: contributions of a model organism.

de Oliveira-Filho, E.C., Matos Lopes, R., Roma Paumgartten, F.J., 2004. Comparative study on the susceptibility of freshwater species to copper-based pesticides. Chemosphere 56, 369–374. https://doi.org/10.1016/J.CHEMOSPHERE.2004.04.026

Degrave, A., Wagner, M., George, P., Coudard, L., Pinochet, X., Ermel, M., Gay, E.J., Fudal, I., Moreno-Rico, O., Rouxel, T., Balesdent, M.H., 2021. A new avirulence gene of *Leptosphaeria maculans*, *AvrLm14,* identifies a resistance source in American broccoli (*Brassica oleracea*) genotypes. Molecular Plant Pathology 00, 1–14. https://doi.org/10.1111/mpp.13131

Deltcheva, E., Chylinski, K., Sharma, C.M., Gonzales, K., Chao, Y., Pirzada, Z.A., Eckert, M.R., Vogel, J., Charpentier, E., 2011. CRISPR RNA maturation by trans-encoded small RNA and host factor RNase III. Nature 2011 471:7340 471, 602–607. https://doi.org/10.1038/nature09886

Dickson, J.G., 1957. Diseases of Field Crops. AIBS Bulletin 7, 39. https://doi.org/10.2307/1292051

Dienes, D., Egyházi, A., Réczey, K., 2004. Treatment of recycled fiber with *Trichoderma* cellulases. Industrial Crops and Products 20, 11–21. https://doi.org/10.1016/J.INDCROP.2003.12.009

Dilmaghani, A., Gout Ab †, L., Moreno-Rico, O., Dias, J.S., Coudard, L., Castillo-Torres, N., Balesdent, M.-H., Rouxel, T., 2013. Clonal populations of *Leptosphaeria maculans* contaminating cabbage in Mexico. Wiley Online Library 62, 520–532. https://doi.org/10.1111/j.1365-3059.2012.02668.x

Dixon, P., 2003. VEGAN, a package of R functions for community ecology. Journal of Vegetation Science 14, 927–930. https://doi.org/10.1111/J.1654-1103.2003.TB02228.X

Dolatabadian, A., Cornelsen, J., Huang, S., Zou, Z., Dilantha Fernando, W.G., 2021. Sustainability on the farm: breeding for resistance and management of major canola diseases in Canada contributing towards an IPM approach. 1–34. https://doi.org/10.1080/07060661.2021.1991480

Doudna, J.A., Charpentier, E., 2014. The new frontier of genome engineering with CRISPR-Cas9. Science 346. https://doi.org/10.1126/SCIENCE.1258096

Edwards, N.M., Peressini, D., Dexter, J.E., Mulvaney, S.J., 2001. Viscoelastic properties of durum wheat and common wheat dough of different strengths. Rheologica Acta 40, 142–153. https://doi.org/10.1007/s003970000147

Egamberdieva, D., Kamilova, F., Validov, S., Gafurova, L., Kucharova, Z., Lugtenberg, B., 2008. High incidence of plant growth-stimulating bacteria associated with the rhizosphere of wheat

grown on salinated soil in Uzbekistan. Environmental Microbiology 10, 1–9. https://doi.org/10.1111/J.1462-2920.2007.01424.X

Elad, Y., Phytopathology, I.C.-, 1987, undefined, n.d. Possible role of competition for nutrients in biocontrol of Pythium damping-off by bacteria. 77, 190-195

Elliott, C.E., Howlett, B.J., 2006. Overexpression of a 3-Ketoacyl-CoA Thiolase in *Leptosphaeria maculans* causes reduced pathogenicity on *Brassica napus*. Molecular Plant-Microbe Interactions MPMI 588, 588–596. https://doi.org/10.1094/MPMI

Erlacher, A., Cardinale, M., Grosch, R., Grube, M., Berg, G., 2014. The impact of the pathogen *Rhizoctonia solani* and its beneficial counterpart *Bacillus amyloliquefaciens* on the indigenous lettuce microbiome. Frontiers in Microbiology 0, 175. https://doi.org/10.3389/FMICB.2014.00175

Escobar, M., science, A.D.-T. in plant, 2003, undefined, n.d. *Agrobacterium tumefaciens* as an agent of disease. Elsevier. https://doi.org/10.1016/S1360-1385(03)00162-6

Evans, H.C., Holmes, K.A., Thomas, S.E., 2003. Endophytes and mycoparasites associated with an indigenous forest tree, *Theobroma gileri*, in Ecuador and a preliminary assessment of their potential as biocontrol agents of cocoa diseases. Mycological Progress 2, 149–160. https://doi.org/10.1007/S11557-006-0053-4

Fardet, A., 2015. Wheat-based foods and non celiac gluten/wheat sensitivity: Is drastic processing the main key issue? Medical Hypotheses 85, 934–939. https://doi.org/10.1016/j.mehy.2015.09.007

Fernando, W.G.D., Paulitz, T.C., Seaman, W.L., Dutilleul, P., Miller, J.D., 1997. Head blight gradients caused by *Gibberella zeae* from area sources of inoculum in wheat field plots. Phytopathology 87, 414–421. https://doi.org/10.1094/PHYTO.1997.87.4.414

Fernando, W.G.D., Zhang, X., Selin, C., Zou, Z., Liban, S.H., McLaren, D.L., Kubinec, A., Parks, P.S., Harunur Rashid, M., Padmathilake, K.R.E., Rong, L., Yang, C., Gnanesh, B.N., Huang, S., 2018. A six-year investigation of the dynamics of avirulence allele profiles, blackleg incidence, and mating type alleles of *Leptosphaeria maculans* populations associated with canola crops in Manitoba, Canada. Plant Disease 102, 790–798. https://doi.org/10.1094/PDIS-05-17-0630-RE/ASSET/IMAGES/LARGE/PDIS-05-17-0630-RE_T5.JPEG

Figueroa, M., Hammond-Kosack, K.E., Solomon, P.S., 2018. A review of wheat diseases—a field perspective. Molecular Plant Pathology 19, 1523–1536. https://doi.org/10.1111/mpp.12618

FILONOW, A.B., 2010. Role of Competition for Sugars by Yeasts in the Biocontrol of Gray Mold of Apple. 8, 243–256. https://doi.org/10.1080/09583159830315

Fitt, B.D.L., Hu, B.C., Li, Z.Q., Liu, S.Y., Lange, R.M., Kharbanda, P.D., Butterworth, M.H., White, R.P., 2008. Strategies to prevent spread of *Leptosphaeria maculans* (phoma stem

canker) onto oilseed rape crops in China; costs and benefits. Plant Pathology 57, 652–664. https://doi.org/10.1111/J.1365-3059.2008.01841.X

Flor, H.H., 1956. The Complementary Genic Systems in Flax and Flax Rust. Advances in Genetics 8, 29–54. https://doi.org/10.1016/S0065-2660(08)60498-8

Food and Agriculture Organization of the United Nations, 2020. FAO Cereal Supply and Demand Brief | World Food Situation | Food and Agriculture Organization of the United Nations [WWW Document]. 05/03/2020. URL http://www.fao.org/worldfoodsituation/csdb/e (accessed 11.4.21).

Foster, A.J., Martin-Urdiroz, M., Yan, X., Wright, H.S., Soanes, D.M., Talbot, N.J., 2018. CRISPR-Cas9 ribonucleoprotein-mediated co-editing and counterselection in the rice blast fungus. Scientific Reports 2018 8:1 8, 1–12. https://doi.org/10.1038/s41598-018-32702-w

Fudal, I., Ross, S., Gout, L., Blaise, F., Kuhn, M.L., Eckert, M.R., Cattolico, L., Bernard-Samain, S., Balesdent, M.H., Rouxel, T., 2007. Heterochromatin-like regions as ecological niches for avirulence genes in the *Leptosphaeria maculans* genome: Map-based cloning of *AvrLm6*. Molecular Plant-Microbe Interactions 20, 459–470. https://doi.org/10.1094/MPMI-20-4-0459

Gao, Z., Karlsson, I., Geisen, S., Kowalchuk, G., Jousset, A., 2019. Protists: Puppet Masters of the Rhizosphere Microbiome. Trends in Plant Science 24, 165–176. https://doi.org/10.1016/J.TPLANTS.2018.10.011

Gardiner, D.M., Cozijnsen, A.J., Wilson, L.M., Soledade, M., Pedras, C., Howlett, B.J., 2004. The sirodesmin biosynthetic gene cluster of the plant pathogenic fungus *Leptosphaeria maculans*. Wiley Online Library 53, 1307–1318. https://doi.org/10.1111/j.1365-2958.2004.04215.x

Garneau, J.E., Dupuis, M.-È., Villion, M., Romero, D.A., Barrangou, R., Boyaval, P., Fremaux, C., Horvath, P., Magadán, A.H., Moineau, S., 2010. The CRISPR/Cas bacterial immune system cleaves bacteriophage and plasmid DNA. Nature 2010 468:7320 468, 67–71. https://doi.org/10.1038/nature09523

Gärtner, B.H., Munich, M., Kleijer, G., Mascher, F., 2008. Characterisation of kernel resistance against Fusarium infection in spring wheat by baking quality and mycotoxin assessments. European Journal of Plant Pathology 120, 61–68. https://doi.org/10.1007/s10658-007-9198-5

Ghanbarnia, K., Fudal, I., Larkan, N.J., Links, M.G., Balesdent, M.-H., Profotova, B., Dilantha Fernando, W.G., Rouxel, T., Hossein Borhan, M., 2014. Rapid identification of the *Leptosphaeria maculans* avirulence gene *AvrLm2* using an intraspecific comparative genomics approach. Wiley Online Library 16, 699–709. https://doi.org/10.1111/mpp.12228

Ghanbarnia, K., Ma, L., Larkan, N.J., Haddadi, P., Fernando, W.G.D., Borhan, M.H., 2018. *Leptosphaeria maculans AvrLm9*: a new player in the game of hide and seek with *AvrLm4-7*. Molecular Plant Pathology 19, 1754–1764. https://doi.org/10.1111/MPP.12658

Gilbert, J., Fernando, W.G.D., 2004. Epidemiology and biological control of *Gibberella zeae* /*Fusarium graminearum*. Canadian Journal of Plant Pathology 26, 464–472. https://doi.org/10.1080/07060660409507166

Gilbert, J., Tekauz, A., 2000. Review: Recent developments in research on Fusarium head blight of wheat in Canada. Canadian Journal of Plant Pathology 22, 1–8. https://doi.org/10.1080/07060660009501155

Glick, B.R., 2012. Plant Growth-Promoting Bacteria: Mechanisms and Applications. Scientifica 2012, 1–15. https://doi.org/10.6064/2012/963401

Goldman, G.H., Kafer, E., 2004. *Aspergillus nidulans* as a model system to characterize the DNA damage response in eukaryotes. Fungal Genetics and Biology 41, 428–442. https://doi.org/10.1016/j.fgb.2003.12.001

González, H.H.L., Moltó, G.A., Pacin, A., Resnik, S.L., Zelaya, M.J., Masana, M., Martínez, E.J., 2008. Trichothecenes and mycoflora in wheat harvested in nine locations in Buenos Aires Province, Argentina. Mycopathologia 165, 105–114. https://doi.org/10.1007/s11046-007-9084-x

Good As Gold. Celebrating 50 Years of Canola [WWW Document], n.d. URL https://www.canolacouncil.org/canola-history/ (accessed 10.20.21).

Goudjal, Y., Zamoum, M., Sabaou, N., Mathieu, F., Zitouni, A., 2016. Potential of endophytic *Streptomyces* spp. for biocontrol of Fusarium root rot disease and growth promotion of tomato seedlings. Biocontrol Science and Technology 26, 1691–1705. https://doi.org/10.1080/09583157.2016.1234584

Gout, L., Eckert, M., Rouxel, T., Ne Balesdent, M.-H., 2006. Genetic variability and distribution of mating type alleles in field populations of *Leptosphaeria maculans* from France. Am Soc Microbiol 72, 185–191. https://doi.org/10.1128/AEM.72.1.185-191.2006

Grosch, R., Scherwinski, K., Lottmann, J., Berg, G., 2006. Fungal antagonists of the plant pathogen *Rhizoctonia solani*: selection, control efficacy and influence on the indigenous microbial community. Mycological Research 110, 1464–1474. https://doi.org/10.1016/j.mycres.2006.09.014

Guida, M., Inglese, M., Meriç, S., 2008. A multi-battery toxicity investigation on fungicides. Desalination 226, 262–270. https://doi.org/10.1016/J.DESAL.2007.04.096

Harman, G.E., Lorito, M., Lynch, J.M., 2004. Uses of *Trichoderma* spp. to alleviate or remediate soil and water pollution. Advances in Applied Microbiology 56, 313–330. https://doi.org/10.1016/S0065-2164(04)56010-0

Heckman, D.S., Geiser, D.M., Eidell, B.R., Stauffer, R.L., Kardos, N.L., Hedges, S.B., 2001. Molecular evidence for the early colonization of land by fungi and plants. Science 293, 1129–1133. https://doi.org/10.1126/science.1061457

Heikinheimo, L., 2002. *Trichoderma* reesei cellulases in processing of cotton.

Heler, R., Samai, P., Modell, J.W., Weiner, C., Goldberg, G.W., Bikard, D., Marraffini, L.A., 2015. Cas9 specifies functional viral targets during CRISPR–Cas adaptation. Nature 2015 519:7542 519, 199–202. https://doi.org/10.1038/nature14245

Hertz, M., Jensen, I.R., Jensen, L.Ø., Thomsen, S.N., Winde, J., Dueholm, M.S., Sørensen, L.H., Wollenberg, R.D., Sørensen, H.O., Sondergaard, T.E., Sørensen, J.L., 2016. The fungal community changes over time in developing wheat heads. International journal of food microbiology 222, 30–39. https://doi.org/10.1016/J.IJFOODMICRO.2016.01.018

Hoffmann, A., Lischeid, G., Koch, M., Lentzsch, P., Sommerfeld, T., Müller, M.E.H., 2021. Co-cultivation of *Fusarium*, *Alternaria*, and *Pseudomonas* on wheat-ears affects microbial growth and mycotoxin production. Microorganisms 9, 1–23. https://doi.org/10.3390/microorganisms9020443

Hooykaas, P.J.J., van Heusden, G.P.H., Niu, X., Reza Roushan, M., Soltani, J., Zhang, X., van der Zaal, B.J., 2018. *Agrobacterium*-mediated transformation of yeast and fungi. Current Topics in Microbiology and Immunology 418, 349–374. https://doi.org/10.1007/82_2018_90

Horvath, P., 2010. CRISPR/Cas, the immune system of bacteria and Archaea. Science 327, 167–170. https://doi.org/10.1126/science.1179555

Howlett, B.J., 2004. Current knowledge of the interaction between *Brassica napus* and *Leptosphaeria maculans*. Canadian Journal of Plant Pathology 26, 245–252. https://doi.org/10.1080/07060660409507141

Howlett, B.J., Idnurm, A., Pedras, M.S.C., 2001. *Leptosphaeria maculans*, the causal agent of blackleg disease of Brassicas. Fungal Genetics and Biology 33, 1–14. https://doi.org/10.1006/fgbi.2001.1274

Hua, L., … K.S.-G. and B., 2007, undefined, 2007. Blackleg disease (*Leptosphaeria maculans*) on oilseed rape-evidence for it being a polycyclic disease in Australia and implications for disease management. Genetics and Breedings: Breeding for Stress Resistance, 416-417.

Idnurm, A., Bailey, A.M., Cairns, T.C., Elliott, C.E., Foster, G.D., Ianiri, G., Jeon, J., 2017. A silver bullet in a golden age of functional genomics: the impact of *Agrobacterium*-mediated transformation of fungi. Fungal Biology and Biotechnology 4:1 4, 1–28. https://doi.org/10.1186/S40694-017-0035-0

Index Mundi, 2015. Wheat Production by Country [WWW Document]. Index Mundi. URL http://www.indexmundi.com/agriculture/?commodity=wheat&graph=production (accessed 11.4.21).

Iqbal, H.M.N., Ahmed, I., Zia, M.A., Irfan, M., 2011. Purification and characterization of the kinetic parameters of cellulase produced from wheat straw by *Trichoderma viride* under SSF and its detergent compatibility. Advances in Bioscience and Biotechnology 02, 149–156. https://doi.org/10.4236/abb.2011.23024

Ishii, H., 2006. Impact of fungicide resistance in plant pathogens on crop disease control and agricultural environment. Japan Agricultural Research Quarterly 40, 205–211. https://doi.org/10.6090/jarq.40.205

Ishino, Y., Shinagawa, H., Makino, K., Amemura, M., Nakata, A., 1987. Nucleotide Sequence of the *iap* gene, responsible for alkaline phosphatase isozyme conversion in *Escherichia coli*, and identification of the gene product. Journal of Bacteriology 169, 5429–5433.

Issariyakul, T., Kulkarni, M.G., Meher, L.C., Dalai, A.K., Bakhshi, N.N., 2008. Biodiesel production from mixtures of canola oil and used cooking oil. Chemical Engineering Journal 140, 77–85. https://doi.org/10.1016/J.CEJ.2007.09.008

Jaggard, K.W., Qi, A., Ober, S., 2010. Possible changes to arable crop yields by 2050. Philosophical transactions of the royal society B: Biological Sciences 365, 2835–2851. https://doi.org/10.1098/RSTB.2010.0153

Jia, M., Chen, L., Xin, H.L., Zheng, C.J., Rahman, K., Han, T., Qin, L.P., 2016. A friendly relationship between endophytic fungi and medicinal plants: A systematic review. Frontiers in Microbiology 7, 906. https://doi.org/10.3389/fmicb.2016.00906

Jinek, M., Chylinski, K., Fonfara, I., Hauer, M., Doudna, J.A., Charpentier, E., 2012. A programmable dual RNA-guided DNA endonuclease in adaptive bacterial immunity. Science 337, 816. https://doi.org/10.1126/SCIENCE.1225829

John, R., Tyagi, R., Prévost, D., Brar, S., protection, S.P.-C., 2010, undefined, 2010. Mycoparasitic *Trichoderma viride* as a biocontrol agent against *Fusarium oxysporum* f. sp. adzuki and *Pythium arrhenomanes* and as a growth promoter of soybean. Elsevier. https://doi.org/10.1016/j.cropro.2010.08.004

Juska, A., Busch, L., Tanaka, K., 1997. The blackleg epidemic in Canadian rapeseed as a "normal agricultural accident." Ecological Applications 7, 1350–1356. https://doi.org/10.1890/1051-0761(1997)007[1350:TBEICR]2.0.CO;2

Kang, Z., Buchenauer, H., 2000. Cytology and ultrastructure of the infection of wheat spikes by *Fusarium culmorum*. Mycological Research 104, 1083–1093. https://doi.org/10.1017/S0953756200002495

Karasawa, S., Araki, T., Nagai, T., Mizuno, H., Miyawaki, A., 2004. Cyan-emitting and orange-emitting fluorescent proteins as a donor/acceptor pair for fluorescence resonance energy transfer. Biochemical Journal 381, 307–312. https://doi.org/10.1042/BJ20040321

Katayama, T., Nakamura, H., Zhang, Y., Pascal, A., Fujii, W., Maruyama, J.I., 2019. Forced recycling of an AMA1-based genome-editing plasmid allows for efficient multiple gene deletion/integration in the industrial filamentous fungus *Aspergillus oryzae*. Applied and Environmental Microbiology 85. https://doi.org/10.1128/AEM.01896-18

Keen, N.T., 1990. Gene-for-gene complementarity in plant-pathogen interactions. Annu. Rev. Genet 24, 447–63.

Kembel, S.W., Cowan, P.D., Helmus, M.R., Cornwell, W.K., Morlon, H., Ackerly, D.D., Blomberg, S.P., Webb, C.O., 2010. Picante: R tools for integrating phylogenies and ecology. Bioinformatics 26, 1463–1464. https://doi.org/10.1093/BIOINFORMATICS/BTQ166

Kemp, N.D., Vaughan, M.M., McCormick, S.P., Brown, J.A., Bakker, M.G., 2020. *Sarocladium zeae* is a systemic endophyte of wheat and an effective biocontrol agent against Fusarium head blight. Biological Control 149, 104329. https://doi.org/10.1016/J.BIOCONTROL.2020.104329

Khan, M.R., Doohan, F.M., 2009. Bacterium-mediated control of Fusarium head blight disease of wheat and barley and associated mycotoxin contamination of grain. Biological Control 48, 42–47. https://doi.org/10.1016/J.BIOCONTROL.2008.08.015

Koch, E., Badawy, H.M.A., Hoppe, H.H., 1989. Differences between aggressive and non-aggressive single spore lines of *Leptosphaeria maculans* in cultural characteristics and phytotoxin production. Journal of Phytopathology 124, 52–62. https://doi.org/10.1111/j.1439-0434.1989.tb04894.x

Köhl, J., Postma, J., Nicot, P., Ruocco, M., Blum, B., 2011. Stepwise screening of microorganisms for commercial use in biological control of plant-pathogenic fungi and bacteria. Biological Control 57, 1–12. https://doi.org/10.1016/J.BIOCONTROL.2010.12.004

Kröber, M., Wibberg, D., Grosch, R., Eikmeyer, F., Verwaaijen, B., Chowdhury P., S.P., Hartmann, A., Pühler, A., Schlüter, A., 2014. Effect of the strain *Bacillus amyloliquefaciens* FZB42 on the microbial community in the rhizosphere of lettuce under field conditions analyzed by whole metagenome sequencing. Frontiers in Microbiology 5, 252. https://doi.org/10.3389/fmicb.2014.00252

Kross, J., Henner, W.D., Haseltine, W.A., Hecht, S.M., 2002. Specificity of deoxyribonucleic acid cleavage by bleomycin, phleomycin, and tallysomycin. Biochemistry 21, 4310–4318. https://doi.org/10.1021/BI00261A021

Kumar, A., Maurya, B.R., Raghuwanshi, R., Meena, V.S., Tofazzal Islam, M., 2017. Co-inoculation with Enterobacter and Rhizobacteria on yield and nutrient uptake by wheat (*Triticum aestivum* L.) in the Alluvial soil under indo-gangetic plain of india. Journal of Plant Growth Regulation 36, 608–617. https://doi.org/10.1007/s00344-016-9663-5

Kutcher, H.R., Yu, F., Brun, H., 2010. Improving blackleg disease management of *Brassica napus* from knowledge of genetic interactions with *Leptosphaeria maculans*. Canadian Journal of Plant Pathology 32, 29–34. https://doi.org/10.1080/07060661003620961

Laddomada, B., Caretto, S., Mita, G., 2015. Wheat bran phenolic acids: Bioavailability and stability in whole wheat-based foods. Molecules 20, 15666–15685. https://doi.org/10.3390/molecules200915666

Lagopodi, A.L., Ram, A.F.J., Lamers, G.E.M., Punt, P.J., van den Hondel, C.A.M.J.J., Lugtenberg, B.J.J., Bloemberg, G. v., 2002. Novel aspects of tomato root colonization and infection by *Fusarium oxysporum* f. sp. radicis-lycopersici Revealed by confocal laser scanning

microscopic analysis using the green fluorescent protein as a marker. Molecular Plant-Microbe Interactions 15, 172–179. https://doi.org/10.1094/MPMI.2002.15.2.172

Larkan, N.J., Lydiate, D.J., Parkin, I.A.P., Nelson, M.N., Epp, D.J., Cowling, W.A., Rimmer, S.R., Borhan, M.H., 2013. The *Brassica napus* blackleg resistance gene *LepR3* encodes a receptor-like protein triggered by the *Leptosphaeria maculans* effector *AvrLm1*. New Phytologist 197, 595–605. https://doi.org/10.1111/NPH.12043

Larkan, N.J., Ma, L., Borhan, M.H., 2015. The *Brassica napus* receptor-like protein *Rlm2* is encoded by a second allele of the *LepR3*/*Rlm2* blackleg resistance locus. Plant Biotechnology Journal 13, 983–992. https://doi.org/10.1111/pbi.12341

Larkan, N.J., Ma, L., Haddadi, P., Buchwaldt, M., Parkin, I.A.P., Djavaheri, M., Borhan, M.H., 2020. The *Brassica napus* wall-associated kinase-like (WAKL) gene *Rlm9* provides race-specific blackleg resistance. The Plant Journal 104, 892–900. https://doi.org/10.1111/TPJ.14966

Larkan, N.J., Yu, F., Lydiate, D.J., Rimmer, S.R., Borhan, M.H., 2016. Single *R* gene introgression lines for accurate dissection of the *Brassica* - *Leptosphaeria* pathosystem. Frontiers in Plant Science 7, 1771. https://doi.org/10.3389/FPLS.2016.01771/BIBTEX

Latz, M.A.C., Kerrn, M.H., Sørensen, H., Collinge, D.B., Jensen, B., Brown, J.K.M., Madsen, A.M., Jørgensen, H.J.L., 2021. Succession of the fungal endophytic microbiome of wheat is dependent on tissue-specific interactions between host genotype and environment. Science of The Total Environment 759, 143804. https://doi.org/10.1016/J.SCITOTENV.2020.143804

Lauber, C.L., Ramirez, K.S., Aanderud, Z., Lennon, J., Fierer, N., 2013. Temporal variability in soil microbial communities across land-use types. The ISME Journal 2013 7:8 7, 1641–1650. https://doi.org/10.1038/ismej.2013.50

LeBlanc, N., 2021. Bacteria in the genus Streptomyces are effective biological control agents for management of fungal plant pathogens: a meta-analysis. BioControl 1–11. https://doi.org/10.1007/s10526-021-10123-5

Lee, S.B., Taylor, J.W., 1990. Isolation of DNA from fungal mycelia and single spores. PCR Protocols 282–287. https://doi.org/10.1016/B978-0-12-372180-8.50038-X

Leifert, C., Li, H., Chidburee, S., Hampson, S., Workman, S., Sigee, D., Epton, H.A.S., Harbour, A., 1995. Antibiotic production and biocontrol activity by *Bacillus subtilis* CL27 and *Bacillus pumilus* CL45. Journal of Applied Bacteriology 78, 97–108. https://doi.org/10.1111/J.1365-2672.1995.TB02829.X

Leplat, J., Friberg, H., Abid, M., Steinberg, C., 2013. Survival of *Fusarium graminearum*, the causal agent of Fusarium head blight. A review. Agronomy for Sustainable Development 33, 97–111. https://doi.org/10.1007/s13593-012-0098-5

Leplat, J., Heraud, C., Gautheron, E., Mangin, P., Falchetto, L., Steinberg, C., 2016. Colonization dynamic of various crop residues by *Fusarium graminearum* monitored through real-time

PCR measurements. Journal of Applied Microbiology 121, 1394–1405. https://doi.org/10.1111/JAM.13259

Lewis, J., protection, G.P.-C., 1991. Biocontrol of plant diseases: the approach for tomorrow. Crop protection, 10, 95-105.

Li, D., Tang, Y., Lin, J., Cai, W., 2017. Methods for genetic transformation of filamentous fungi. Microbial Cell Factories 16, 1–13. https://doi.org/10.1186/s12934-017-0785-7

Li, G., Zhou, Z., Liu, G., Zheng, F., He, C., 2007. Characterization of T-DNA insertion patterns in the genome of rice blast fungus *Magnaporthe oryzae*. Current Genetics 51, 233–243. https://doi.org/10.1007/S00294-007-0122-5/FIGURES/5

Li, H., Smyth, F., Barbetti, M., Research, K.S.-F.C., 2006. Relationship between *Brassica napus* seedling and adult plant responses to *Leptosphaeria maculans* is determined by plant growth stage at inoculation and. Elsevier 96, 428–437. https://doi.org/10.1016/j.fcr.2005.08.006

Li, Hua, Krishnapillai, ·, Martin, S., Barbetti, J., Kuo, John, Li, H, Sivasithamparam, · K, Barbetti, M.J., Kuo, J, 2004. Germination and invasion by ascospores and pycnidiospores of *Leptosphaeria maculans* on spring-type *Brassica napus* canola varieties with varying susceptibility to blackleg. Fungal Diseases J Gen Plant Pathol 70, 261–269. https://doi.org/10.1007/s10327-004-0125-8

Li, J., Zhang, Yanhua, Zhang, Yucheng, Yu, P.L., Pan, H., Rollins, J.A., 2018. Introduction of large sequence inserts by CRISPR-cas9 to create pathogenicity mutants in the multinucleate filamentous pathogen sclerotinia sclerotiorum. mBio 9. https://doi.org/10.1128/mBio.00567-18

Li, M., Li, G., Metabolites, K.Z.-, 2019, undefined, 2019. Non-volatile metabolites from *Trichoderma* spp. Metabolites 9, 58. https://doi.org/10.3390/metabo9030058

Liban, S.H., Cross, D.J., Kutcher, H.R., Peng, G., Fernando, W.G.D., 2016. Race structure and frequency of avirulence genes in the western Canadian *Leptosphaeria maculans* pathogen population, the causal agent of blackleg in brassica species. Plant Pathology 65, 1161–1169. https://doi.org/10.1111/ppa.12489

Lin, L., Allemekinders, H., Dansby, A., Campbell, L., Durance-Tod, S., Berger, A., Jones, P.J., 2013. Evidence of health benefits of canola oil. Nutrition Reviews 71, 370–385. https://doi.org/10.1111/NURE.12033

Lindow, S.E., Brandl, M.T., 2003. Microbiology of the phyllosphere. Applied and Environmental Microbiology 69, 1875–1883. https://doi.org/10.1128/AEM.69.4.1875-1883.2003

Liu, F., Zou, Z., Peng, G., Fernando, W.G.D., 2021. *Leptosphaeria maculans* isolates reveal their allele frequency in Western Canada. Plant Disease 105. https://doi.org/10.1094/PDIS-08-20-1838-RE

Lorang, J.M., Tuori, R.P., Martinez, J.P., Sawyer, T.L., Redman, R.S., Rollins, J.A., Wolpert, T.J., Johnson, K.B., Rodriguez, R.J., Dickman, M.B., Ciuffetti, L.M., 2001. Green fluorescent

protein is lighting up fungal biology. Applied and Environmental Microbiology 67, 1987–1994. https://doi.org/10.1128/AEM.67.5.1987-1994.2001

MacCabe, A.P., Orejas, M., Ramón, D., 2001. *Aspergillus nidulans* as a model organism for the study of the expression of genes encoding enzymes of relevance in the food industry. Applied Mycology and Biotechnology 1, 239–265. https://doi.org/10.1016/S1874-5334(01)80011-3

Mali, P., Yang, L., Esvelt, K.M., Aach, J., Guell, M., DiCarlo, J.E., Norville, J.E., Church, G.M., 2013. RNA-guided human genome engineering via Cas9. Science (New York, N.Y.) 339, 823. https://doi.org/10.1126/SCIENCE.1232033

Manokaran, R., Lòpez, A., 2016. Use of *Trichoderma* spp. in biodegradation of Carbendazim. Indian J. Agric. Sci 86, 59-62.

Manstretta, V., Rossi, V., 2016. Effects of temperature and moisture on development of Fusarium graminearum perithecia in maize stalk residues. Applied and Environmental Microbiology 82, 184–191. https://doi.org/10.1128/AEM.02436-15/ASSET/9B424583-AB76-47FA-AF3B-D5153BFF0B06/ASSETS/GRAPHIC/ZAM9991168140006.JPEG

Maor, R., Puyesky, M., Horwitz, B.A., Sharon, A., 1998. Use of green fluorescent protein (GFP) for studying development and fungal-plant interaction in *Cochliobolus heterostrophus*. Mycological Research 102, 491–496. https://doi.org/10.1017/S0953756297005789

Massart, S., Margarita, M.M., Jijakli, M.H., 2015. Biological control in the microbiome era: Challenges and opportunities. Biological Control 89, 98–108. https://doi.org/10.1016/J.BIOCONTROL.2015.06.003

Masuda, H., Takenaka, Y., Yamaguchi, A., Nishikawa, S., Mizuno, H., 2006. A novel yellowish-green fluorescent protein from the marine copepod, *Chiridius poppei*, and its use as a reporter protein in HeLa cells. Gene 372, 18–25. https://doi.org/10.1016/J.GENE.2005.11.031

Matarese, F., Sarrocco, S., Gruber, S., Seidl-Seiboth, V., Vannacci, G., 2012a. Biocontrol of Fusarium head blight: Interactions between *Trichoderma* and mycotoxigenic Fusarium. Microbiology 158, 98–106. https://doi.org/10.1099/mic.0.052639-0

Matarese, F., Sarrocco, S., Gruber, S., Seidl-Seiboth, V., Vannacci, G., 2012b. Biocontrol of Fusarium head blight: Interactions between *Trichoderma* and mycotoxigenic *Fusarium*. Microbiology 158, 98–106. https://doi.org/10.1099/mic.0.052639-0

McDonald, B.A., McDermott, J.M., 1993. Population genetics of plant pathogenic fungi. BioScience 43, 311–319. https://doi.org/10.2307/1312063

McMullen, M., Bergstrom, G., de Wolf, E., Dill-Macky, R., Hershman, D., Shaner, G., van Sanford, D., 2012. A unified effort to fight an enemy of wheat and barley: Fusarium Head Blight. https://doi.org/10.1094/PDIS-03-12-0291-FE 96, 1712–1728. https://doi.org/10.1094/PDIS-03-12-0291-FE

McMurdie, P.J., Holmes, S., 2013. phyloseq: An R Package for reproducible interactive analysis and graphics of microbiome census data. PLOS ONE 8, e61217. https://doi.org/10.1371/JOURNAL.PONE.0061217

McVetty, P.B.E., Duncan, R.W., 2015. Canola, Rapeseed, and Mustard: For biofuels and bioproducts. Industrial Crops: Breeding for Bioenergy and Bioproducts 133–156. https://doi.org/10.1007/978-1-4939-1447-0_7

Mendes-Pereira, E., Balesdent, M.H., Brun, H., Rouxel, T., 2003. Molecular phylogeny of the *Leptosphaeria maculans-L. biglobosa* species complex. Mycological Research 107, 1287–1304. https://doi.org/10.1017/S0953756203008554

Mesterházy, A., 1995. Types and components of resistance to Fusarium head blight of wheat. Plant Breeding 114, 377–386. https://doi.org/10.1111/J.1439-0523.1995.TB00816.X

Meyer, M., Zhou, L., Balesdent, M.-H., Blaise, F., Rémy, E., Narcy, J.-P., Roux, J., Ne Balesdent, M.-H., Rouxel, T., 2016. A critical assessment of *Agrobacterium tumefaciens*-mediated transformation as a tool for pathogenicity gene discovery in the phytopathogenic fungus *Leptosphaeria*. Elsevier. https://doi.org/10.1016/j.fgb.2006.07.006

Michaud, A.M., Chappellaz, C., Hinsinger, P., 2008. Copper phytotoxicity affects root elongation and iron nutrition in durum wheat (*Triticum turgidum durum* L.). Plant and Soil 310, 151–165. https://doi.org/10.1007/S11104-008-9642-0

Michielse, C.B., Hooykaas, P.J.J., van den Hondel, C.A.M.J.J., Ram, A.F.J., 2005. *Agrobacterium*-mediated transformation as a tool for functional genomics in fungi. Current Genetics 48, 1–17. https://doi.org/10.1007/s00294-005-0578-0

Mikosch, T.S.P., Lavrijssen, B., Sonnenberg, A.S.M., van Griensven, L.J.L.D., 2001. Transformation of the cultivated mushroom *Agaricus bisporus* (Lange) using T-DNA from *Agrobacterium tumefaciens*. Current Genetics 39, 35–39. https://doi.org/10.1007/s002940000178

Mishra, N.C., Tatum, E.L., 1973. Non-mendelian inheritance of DNA-induced inositol independence in *Neurospora* (exosome/integration/meiosis/transformation). Part 70, 3875–3879.

Monte, E., 2001. Understanding *Trichoderma*: between biotechnology and microbial ecology. International microbiology: the official journal of the Spanish Society for Microbiology 4, 1–4. https://doi.org/10.1007/s101230100001

Mora-Lugo, R., Zimmermann, J., Rizk, A.M., Fernandez-Lahore, M., 2014. Development of a transformation system for *Aspergillus sojae* based on the *Agrobacterium tumefaciens*-mediated approach. BMC Microbiology 14, 1–8. https://doi.org/10.1186/S12866-014-0247-X/FIGURES/5

Müller, T., Ruppel, S., Behrendt, U., Lentzsch, P., Müller, M.E.H., 2018. Antagonistic potential of fluorescent *Pseudomonads* colonizing wheat heads against mycotoxin producing

*Alternaria* and fusaria. Frontiers in Microbiology 9, 2124. https://doi.org/10.3389/fmicb.2018.02124

Mullins, E.D., Kang, S., 2001. Transformation: a tool for studying fungal pathogens of plants. CMLS, Cell. Mol. Life Sci 58, 2043–2052.

Nakamura, M., Kuwahara, H., Onoyama, K., Iwai, H., 2012. *Agrobacterium tumefaciens*-mediated transformation for investigating pathogenicity genes of the phytopathogenic fungus *Colletotrichum sansevieriae*. Current Microbiology 65, 176–182. https://doi.org/10.1007/S00284-012-0140-5/FIGURES/6

Occhipinti, A., 2013. Plant coevolution: Evidences and new challenges. Journal of Plant Interactions 8, 188–196. https://doi.org/10.1080/17429145.2013.816881

Oghenekaro, A.O., Oviedo-Ludena, M.A., Serajazari, M., Wang, X., Henriquez, M.A., Wenner, N.G., Kuldau, G.A., Navabi, A., Kutcher, H.R., Fernando, W.G.D., 2021. Population genetic structure and chemotype diversity of *Fusarium graminearum* populations from wheat in Canada and north eastern United States. Toxins 2021, Vol. 13, Page 180 13, 180. https://doi.org/10.3390/TOXINS13030180

Olmedo-Monfil, V., Cortés-Penagos, C., Herrera-Estrella, A., 2004. Three decades of fungal transformation. Methods in molecular biology (Clifton, N.J.) 267, 297–313. https://doi.org/10.1385/1-59259-774-2:297

Osborne, L.E., Stein, J.M., 2007. Epidemiology of Fusarium head blight on small-grain cereals. International Journal of Food Microbiology 119, 103–108. https://doi.org/10.1016/J.IJFOODMICRO.2007.07.032

Park, S.-Y., Vaghchhipawala, Z., Vasudevan, B., Lee, L.-Y., Shen, Y., Singer, K., Waterworth, W.M., Zhang, Z.J., West, C.E., Mysore, K.S., Gelvin, S.B., 2015. *Agrobacterium* T-DNA integration into the plant genome can occur without the activity of key non-homologous end-joining proteins. Plant Journal 81, 934–946. https://doi.org/10.1111/tpj.12779

Parlange, F., Daverdin, G., Fudal, I., Kuhn, M.-L., Balesdent, M.-H., Blaise, F., Grezes-Besset, B., Rouxel, T., 2008. *Leptosphaeria maculans* avirulence gene *AvrLm4-7* confers a dual recognition specificity by the *Rlm4* and *Rlm7* resistance genes of oilseed rape and circumvents *Rlm4*-mediated recognition through a single amino acid change. https://doi.org/10.1111/j.1365-2958.2008.06547.x

Perazzolli, M., Antonielli, L., Storari, M., Puopolo, G., Pancher, M., Giovannini, O., Pindo, M., Pertot, I., 2014. Resilience of the natural phyllosphere microbiota of the grapevine to chemical and biological pesticides. Applied and Environmental Microbiology 80, 3585–3596. https://doi.org/10.1128/AEM.00415-14

Pestka, J.J., 2010. Deoxynivalenol: mechanisms of action, human exposure, and toxicological relevance. Arch Toxicol 84, 663–679. https://doi.org/10.1007/s00204-010-0579-8

Petersen, J., Wilmann, P.G., Beddoe, T., Oakley, A.J., Devenish, R.J., Prescott, M., Rossjohn, J., 2003. The 2.0-Å Crystal Structure of eqFP611, a far red fluorescent protein from the Sea Anemone *Entacmaea quadricolor* *. Journal of Biological Chemistry 278, 44626–44631. https://doi.org/10.1074/JBC.M307896200

Petit-Houdenot, Y., Degrave, A., Meyer, M., ßoise Blaise, F., en edicte Ollivier, B., Marais, C.-L., Jauneau, A., Audran, C., Rivas, S., Veneault-Fourrey, C., Brun, H., Rouxel, T., Fudal, I., el ene Balesdent, M.-H., 2019. A two genes – for – one gene interaction between *Leptosphaeria maculans* and *Brassica napus*. Wiley Online Library 223, 397–411. https://doi.org/10.1111/nph.15762

Plissonneau, C., Daverdin, G., Ollivier, B., Blaise, F., Degrave, A., Fudal, I., Rouxel, T., Balesdent, M.H., 2016. A game of hide and seek between avirulence genes *AvrLm4-7* and *AvrLm3* in *Leptosphaeria maculans*. New Phytologist 209, 1613–1624. https://doi.org/10.1111/nph.13736

Podolich, O., Ardanov, P., Zaets, I., Pirttilä, A.M., Kozyrovska, N., 2014. Reviving of the endophytic bacterial community as a putative mechanism of plant resistance. Plant and Soil 2014 388:1 388, 367–377. https://doi.org/10.1007/S11104-014-2235-1

Pöggeler, S., Masloff, S., Hoff, B., Mayrhofer, S., Kück, U., 2003. Versatile EGFP reporter plasmids for cellular localization of recombinant gene products in filamentous fungi. Current Genetics 2003 43:1 43, 54–61. https://doi.org/10.1007/S00294-003-0370-Y

Prandini, A., Sigolo, S., Filippi, L., Battilani, P., Piva, G., 2009. Review of predictive models for Fusarium head blight and related mycotoxin contamination in wheat. Food and Chemical Toxicology 47, 927–931. https://doi.org/10.1016/J.FCT.2008.06.010

Punt, P.J., van den Hondel, C.A.M.J.J., 1992. [39] Transformation of filamentous fungi based on hygromycin b and phleomycin resistance markers. Methods in Enzymology 216, 447–457. https://doi.org/10.1016/0076-6879(92)16041-H

Qian, X.B., Chen, T., Xu, Y.P., Chen, L., Sun, F.X., Lu, M.P., Liu, Y.X., 2020. A guide to human microbiome research: Study design, sample collection, and bioinformatics analysis. Chinese Medical Journal 133, 1844–1855. https://doi.org/10.1097/CM9.0000000000000871

Quast, C., Pruesse, E., Yilmaz, P., Gerken, J., Schweer, T., Yarza, P., Peplies, J., Glöckner, F.O., 2013. The SILVA ribosomal RNA gene database project: improved data processing and web-based tools. Nucleic Acids Research 41, D590. https://doi.org/10.1093/NAR/GKS1219

Raman, H., Raman, R., Coombes, N., Song, J., Diffey, S., Kilian, A., Lindbeck, K., Barbulescu, D.M., Batley, J., Edwards, D., Salisbury, P.A., Marcroft, S., 2016. Genome-wide association study identifies new loci for resistance to *Leptosphaeria maculans* in canola. Frontiers in Plant Science 7, 1513. https://doi.org/10.3389/FPLS.2016.01513/BIBTEX

Raman, H., Raman, R., Qiu, Y., Zhang, Y., Batley, J., Liu, S., 2021. The *Rlm13* gene, a new player of *Brassica napus–Leptosphaeria maculans* interaction maps on chromosome C03 in canola. Frontiers in Plant Science 12, 675. https://doi.org/10.3389/fpls.2021.654604

Rashid, M., Zou, Z., Breeding, W.F.-P., 2018, undefined, 2018. Development of molecular markers linked to the *Leptosphaeria maculans* resistance gene *Rlm6* and inheritance of SCAR and CAPS markers in *Brassica napus*. Wiley Online Library 137, 402–411. https://doi.org/10.1111/pbr.12587

Raymer, P.L., 2002. Canola: An Emerging Oilseed Crop. Trends in New Crops and New Uses 1, 122-126

Remington, S.J., 2011. Green fluorescent protein: A perspective. Protein Science 20, 1509–1519. https://doi.org/10.1002/PRO.684

Rimmer, S.R., 2006. Resistance genes to *Leptosphaeria maculans* in *Brassica napus*. Canadian Journal of Plant Pathology 28, 288–297. https://doi.org/10.1080/07060660609507386

Rinu, K., Sati, P., Pandey, A., 2014. *Trichoderma gamsii* (NFCCI 2177): A newly isolated endophytic, psychrotolerant, plant growth promoting, and antagonistic fungal strain. Journal of Basic Microbiology 54, 408–417. https://doi.org/10.1002/JOBM.201200579

Riquelme, M., Martínez-Nñez, L., 2016. Hyphal ontogeny in *Neurospora crassa*: A model organism for all seasons. F1000Research 5. https://doi.org/10.12688/f1000research.9679.1

Rodríguez, M., Evans, H.C., de Abreu, L.M., de Macedo, D.M., Ndacnou, M.K., Bekele, K.B., Barreto, R.W., 2021. New species and records of *Trichoderma* isolated as mycoparasites and endophytes from cultivated and wild coffee in Africa. Scientific Reports 11, 1–30. https://doi.org/10.1038/s41598-021-84111-1

Saika, H., Nishizawa-Yokoi, A., Toki, S., 2014. The non-homologous end-joining pathway is involved in stable transformation in rice. Frontiers in Plant Science 5, 560. https://doi.org/10.3389/FPLS.2014.00560/BIBTEX

Sample, V., Newman, R.H., Zhang, J., 2009. The structure and function of fluorescent proteins. Chemical Society Reviews 38, 2852–2864. https://doi.org/10.1039/B913033K

Samuels, G., … R.P.-S.-M., 2000, undefined, 2021. *Trichoderma stromaticum* sp. nov., a parasite of the cacao witches broom pathogen. cambridge.org. https://doi.org/10.1017/S0953756299001938

Samuels, G.J., 2006. The Nature and Application of Biocontrol Microbes II: *Trichoderma* spp. *Trichoderma*: Systematics, the Sexual State, and Ecology. Phytopathology 96, 195. https://doi.org/10.1094/PHYTO-96-0195

Samuels, G.J., 1996. *Trichoderma*: a review of biology and systematics of the genus. Mycological Research 100, 923–935. https://doi.org/10.1016/S0953-7562(96)80043-8

Šantić, Ž., Puvačić, Z., Radović, S., Puvačić, S., 2005. Higher mortality risk of lungs carcinoma in vineyard sprayers. Bosnian Journal of Basic Medical Sciences 5, 65.

Sarrocco, S., Esteban, P., Vicente, I., Bernardi, R., Plainchamp, T., Domenichini, S., Puntoni, G., Baroncelli, R., Vannacci, G., Dufresne, M., 2021. Straw competition and wheat root

endophytism of *Trichoderma gamsii* T6085 as useful traits in the biological control of Fusarium head blight. Phytopathology. https://doi.org/10.1094/PHYTO-09-20-0441-R

Sarrocco, S, Matarese, F., … L.M.-J. of P., 2013, undefined, 2013. Biocontrol of Fusarium head blight by spike application of *Trichoderma gamsii*. search.ebscohost.com.

Sarrocco, S., Matarese, F., Moncini, L., Pachetti, G., Ritieni, A., Moretti, A., Vannacci, G., 2013. Biocontrol of Fusarium head blight by spike application of *Trichoderma gamsii*. Journal of Plant Pathology 1.

Sarrocco, S., Valenti, F., Manfredini, S., Esteban, P., Bernardi, R., Puntoni, G., Baroncelli, R., Haidukowski, M., Moretti, A., Vannacci, G., 2019. Is exploitation competition involved in a multitrophic strategy for the biocontrol of Fusarium head blight? Phytopathology 109, 560–570. https://doi.org/10.1094/PHYTO-04-18-0123-R/ASSET/IMAGES/LARGE/PHYTO-04-18-0123-R_T6.JPEG

Scherm, B., Orrù, M., Balmas, V., Spanu, F., Azara, E., Delogu, G., Hammond, T.M., Keller, N.P., Migheli, Q., 2011. Altered trichothecene biosynthesis in TRI6-silenced transformants of *Fusarium culmorum* influences the severity of crown and foot rot on durum wheat seedlings. Molecular Plant Pathology 12, 759–771. https://doi.org/10.1111/J.1364-3703.2011.00709.X

Scherwinski, K., Wolf, A., Berg, G., 2007. Assessing the risk of biological control agents on the indigenous microbial communities: *Serratia plymuthica* HRO-C48 and *Streptomyces* sp. HRO-71 as model bacteria. BioControl 52, 87–112. https://doi.org/10.1007/s10526-006-9006-8

Schiro, G., Verch, G., Grimm, V., Müller, M.E.H., 2018. *Alternaria* and *Fusarium* fungi: Differences in distribution and spore deposition in a topographically heterogeneous wheat field. Journal of Fungi 4, 63. https://doi.org/10.3390/jof4020063

Schliep, K.P., 2011. phangorn: phylogenetic analysis in R. Bioinformatics 27, 592–593. https://doi.org/10.1093/BIOINFORMATICS/BTQ706

Schoch, C.L., Seifert, K.A., Huhndorf, S., Robert, V., Spouge, J.L., Levesque, C.A., Chen, W., 2012. Nuclear ribosomal internal transcribed spacer (*ITS*) region as a universal DNA barcode marker for Fungi. Proceedings of the National Academy of Sciences of the United States of America 109, 6241–6246. https://doi.org/10.1073/pnas.1117018109

Sexton, A.C., Howlett, B.J., 2001. Green fluorescent protein as a reporter in the *Brassica-Leptosphaeria maculans* interaction [WWW Document]. Physiological and Molecular Plant Pathology. https://doi.org/10.1006/pmpp.2000.0307

Shah, L., Ali, A., Yahya, M., Zhu, Y., Wang, S., Si, H., Rahman, H., Ma, C., 2018. Integrated control of Fusarium head blight and deoxynivalenol mycotoxin in wheat. Plant Pathology 67, 532–548. https://doi.org/10.1111/PPA.12785

Shewry, P.R., 2009. Wheat. Journal of Experimental Botany 60, 1537–1553. https://doi.org/10.1093/jxb/erp058

Shimomura, O., Johnson, F.H., Saiga, Y., 1962. Extraction, purification and properties of aequorin, a bioluminescent. Journal of cellular and comparative physiology 59, 223–239. https://doi.org/10.1002/JCP.1030590302

Shoemaker, R.A., Brun, H., 2001. The teleomorph of the weakly aggressive segregate of *Leptosphaeria maculans*. Canadian Journal of Botany 79, 412–419. https://doi.org/10.1139/b01-019

Simopoulos, A.P., 2008. The Importance of the Omega-6/Omega-3 fatty acid ratio in cardiovascular disease and other chronic diseases: Experimental biology and medicine, 233, 674-688. https://doi.org/10.3181/0711-MR-311

Sivan, A., Phytopathology, I.C.-, 1989, undefined, n.d. The possible role of competition between *Trichoderma harzianum* and *Fusarium oxysporum* on rhizosphere colonization. Phytopathology 79, 198-203.

Smith, K.P., Goodman, R.M., 1999. Host variation for interactions with beneficial plant-associated microbes. Annual Review of Phytopathology 37, 473–491. https://doi.org/10.1146/annurev.phyto.37.1.473

Somda, I., Harkous, S., Brun, H., 1997. Bipolar heterothallism in B-group isolates of *Leptosphaeria maculans*. Plant Pathology 46, 890–896. https://doi.org/10.1046/j.1365-3059.1997.d01-80.x

Sonah, H., Zhang, X., Deshmukh, R.K., Hossein Borhan, M., Dilantha Fernando, W.G., Bélanger, R.R., 2016. Comparative transcriptomic analysis of virulence factors in *Leptosphaeria maculans* during compatible and incompatible interactions with canola. Frontiers in Plant Science 7, 1784. https://doi.org/10.3389/fpls.2016.01784

Sørensen, L.Q., Lysøe, E., Larsen, J.E., Khorsand-Jamal, P., Nielsen, K.F., Frandsen, R.J.N., 2014. Genetic transformation of *Fusarium avenaceum* by *Agrobacterium tumefaciens* mediated transformation and the development of a USER-Brick vector construction system. BMC Molecular Biology 15, 1–15. https://doi.org/10.1186/1471-2199-15-15/FIGURES/7

Spellerberg, I.F., Fedor, P.J., 2003. A tribute to Claude-Shannon (1916-2001) and a plea for more rigorous use of species richness, species diversity and the "Shannon-Wiener" Index. Global Ecology and Biogeography 12, 177–179. https://doi.org/10.1046/j.1466-822X.2003.00015.x

Spellig, T., Bottin, A., Kahmann, R., 1996. Green fluorescent protein (GFP) as a new vital marker in the phytopathogenic fungus *Ustilago maydis*. Molecular and General Genetics MGG 1996 252:5 252, 503–509. https://doi.org/10.1007/BF02172396

Stokowa-Sołtys, K., Dzyhovskyi, V., Wieczorek, R., Jeżowska-Bojczuk, M., 2019. Phleomycin complex – Coordination mode and in vitro cleavage of DNA. Journal of Inorganic Biochemistry 195, 71–82. https://doi.org/10.1016/J.JINORGBIO.2019.03.010

Strange, R.N., Majer, J.R., Smith, H., 1974. The isolation and identification of choline and betaine as the two major components in anthers and wheat germ that stimulate *Fusarium*

*graminearum* in vitro. Physiological Plant Pathology 4, 277–290. https://doi.org/10.1016/0048-4059(74)90015-0

Strzyz, P., 2020. CRISPR–Cas9 wins Nobel. Nature Reviews Molecular Cell Biology 2020 21:12 21, 714–714. https://doi.org/10.1038/s41580-020-00307-9

Sugui, J.A., Chang, Y.C., Kwon-Chung, K.J., 2005. *Agrobacterium tumefaciens*-mediated transformation of *Aspergillus fumigatus*: an efficient tool for insertional mutagenesis and targeted gene disruption. Applied and Environmental Microbiology 71, 1798–1802. https://doi.org/10.1128/AEM.71.4.1798-1802.2005

Sutton, J.C., 1982. Epidemiology of wheat head blight and maize ear rot caused by *Fusarium graminearum*. Canadian Journal of Plant Pathology 4, 195–209. https://doi.org/10.1080/07060668209501326

Takahara, Hiroyuki, Tsuji, Gento, Kubo Mikihiro Yamamoto, Y., Toyoda Yoshishige Inagaki, K., Ichinose, Yuki, Shiraishi, Tomonori, Takahara, H, Tsuji, G, Yamamoto, M., Toyoda, K., Inagaki, Y., Ichinose, Y, Shiraishi, T, Kubo, Y., 2004. *Agrobacterium tumefaciens*-mediated transformation as a tool for random mutagenesis of *Colletotrichum trifolii*. J Gen Plant Pathol 70, 93–96. https://doi.org/10.1007/s10327-003-0099-y

Tekauz, A., McCallum, B., Ames, N., Fetch, J.M., 2010. Fusarium head blight of oat — current status in western Canada. Canadian journal of plant pathology 26, 473-479. https://doi.org/10.1080/07060660409507167

Thompson, J.N., Burdon, J.J., 1992. Gene-for-gene coevolution between plants and parasites. Nature 360, 121–125. https://doi.org/10.1038/360121a0

Tilman, D., Balzer, C., Hill, J., Befort, B.L., 2011. Global food demand and the sustainable intensification of agriculture. Proceedings of the National Academy of Sciences of the United States of America 108, 20260–20264. https://doi.org/10.1073/PNAS.1116437108/-/DCSUPPLEMENTAL

Toju, H., Tanabe, A.S., Yamamoto, S., Sato, H., 2012. High-coverage *ITS* primers for the DNA-based identification of ascomycetes and basidiomycetes in environmental samples. PLoS ONE 7. https://doi.org/10.1371/journal.pone.0040863

Toljander, J.F., Artursson, V., Paul, L.R., Jansson, J.K., Finlay, R.D., 2006. Attachment of different soil bacteria to arbuscular mycorrhizal fungal extraradical hyphae is determined by hyphal vitality and fungal species. FEMS Microbiology Letters 254, 34–40. https://doi.org/10.1111/j.1574-6968.2005.00003.x

Trail, F., 2009. For blighted waves of grain: *Fusarium graminearum* in the postgenomics era. Plant Physiology 149, 103–110. https://doi.org/10.1104/pp.108.129684

Trotel-Aziz, P., Couderchet, M., Biagianti, S., Aziz, A., 2008. Characterization of new bacterial biocontrol agents *Acinetobacter*, *Bacillus*, *Pantoea* and *Pseudomonas* spp. mediating

grapevine resistance against *Botrytis cinerea*. Environmental and Experimental Botany 64, 21–32. https://doi.org/10.1016/J.ENVEXPBOT.2007.12.009

Turner, D., Kovacs, W., Kuhls, K., Lieckfeldt, E., Peter, B., Arisan-Atac, I., Strauss, J., Samuels, G.J., Börner, T., Kubicek, C.P., 1997. Biogeography and phenotypic variation in *Trichoderma* sect. *Longibrachiatum* and associated *Hypocrea* species. Mycological Research 101, 449–459. https://doi.org/10.1017/S0953756296002845

Turner, T.R., James, E.K., Poole, P.S., 2013. The plant microbiome. Genome Biology 2013 14:6 14, 1–10. https://doi.org/10.1186/GB-2013-14-6-209

Ueki, A., Takehara, T., Ishioka, G., Kaku, N., Ueki, K., 2017. Degradation of the fungal cell wall by clostridial strains isolated from soil subjected to biological soil disinfestation and biocontrol of Fusarium wilt disease of spinach. Applied Microbiology and Biotechnology 2017 101:22 101, 8267–8277. https://doi.org/10.1007/S00253-017-8543-7

Updated clubroot maps and survey results | The Canola Council of Canada [WWW Document], n.d. URL https://www.canolacouncil.org/canola-watch/2021/01/14/updated-clubroot-maps-and-survey-results/ (accessed 10.25.21).

Valdivia, R.H., Hromockyj, A.E., Monack, D., Ramakrishnan, L., Falkow, S., 1996. Applications for green fluorescent protein (GFP) in the study of host pathogen interactions. Gene 173, 47–52. https://doi.org/10.1016/0378-1119(95)00706-7

van de Wouw, A.P., Pettolino, F.A., Howlett, B.J., Elliott, C.E., 2009. Mutations to LmIFRD affect cell wall integrity, development and pathogenicity of the ascomycete *Leptosphaeria maculans*. Fungal Genetics and Biology 46, 695–706. https://doi.org/10.1016/J.FGB.2009.06.004

van der Lee, T., Zhang, H., van Diepeningen, A., Waalwijk, C., 2015. Biogeography of *Fusarium graminearum* species complex and chemotypes: a review. https://doi.org/10.1080/19440049.2014.984244

Venn, L., 1979. The genetic control of sexual compatibility in *Leptosphaeria maculans*. Australasian Plant Pathology 8, 5–6. https://doi.org/10.1071/APP9790005

Vieira, A.A., Vianna, G.R., Carrijo, J., Aragão, F.J.L., Vieira, P.M., 2021. Generation of *Trichoderma harzianum* with pyr4 auxotrophic marker by using the CRISPR/Cas9 system. Scientific Reports 2021 11:1 11, 1–7. https://doi.org/10.1038/s41598-020-80186-4

Walter, S., Nicholson, P., Doohan, F.M., 2010. Action and reaction of host and pathogen during Fusarium head blight disease. New Phytologist 185, 54–66. https://doi.org/10.1111/j.1469-8137.2009.03041.x

Wang, S., Chen, H., Wang, Y., Tang, X., Zhang, H., Chen, W., Chen, Y.Q., 2018. Optimization of *Agrobacterium tumefaciens*-mediated transformation method of oleaginous filamentous fungus *Mortierella alpina* on co-cultivation materials choice. Journal of Microbiological Methods 152, 179–185. https://doi.org/10.1016/J.MIMET.2018.08.002

Wei, F., Hu, X., Xu, X., 2016. Dispersal of *Bacillus subtilis* and its effect on strawberry phyllosphere microbiota under open field and protection conditions. Scientific Reports 2016 6:1 6, 1–9. https://doi.org/10.1038/srep22611

Weiss, P.S., 2008. Nobel prize in chemistry: green fluorescent protein, its variants and implications. ACS Nano 2, 1977. https://doi.org/10.1021/NN800671H

Weld, R.J., Plummer, K.M., Carpenter, M.A., Ridgway, H.J., 2006. Approaches to functional genomics in filamentous fungi. Cell Research 2006 16:1 16, 31–44. https://doi.org/10.1038/sj.cr.7310006

Woo, S.L., Ruocco, M., Vinale, F., Nigro, M., Marra, R., Lombardi, N., Pascale, A., Lanzuise, S., Manganiello, G., Lorito, M., 2014. *Trichoderma*-based Products and their Widespread Use in Agriculture. The Open Mycology Journal 8, 71–126. https://doi.org/10.2174/1874437001408010071

Wright, A.L., Wahoush, O., Ballantyne, M., Gabel, C., Jack, S.M., 2016. Qualitative health research involving indigenous peoples: culturally appropriate data collection methods. The Qualitative Report 21, 2230–2245. https://doi.org/10.46743/2160-3715/2016.2384

Wu, J., Wang, Y., Park, S.Y., Kim, S.G., Yoo, J.S., Park, S., Gupta, R., Kang, K.Y., Kim, S.T., 2016. Secreted Alpha-N-Arabinofuranosidase B protein is required for the full virulence of *Magnaporthe oryzae* and triggers host defences. PLOS ONE 11, e0165149. https://doi.org/10.1371/JOURNAL.PONE.0165149

Xu, X.M., Nicholson, P., Thomsett, M.A., Simpson, D., Cooke, B.M., Doohan, F.M., Brennan, J., Monaghan, S., Moretti, A., Mule, G., Hornok, L., Beki, E., Tatnell, J., Ritieni, A., Edwards, S.G., 2008. Relationship between the fungal complex causing Fusarium head blight of wheat and environmental conditions. Phytopathology 98, 69–78. https://doi.org/10.1094/PHYTO-98-1-0069

Yang, C., Hamel, C., Vujanovic, V., Gan, Y., 2011. Fungicide: modes of action and possible impact on nontarget microorganisms. International Scholarly Research Network ISRN Ecology 2011. https://doi.org/10.5402/2011/130289

Yang, L., Ukil, L., Osmani, A., Nahm, F., Davies, J., de Souza, C.P.C., Dou, X., Perez-Balaguer, A., Osmani, S.A., 2004. Rapid production of gene replacement constructs and generation of a green fluorescent protein-tagged centromeric marker in *Aspergillus nidulans*. Eukaryotic Cell 3, 1359–1362. https://doi.org/10.1128/EC.3.5.1359-1362.2004/ASSET/39F93423-2275-4C4B-BE54-ADC6A56EB8A8/ASSETS/GRAPHIC/ZEK0050423070004.JPEG

Yao, Y.R., Tian, X.L., Shen, B.M., Mao, Z.C., Chen, G. hua, Xie, B.Y., 2015. Transformation of the endophytic fungus Acremonium implicatum with GFP and evaluation of its biocontrol effect against *Meloidogyne incognita*. World Journal of Microbiology and Biotechnology 31, 549–556. https://doi.org/10.1007/s11274-014-1781-2

Yin, D., Wang, N., Xia, F., Li, Q., Wang, W., 2013. Impact of biocontrol agents *Pseudomonas fluorescens* 2P24 and CPF10 on the bacterial community in the cucumber rhizosphere. European Journal of Soil Biology 59, 36–42. https://doi.org/10.1016/J.EJSOBI.2013.09.001

Yoshida, K., Schuenemann, V.J., Cano, L.M., Pais, M., Mishra, B., Sharma, R., Lanz, C., Martin, F.N., Kamoun, S., Krause, J., Thines, M., Weigel, D., Burbano, H.A., 2013. The rise and fall of the *Phytophthora infestans* lineage that triggered the Irish potato famine. eLife 2013. https://doi.org/10.7554/eLife.00731

Yuan, W.M., Crawford, D.L., 1995. Characterization of *Streptomyces lydicus* WYEC108 as a potential biocontrol agent against fungal root and seed rots. Applied and Environmental Microbiology 61, 3119–3128. https://doi.org/10.1128/AEM.61.8.3119-3128.1995/FORMAT/PDF

Zafra, G., Cortés-Espinosa, D. v., 2015. Biodegradation of polycyclic aromatic hydrocarbons by *Trichoderma* species: a mini review. Environmental Science and Pollution Research 2015 22:24 22, 19426–19433. https://doi.org/10.1007/S11356-015-5602-4

Zambiazi, R., Przybylski, R., Alimentos, M.Z.-… de, 2007. Fatty acid composition of vegetable oils and fats. . Boletim do Centro de Pesquisa de Processamento de Alimentos 25, 111–120.

Zhai, C., Liu, X., Song, T., Yu, F., Peng, G., 2021. Genome-wide transcriptome reveals mechanisms underlying *Rlm1*-mediated blackleg resistance on canola. Scientific Reports 11, 1–17. https://doi.org/10.1038/s41598-021-83267-0

Zhang, S., Gan, Y., Xu, B., 2016. Application of plant-growth-promoting fungi *Trichoderma longibrachiatum* T6 enhances tolerance of wheat to salt stress through improvement of antioxidative defense system and gene expression. Frontiers in Plant Science 0, 1405. https://doi.org/10.3389/FPLS.2016.01405

Zhang, X., Fernando, W.G.D., 2017. Insights into fighting against blackleg disease of *Brassica napus* in Canada. Crop and Pasture Science 69, 40–47. https://doi.org/10.1071/CP16401

Zhang, X., Peng, G., Kutcher, H.R., Balesdent, M.H., Delourme, R., Fernando, W.G.D., 2016. Breakdown of *Rlm3* resistance in the *Brassica napus–Leptosphaeria maculans* pathosystem in western Canada. European Journal of Plant Pathology 145, 659–674. https://doi.org/10.1007/S10658-015-0819-0/TABLES/5

Zhong, Y., Yu, H., Wang, X., Lu, Y., Wang, T., 2010. Towards a novel efficient T-DNA-based mutagenesis and screening system using green fluorescent protein as a vital reporter in the industrially important fungus *Trichoderma reesei*. Molecular Biology Reports 2010 38:6 38, 4145–4151. https://doi.org/10.1007/S11033-010-0534-Z

Zhou, X., Liu, L., Chen, Y., Xu, S., Chen, J., 2007. Efficient biodegradation of cyanide and ferrocyanide by Na-alginate beads immobilized with fungal cells of *Trichoderma koningii*. Canadian Journal of Microbiology 53, 1033–1037. https://doi.org/10.1139/W07-070

Zou, Z., Liu, F., Fernando, W.G.D., 2018. Rapid detection of *Leptosphaeria maculans* avirulence gene *AvrLm4-7* conferring the avirulence/virulence specificity on *Brassica napus* using a tetra-primer ARMS-PCR. European Journal of Plant Pathology 152, 515–520. https://doi.org/10.1007/S10658-018-1465-0/TABLES/1

Zou, Z., Liu, F., Selin, C., Fernando, W.G.D., 2020. Generation and characterization of a virulent *Leptosphaeria maculans* isolate carrying a mutated *AvrLm7* gene using the CRISPR/Cas9 system. Frontiers in Microbiology 0, 1969. https://doi.org/10.3389/FMICB.2020.01969

# 7.0 APPENDICES

## 7.1 List of abbreviations

| | |
|---|---|
| ANOVA | Analysis of variance |
| APR | Adult plant resistance |
| ATMT | *Agrobacterium tumefaciens* mediated transformation |
| *Avr* | Avirulence |
| Cas | CRISPR associated |
| crRNA | CRISPR RNA |
| DON | Deoxynivalenol |
| dpi | Days post inoculation |
| DS | Disease severity |
| FHB | Fusarium Head Blight |
| FP | Fluorescent protein |
| GFP | Green Fluorescent Protein |
| HR | Hypersensitive reaction |
| IR | Intermediate resistance |
| LDL | low-density lipoproteins |
| MDS | Mean disease score |
| mJN3 | Mutant JN3 |
| NIV | Nivalenol |
| OTU | Operational taxonomic unit |
| PAM | Protospacer adjacent motif |
| pre-crRNA | Precursor CRISPR RNA |
| qPCR | Quantitative PCR |
| *R* | Resistant |
| RNP | Ribonucleoprotein |
| S | Susceptible |
| sgRNA | Single guide RNA |
| Ti | Tumor inducing |

| | |
|---|---|
| tracrRNA | Trans-activating crRNA |